NUMERICAL MODELLING OF ICE-SEABED INTERACTION IN LAYERED SEABED

by

© Seyedhossein Hashemi

A Thesis submitted to the

School of Graduate Studies

in partial fulfillment of the requirements for the degree of

Doctor of Philosophy

Faculty of Engineering and Applied Science

Memorial University of Newfoundland

June 2022

St. John's Newfoundland Canada

ABSTRACT

Traveling icebergs may threat the structural integrity of the offshore pipelines in any territories that they can reach. Arctic offshore pipeline are usually buried for physical protection against ice gouging. Burying the pipeline in a trench immediately deeper than the maximum-recorded ice gouge depth is not sufficient to ensure the safety of the pipeline. The subgouge soil displacement is not limited to the depth of the ice keel tip. The shear resistance of the seabed soil causes the subgouge soil deformation to extend much deeper than the ice keel tip. This, in turn, threats the subsea pipelines and mandates achieving a sufficient burial depth to ensure the structural integrity of the pipeline. Finding the best burial depth satisfying the safety and economical consideration is a challenging aspect. In practice, a decoupled approach is usually undertaken by engineers, where, first, a continuum large deformation finite element analysis of free field ice gouging process is conducted. Then, the results of subgouge soil deformations are transferred to a simplified beam-spring model to obtain the structural response of the pipeline. Therefore, the free-field ice gouging analysis is a key part of the design practice. However, the seabed is usually represented by a uniform material domain ignoring the complexities and implications that may arise from layered seabeds that are quite common in many of the Arctic geographical locations (e.g., Chukchi Sea (Winters and Lee, 1984; C-CORE, 2008), Alaskan Beaufort Shelf (C-CORE, 2008), Russian Sakhalin Island (C-CORE, 1995e), etc.). Therefore, there exists a knowledge gap in the literature digging in to the ice gouging event in a complex non-uniform layered soil strata.

In this study, the response of different layered seabed comprising soft over stiff clay, stiff over soft clay, and the loose and dense sand over soft and stiff clay to the ice gouging were

investigated by performing large deformation finite element (LDFE) analysis using a Coupled Eulerian Lagrangian (CEL) algorithm. The CEL allows the material to flow through the Eulerian fixed mesh and supress the mesh distortion and numerical instability issues. Despite the conventional studies that typically consider a uniform soil strata with an elastic perfect plastic seabed soil material obeying von Mises or Tresca criterion, the current study incorporated the strain rate and strain softening effects of the cohesive soil as well to improve the accuracy of the predictions. This was conducted by coding the modified soil model into a user-defined subroutine (VUSDFLD) and linking to the main model. Strain rate dependency and strain softening during shearing and remoulding are two natural behaviours of cohesive soils affecting the value of soil undrained shear strength. It is generally agreed that increasing shear strain rate leads to increase in undrained shear strength. Also, within large shear strains, the strain softening causes a gradual loss of shear strength. Including these effects in the current study improved the accuracy of simulating of ice gouging process in layered seabed as a high velocity geotechnical problem involving large deformations. During the analysis, the user subroutine is incrementally called by ABAQUS to update the undrained shear strength of the soil based on the incremental values of the currently accumulated absolute plastic shear strain and the calculated maximum shear strain rate with zero value adopted for friction and dilation angles. The performance of the modified soil model was verified through comparisons with published experimental studies and conventional soil models. Comprehensive parametric studies were conducted to examine the ice keel-seabed interaction in a range of layered seabed with different configurations. The effect of different input parameters including the ice keel geometry, gouge depth, seabed soil strength, and layering condition on the keel reaction

forces, subgouge soil deformation, the side berm and frontal mound formations, and the progressive plastic shear strain distribution were examined through a large number of case scenarios.

It was observed that replacing a layered seabed with a uniform seabed for simplicity could be significantly misleading resulting in non-reliable subgouge soil deformation magnitudes and keel reaction forces. The study showed that an interactive mechanism between the different soil layers might significantly affect the soil failure mechanism near the ice keel and cause unexpected subgouge soil deformations in underlying layers. The new findings of the conducted study are quite significant in terms of practical considerations for pipeline design. Based on the observations, several practical recommendations were made to improve the safety of the Arctic pipelines to be buried in complex layered seabed soil strata.

STATEMENT OF AUTHORSHIP

Among the outcomes of this work, I as the main author am credited for the methodology, modeling, data curation, visualization, investigation, validation and writing-original draft, my supervisor Dr. Hodjat Shiri is credited for conceptualization, supervision, writing-review and editing and funding acquisition and Dr. Xiaoyu Dong is credited for writing-review and editing one of the published papers shown below:

- Hashemi, S., and Shiri, H., 2022b. "Numerical Modeling of Ice–Seabed Interaction in Clay by Incorporation of the Strain Rate and Strain-Softening Effects." ASME. J. Offshore Mech. Arct. Eng. August 2022; 144(4): 042101. https://doi.org/10.1115/1.4053871
- Hashemi, S., Shiri, H. and Dong, X., 2022a. The influence of layered soil on ice-seabed interaction: Soft over stiff clay, Applied Ocean Research, Volume 120, March 2022, 103033, ISSN 0141-1187, https://doi.org/10.1016/j.apor.2021.103033
- Hashemi, S., Shiri, H., 2022. Numerical Modeling of Ice-seabed Interaction in Layered Soil: Stiff over Soft Clay, Submitted to the Applied Ocean Research.
- Hashemi, S., Shiri, H., 2022. The Response of Layered Seabed to Ice Gouging: Sand over Clay, Submitted to the Ocean Engineering.
- Hashemi, S., Shiri, H., 2023, Simulation of the response of layered seabed to the ice gouging, International Conference on Port and Ocean Engineering under Arctic Conditions, POAC 2023, Glasgow, UK (to be submitted).

ACKNOWLEDGMENT

Thanks God, the merciful and the passionate, for providing me the opportunity to step in the excellent world of science.

I would like to express my special appreciation and thanks to my supervisor, Dr. Hodjat Shiri, who provided me excellent opportunity to join his research team and involved me in a challenging research topic. I am grateful for his unconditional supports, keen supervision, and guidance thorough out this study, and especially for his confidence in me. His knowledge and industrial experiences provided valuable insight for academic research.

I gratefully acknowledge the financial support of the Wood Group PLC, which established a Research Chair program in Arctic and Harsh Environment Engineering at Memorial University of Newfoundland, the "Natural Science and Engineering Research Council of Canada (NSERC)" through "CRD" program, and the "Newfoundland Research and Development Corporation (RDC) (now TCII)" through "Ignite" and "Collaborative Research and Developments Grants (CRD)". Special thanks are extended to School of Graduate Studies (SGS), and Faculty of Engineering and Applied Science at Memorial University for providing financial supports and excellent resources to conduct this research project.

I owe hugely to my dear parents. When I look at to my academic path in behind, I see nothing except encouragement, support and pray from them. Thank you is a very small phrase to convey my gratitude towards them. I am incredibly grateful to them.

Finally, but definitely not the least, I express my gratitude to my dear wife who warmly encouraged me during my studies. I am so appreciative for her unconditional love, understanding and patience.

This thesis is dedicated to my dear parents and my wife

Contents

List of Figures

List of Tables

List of Abbreviations and Symbols

Abbreviations

ALE	Arbitrary Lagrangian-Eulerian
CEL	Coupled Eulerian-Lagrangian
DS	Dense sand
FEA	Finite element analysis
FM	Frontal mound
FMH	Frontal mound height
FML	Frontal mound length
FV	Field variable
LDFE	Large Deformation Finite Element
LS	Loose sand
MC	Mohr-Coulomb
OC	Over-consolidated clay
OCR	Over-consolidation ratio
PI	Plasticity index
PIC	Particle-In-Cell
PRISE	Pressure Ridge Ice Scour Experiments
RF1	Ultimate horizontal keel reaction force
RF3	Ultimate vertical keel reaction force

SB	Side berms
SBH	Side berms height
SBW	Side berms width
SoC	Soft clay
StC	Stiff clay
VLS	Very loose sand

English Symbols

Z	Depth
G	Shear modulus
G_{50}	Shear modulus at 50% mobilized strength
E	Modulus of elasticity
E_{u50}	Undrained modulus of elasticity at 50% mobilized strength
I_R	Rigidity index
S_t	Soil sensitivity
s_{ui}	In situ undrained shear strength
Δt	Time increment
s_{um}	Mudline undrained shear strength
k	Gradient of linear profile of undrained shear strength
$s_{ui\ stiff}$	Intercept undrained shear strength magnitude of stiff layer
$s_{ui\ soft}$	Intercept undrained shear strength magnitude of soft layer

Greek Symbols

ν	Poisson's ratio
μ	Increase rate of the shear strength per log cycle
$\dot{\gamma}_{ref}$	Reference shear strain rate
$\dot{\gamma}_{max}$	Maximum shear strain rate
δ_{rem}	Ratio of fully remoulded to initial shear strength
ξ	Accumulated absolute plastic shear strain
ξ_{95}	Accumulated absolute plastic shear strain for 95% reduction in strength due to remoulding
ρ	Mass density
$\Delta\varepsilon_1$	Cumulative major principal strains
$\Delta\varepsilon_3$	Cumulative minor principal strains
τ_y	Cohesion yield stress
τ_{max}	Limited allowable keel-soil interface shear stress
ε^p	Plastic strain components

Chapter 1

Introduction

1.1. Background

The current thesis is presented paper-based, where each chapter has its own introduction and literature review. However, a summary introduction representing all chapters is brought here as Chapter 1.

Floating ice in shape of icebergs or ice ridges travel through the Arctic oceans and neighbour territories and scour the seabed in shallow water. This phenomenon that is called "Ice gouging" may jeopardize the structural integrity of the crossed subsea pipelines. Therefore, pipelines are buried in trenches for physical protection against ice attack. However, the best burial depth of the pipeline is still a challenging question in practice. A trench immediately deeper than the maximum-recorded ice gouge depth in the region does not suffice the integrity and the safety of the pipeline. The shear resistance of the seabed soil causes the subgouge soil deformation to extend much deeper than the ice keel tip. This, in turn, threats the subsea pipelines and mandates achieving a sufficient burial depth to ensure the structural integrity of the pipeline. Determining the safest and the most economical burial depth requires accurate estimation of the subgouge soil deformation. In practice, it is determined by performing a decoupled large deformation finite element (LDFE) analysis of ice gouging, where the subgouge soil deformations obtained from a free-field (no pipeline) ice gouging analysis are transferred to the end of the lateral springs in abeam-spring model to obtain the pipeline response (Woodworth-Lynas et al., 1996; Phillips and Barrett, 2012). Although the accuracy of this approach suffer from the

superposition of idealization and directional load decoupling as two sources of errors (Konuk and Gracie, 2004; Nobahar et al., 2007b; Lele et al., 2011; Peek and Nobahar, 2012; Phillips and Barrett, 2012; Eltaher, 2014; Pike and Kenny, 2016), but it is still used in industry as an acceptable and cost-effective estimation. Therefore, an accurate free-field ice gouging analysis is significantly important in obtaining reliable results. However, the seabed is usually represented by a uniform material domain ignoring the complexities and implications that may arise from layered seabed (e.g., Konuk and Gracie, 2004; Nobahar et al., 2007b; Lele et al., 2011; Peek and Nobahar, 2012; Phillips and Barrett, 2012; Eltaher, 2014; Pike and Kenny, 2016), while layered seabed has been broadly observed in Arctic offshore areas with ongoing offshore energy activities (e.g., Chukchi Sea (Winters and Lee, 1984; Clark and Guigné, 1988; C-CORE, 2008), Alaskan Beaufort Shelf (C-CORE, 2008), Russian Sakhalin Island (C-CORE, 1995e), etc.). The layered soil observed in these studies includes soft over stiff clay in the western Chukchi Sea (Winters and Lee, 1984), stiff over soft clay in Alaskan Beaufort Sea (Miller and Bruggers, 1980), and non-uniform sand over clay in North Sakhalin Island (C-CORE, 1995e). These layered soil strata have been widely investigated in the current study.

1.2. Motivation

There are only a few published experimental and numerical studies investigating the ice gouging in layered seabed that have considered the layered soil in a very limited scope (e.g., Miller and Bruggers, 1980; Allersma and Schoonbeek, 2005; Pressure Ridge Ice Scour Experiments (PRISE) JIP, C-CORE, 1995e). The significance of the impact of layered seabed soil on ice gouging process has been highlighted in the literature as an important knowledge gap (NRC-PERD, 2014; BSEE-WGK, 2015; Winters and Lee, 1984;

Babaei and Sudom, 2014; Alba, 2015). In this research program, the response of complex layered seabed strata comprising different configurations including soft over stiff clay, stiff over soft clay, and sand (loose and dense) over clay (stiff and soft) to the ice gouging were investigated by performing advanced large deformation finite element (LDFE) analysis using a Coupled Eulerian Lagrangian (CEL) in a fashion similar to earlier studies (e.g., Konuk and Gracie, 2004; Babaei and Sudom, 2014; Pike and Kenny, 2016). The LDFE analysis of ice gouging is highly affected by strain localization that could suffer from mesh distortion and instability issues if a Lagrangian approach was undertaken. The reason is the loss of mathematical well-posedness of initial or boundary value problems that result in the solution uniqueness and dependency on the boundary data. Early efforts towards overcoming these limitations lead to introduce two robust and efficient techniques like Coupled Eulerian-Lagrangian (CEL) and Arbitrary Lagrangian-Eulerian (ALE) which are able to model ice gouging event as a complex interaction based large deformation problem (Konuk and Gracie, 2004; Babaei and Sudom, 2014; Pike and Kenny, 2016). The Arbitrary Lagrangian-Eulerian (ALE) method has been used for LDFE analysis by researchers but the limited allowable mesh distortion is the major concern suffering the method (Banneyake et al., 2011). The CEL formulation available in ABAQUS/Explicit software in a friendly framework offers large deformation analysis in which Eulerian body (e.g., soil) can flow in fixed Eulerian meshes without any concern about the mesh over-distortion and allows Eulerian body and Lagrangian body (e.g., ice) to interact with each other without any instability during the analysis. Therefore, in this study, the LDFE analysis was conducted using the CEL approach in ABAQUS/Explicit.

However, despite the conventional studies that have typically considered uniform soil strata with an elastic perfect plastic seabed soil material obeying von Mises or Tresca criterion, the current study incorporated the strain rate and strain softening effects in cohesive soil layers as well, through coding a user-defined subroutine (VUSDFLD) and modifying the classical Tresca soil model using the equation proposed by Einav and Randolph (2005). Strain rate dependency and strain softening during shearing and remoulding are two natural behaviours of cohesive soils affecting the value of soil undrained shear strength. It is generally agreed that increasing shear strain rate leads to increase in undrained shear strength (e.g., Biscontin and Pestana, 2001; DeGroot et al., 2007; Lunne and Andersen, 2007; DeJong et al., 2012). Also, within large shear strains, the strain softening causes a gradual loss of shear strength (Hossain and Randolph, 2009). Including these effects in the current study improved the accuracy of simulating of ice gouging process in layered seabed as a high velocity geotechnical problem involving large deformations. During the analysis, the user subroutine is incrementally called by ABAQUS to update the undrained shear strength of the soil based on the incremental values of the currently accumulated absolute plastic shear strain and the calculated maximum shear strain rate with zero value adopted for friction and dilation angles. The performance of the model was verified through comparisons with published experimental studies (Allersma and Schoonbeek, 2005; Lach, 1996).

A comprehensive parametric study was conducted to examine the ice keel-seabed interaction in a layered seabed and the effect of a range of different input parameters including the ice keel geometry, gouge depth, seabed soil strength, and layering condition on the keel reaction forces, subgouge soil deformation, the side berms and frontal mound

formations, and the progressive plastic shear strains distribution measured when gouging was developed in steady state condition.

It was observed that replacing a layered seabed with a uniform soil for simplicity can be significantly misleading resulting in non-reliable subgouge soil deformation magnitudes and keel reaction forces. The study revealed interactive soil failure mechanisms between the soil layers that may cause unexpected subgouge soil deformation in deep layers. The new findings of the current study have never been reported in earlier studies. Based on the observations of the current study, several practical recommendations were made to improve the safety of the Arctic pipelines threatened by icebergs. The developed numerical model was found to be a simple but robust tool that could be used in current engineering practice to estimate a reliable response of uniform and layered seabed to ice gouging event in Arctic seas.

1.3. Key objectives

The key objectives of the current research project that were achieved throughout the project were as follows:

- Review the literature and identify a key knowledge gap,
- Develop the CEL model for LDFE analysis of free-field ice gouging in uniform cohesive seabed,
- Develop a coded user-defined subroutine in FORTRAN to incorporate the effects of strain rate dependency and strain-softening on the undrained shear strength of the cohesive soil layer,
- Verify the developed model in uniform seabed against the published experimental and numerical studies,

- Extract the configuration of different layered seabed from the published data in the literature,
- Develop the CEL models for various layered seabed strata and perform comprehensive parametric study,
- Investigate the soil failure mechanism in layered seabed under the ice gouging process and its influence on the ice keel reaction forces, subgouge soil deformations, side berms and frontal mound formations, and the plastic shear strain distribution,
- Examine the influences of various key parameters on the ice-seabed interaction process in the layered seabed, layered .Provide technical advices to be considered in practice for improving the safety of the Arctic offshore pipelines.

1.4. Organization of the Thesis

The thesis is prepared paper-based, presenting each journal paper as an independent chapter added by three more chapters as the introduction, a short literature review, and conclusions and recommendations.

Chapter 1 is an introduction to the research topic containing the background, research motivations, research objectives, the thesis structure, and the research outcome. Chapter 2 includes a short literature review of the numerical and experimental studies investigating the ice gouging process. In addition, each chapter has its specific literature review as an independent journal paper. Chapter 3 presents developing and verifying a CEL model for LDFE analysis of ice gouging in uniform clay along with the incorporation of the strain rate dependency and strain softening effects. A comprehensive parametric study was also conducted to explore the effects of different parameters of iceberg and seabed soil on the

ice keel-seabed interaction. This chapter was published as a journal paper in *Journal of Offshore Mechanics and Arctic Engineering* (ASME). Chapter 4 presents developing a CEL model for LDFE analysis of ice gouging in layered soft over stiff clay that is observed in many Arctic geographical locations. The interactive response of the layered soft over stiff clay to the ice gouging was investigated and the observations resulted in technical advices for improvement of the design practice. The numerical results were verified against the published centrifuge test results. This chapter was published as a journal paper in *Applied Ocean Research* (Elsevier). Chapter 5 discusses the CEL model developed for the LDFE analysis of ice gouging in a complex layered stiff over soft clay that has been reported in geotechnical site investigations in various Arctic regions. The study resulted in observing a very interesting wavy profile in subgouge soil deformation and technical advices for enhancing the design practice. A comprehensive parametric study was also conducted to investigate the effect of key model parameters on the keel reaction forces, subgouge soil deformations, side berms and frontal mound formations, and plastic shear strain distributions. This chapter has been submitted as a manuscript to the journal of *Applied Ocean Research (*Elsevier). Chapter 6 presents the numerical model developed and verified for LDFE analysis of ice gouging in layered sand over clay seabed. Loose and dense sand over stiff and soft clay were investigated and the interactive soil failure mechanism in front of the ice keel was captured. A comprehensive parametric study was conducted and practical advices were provided to improve the design practice. The accuracy of the developed model was verified through comparing the numerical results with the PRISE centrifuge test results reported by C-CORE (1995e). This chapter was submitted as a manuscript to the journal of *Ocean Engineering* (Elsevier). Chapter 7

presents the summary of the key observations, technical advices for practical applications, and the recommendations for future studies.

1.5. Research outcome

The research work provided a valuable insight into the numerical modelling of free-field ice gouging in uniform and layered clay seabed. More specifically the significant effect of incorporation of the strain rate dependency and strain-softening effects in to the constitutive soil model was investigated. These effects are more visible on the keel reaction forces, subgouge soil deformations, and the formation of the side berms and frontal mounds. The study improved the accuracy of free-field ice gouging analysis and the resultant subgouge soil displacements in uniform and layered seabed. The study revealed the significance of soil layer interactions and its impact on the soil failure mechanisms during the ice gouging process. Technical advices were provided for engineering industry to take the advantage of these new observations to improve the safety and cost-effectiveness of pipeline design against ice gouging in practice. The research outcome was disseminated through four journal papers and a peer-reviewed conference paper as follows:

- Hashemi, S., and Shiri, H., 2022b. "Numerical Modeling of Ice–Seabed Interaction in Clay by Incorporation of the Strain Rate and Strain-Softening Effects." ASME. J. Offshore Mech. Arct. Eng. August 2022; 144(4): 042101. https://doi.org/10.1115/1.4053871
- Hashemi, S., Shiri, H. and Dong, X., 2022a. The influence of layered soil on ice-seabed interaction: Soft over stiff clay, Applied Ocean Research, Volume 120, March 2022, 103033, ISSN 0141-1187, https://doi.org/10.1016/j.apor.2021.103033

- Hashemi, S. and Shiri, H., 2022. Numerical Modeling of Ice-seabed Interaction in Layered Soil: Stiff over Soft Clay. Submitted to the Applied Ocean Research.
- Hashemi, S. and Shiri, H., 2022. The Response of Layered Seabed to Ice Gouging: Sand over Clay. Submitted to the Ocean Engineering.
- Hashemi, S. and Shiri, H., 2023, Simulation of the response of layered seabed to the ice gouging, International Conference on Port and Ocean Engineering under Arctic Conditions, POAC 2023, Glasgow, UK (to be submitted).

References

Alba, J. L. , 2015, Ice Scour and Gouging Effects With Respect to Pipeline and Wellhead Placement and Design, Bureau of Safety and Environmental Enforcement (BSEE), Wood Group Kenny, Report No. 100100.01.PL.REP.004, Houston, TX.

Allersma, H.G.B., and Schoonbeek, I.S.S. (2005). Centrifuge modelling of scouring ice keels in clay. Int. Conference on Offshore and Polar Engineering, ISOPE2005, Seoul, June 19-24, paper 2005-JSC-427, pp.404-409

Babaei, M. H., & Sudom, D. (2014). Ice-seabed gouging database: review and analysis of available numerical models. In *OTC Arctic Technology Conference*. Offshore Technology Conference.

Banneyake, R., Hossain, M. K., Eltaher, A., Nguyen, T., Jukes, P., 2011. Ice-soil pipeline interactions using coupled eulerian-lagrangian (CEL) ice gouge simulations extracts from ice pipe JIP. Paper presented at the OTC Arctic Technology Conference.

Biscontin, G., Pestana, J.M., 2001. Influence of peripheral velocity on vane shear strength of an artificial clay. Geotech. Test.J. 24(4), 423–429.

BSEE-WGK (2015). Ice Scour and Gouging Effects with Respect to Pipeline and Wellhead, Final Report, 100100.01.PL.REP.004, Rev0.

C-CORE. (1995e). Pressure Ridge Ice Scour Experiment, PRISE: Phase 3-Centrifuge Modelling of Ice Keel Scour: Draft Final Report. April 1995. Publication 95-C12, 52p.

C-CORE. (2008). Design Options for Offshore Pipelines in the US Beaufort and Chukchi Seas. April 2008. Report R-07-078-519.

Clark J. I., Guigné J. Y., 1988. Twenty-fifth anniversary special paper: Marine geotechnical engineering in Canada. Canadian Geotechnical Journal, 1988, 25(2): 179-198.

DeGroot, D. J., DeJong, J. T., Yafrate, N. J., Landon, M. M., Sheahan, T. C., 2007. Application of recent developments in terrestrial soft sediment characterization methods to offshore environments. Proc., Offshore Technology Conf., Houston, OTC 18737.

DeJong, J., DeGroot, D., Yafrate, N., 2012. Evaluation of undrained shear strength using full-flow penetrometers. J. Geotech. Geoenviron. Eng.138(6),765–767.

Einav, I., Randolph, M. F., 2005. Combining Upper Bound and Strain Path Methods for Evaluating Penetration Resistance. International Journal for Numerical Methods in Engineering, Vol. 63, No. 14, pp. 1991-2016.

Eltaher, A., 2014. Gaps in Knowledge and Analysis Technology of Ice Gouge Pipeline Interaction. Proceedings of the Arctic Technology Conference, February 10 - 12, 2014, 10p.

Hossain, MS, Randolph, MF, 2009. Effect of Strain Rate and Strain Softening on the Penetration Resistance of Spudcan Foundations on Clay. International Journal of Geomechanics, Vol 9, No 3, pp 122-132.

Konuk, I. & Gracie, R. 2004, "A 3-Dimensional Eulerian Finite Element Model for Ice Scour", Proceedings of the 5th International Pipeline Conference, October 4 - 8, 2004, pp. 1911-1918.

Lach, P.R. 1996, Centrifuge modelling of large soil deformation due to ice scour, Ph.D., Memorial University of Newfoundland (Canada).

Lele, S., Hamilton, J., Panico, M., Arslan, H., Minnaar, K., 2011. 3D continuum simulations to determine pipeline strain demand due to ice-gouge hazards. Arctic Technology Conference, ATC.

Lunne, T., Andersen, K. H., 2007. Soft clay shear strength parameters for deepwater geotechnical design. Proc., 6th Int. Offshore Site Investigation and Geotechnics Conf.: Confronting New Challenges and Sharing Knowledge, Vol. 1, Society for Underwater Technology, London, 151–176.

Miller, D. L. and Bruggers, D. E. (1980). Soil and Permafrost Conditions in the Alaskan Beaufort Sea, Offshore Technology Conference OTC 3887.

Nobahar, A., Kenny, S., Phillips, R., 2007b. Buried pipelines subject to subgouge deformations. International Journal of Geomechanics, vol. 7, no. 3, pp. 206-216.

NRC-PERD (2014), Ice-Seabed Gouging Database: Review & Analysis of Available Numerical Models (Babae, M.H. and Sudom, D. (2014)); Physical Simulations of Seabed Scouring by Ice: Review and Database (Barrette, P. and Sudom, D. (2014)).

Peek, R., Nobahar, A., 2012. Ice gouging over a buried pipeline: Superposition error of simple beam-and-spring models. International Journal of Geomechanics, vol. 12, no. 4, pp. 508-516.

Phillips, R., Barrett, J., 2012. PIRAM: Pipeline Response to Ice Gouging. Proceedings of the Arctic Technology Conference, December 3 - 5, 2012, 6p.

Pike, K., Kenny, S., 2016. Offshore pipelines and ice gouge geohazards: Comparative performance assessment of decoupled structural and coupled continuum models. Canadian Geotechnical Journal, 53(11), 1866-1881.

Winters, W. J. and Lee, H. J. (1984). Geotechnical properties of samples from borings obtained in the Chukchi Sea, Alaska. USGS Report 85-23.

Woodworth-Lynas, C., Nixon, D., Phillips, R., Palmer, A., 1996. Subgouge Deformations and the Security of Arctic Marine Pipelines. Proc. 28th OTC, Vol. 4, Paper No. 8222, pp. 657–664.

Chapter 2

Literature Review

2.1. Overview

Since the thesis is paper based, each chapter has its own literature review. However, a short literature review is provided in this chapter to facilitate reading through the thesis.

2.2. Literature review

2.2.1. Numerical modelling of ice gouging

Konuk and Gracie (2004) investigated the performance of ice gouging in soft and stiff clay using the ALE method offered by LS-Dyna Explicit FE software. In their 3D finite element model, the seabed soil was modelled using CAP plasticity constitutive model with inclusion of nonlinear kinematic hardening. Konuk and Gracie (2004) confirmed that the LS-Dyna CAP soil model was capable to handle the corner between the CAP and the failure surface in a consistent way allowing a continuous transition from hardening to failure. The undrained condition of soil was adopted. The authors reported that the horizontal soil displacement obtained from their FEA model, were lower than what C-CORE functions (Woodworth-Lynas et al., 1996) predicted.

Konuk and Fredj (2004b) investigated how the gouging performance and forces on the pipeline can be affected by the pipeline trench using the ALE finite element approach. In their model, pipe was fixed in its position and was defined as a rigid structure. The trench was filled with two types of soils in which the materials behaviour were defined to follow the Cap soil model. The results of soil deformation confirmed the significance of modeling trench in ice gouging process. Although the magnitudes of the resulted loads on the pipe

were in upper limit due to its condition but still were lower than what the structural Winkler model predicted. As it was expected, the more stiff the infill soil materials, the larger the resulted magnitude of the horizontal and vertical loads on the pipe. The authors recommended that the analysis of the unburied flexible pipe and more investigation about the material properties of the infilled soil could improve the design process.

Konuk et al. (2006) conducted the decoupled analysis of ice-soil-pipe interaction following the Winkler idealized beam-spring method and compared the results with the predicted ones from a continuum model. The subgouge soil deformation as an main input for the beam-spring model, obtained from a free-field analysis of ice gouging in clay with avearage undrained shear strength of 10 kPa and 50 kPa using the ALE method and also PRISE engineering equation. The load-displacement relationships was defined for the Winkler spring model and the response of the pipe was monitored. The authors pointed that there was some differences in the method of defining the clay soil properties for two kinds of analysis, coupled and decoupled. The authors concluded that the pipe responses was overstimated when the subgouge soil diformation attained from PRISE model. The authors noted that following decoupled analysis of ice-soil-pipe interaction and using Winkler beam spring model to estimate the pipe response, might cause selecting a deeper burial depth for pipe in design process in comparison to continuum model.

Kenny et al. (2007) conducted a 3D finite element model of ice gouging in clay using Arbitrary Lagrangian Eulerian (ALE) method with adaptive mesh technique provided by ABAQUS/Explicit. The clay soil was considered as a single-phase material (i.e. no pore water pressure) which was assumed under undrained condition of loading. Clay seabed was modeled as an elastic-perfectly plastic material obeying the von Mises criterion. The results

of their free-field ice gouging analysis were verified against the selected PRISE centrifuge test data and also the PRISE empirical function (Woodworth-Lynas et al., 1996). The result of subgouge soil deformation obtained from their numerical work was in general agreement with PRISE centrifuge test data for soil particles located in greater depth than one gouge depth from keel base. The PRISE engineering model provided conservative result compared to the test data.

Nobahar et al. (2007) studied the coupled analysis of ice-soil-pipe interaction and compared the outcome FE results with the decoupled analysis approach following the structural Winkler model. In their FE model, the pipe-soil contact was modeled following the Coulomb frictional model. The authors concluded that the quality of soil failure mechanism and the depth of development of the failure plastic wedges were significantly affected by ice attack angle and interaction properties of the contact areas. The results showed that undrained loading of the clay soil in various direction could result in soil failure in lower level of loads when compared with undrained loading in just single direction. The authors reported that the magnitude of stresses and strains experienced by the pipe were lower when compared with those estimated by the decoupled approach following the structural Winkler model. They noted that the predictions made by the structural approach were reasonably conservative.

Abdalla et al. (2009) conducted a 3D finite element model of ice gouging in cohesive soil using the Coupled Eulerian Lagrangian approach (CEL) offered by ABAQUS/Explicit. The Authors modelled the soft clay soil material in undrained condition using the modified Dracker-Prager/Cap constitutive model. In order to control the volume dilatancy of the soil under high plastic shear deformation and pressure, a Cap yield surface was added to the

linear Drucker-Prager. In case of validation, the free-field subgouge soil deformation result was compared to the selected PRISE centrifuge test data and the proposed PRISE empirical function (Woodworth-Lynas et al., 1996) and also the results of two other numerical works conducted by Konuk et al. (2005) and Kenny et al. (2007). Abdalla et al. (2009) confirmed that they made some reasonable assumptions for soil parameters due to lack of reported soil data. The subgouge soil deformation obtained from their study was in general agreement with the trends of the PRISE experimental results and the PRISE Engineering Model. The CEL results was also in good agreement with the numerical results predicted by Kenny et al. (2007) and Konuk et al. (2005) specifically for the shallow keel angle (15 degrees).

Sayed and Timco (2009) conducted 2D finit element analysis of ice gouging in sand following the Particle-In-Cell (PIC) advection method to handle such that large deformation problem and treated the soil as a viscous non-Newtonian fluid. It sould be noted that in their model, the rigid ice was allowed to have just vertical movements. Following the PIC approach, the soil material was modelled as discrete particles which were able to move during analysis. Strength behaviour of the soil under loading followed the rigid plastic Mohr Coulomb model. Displacement in sand was assumed to be occurred in critical state. The results of their model were in good agreement with the predictions of PRISE engineering equation. The results showed that by increasing the value of gouge depth and the angle of friction of the sand the mean normal stress was increased.

Eskandari et al., (2010) and (2011) simulated a free-field ice gouging process in sand following ALE approach offered by Abaqus/Explicit FEA software as part of the Pipeline Ice Risk Assessment and Mitigation, PIRAM, Joint Industry Project (JIP). The sand soil

strength behaviour under loading, was defined following the NorSand critical state constitutive soil model. The undrained condition of the soil was enforced following the volume constraint method. Ice keel was simulated as a rigid body. Although the capability of the model was approved when the results of their study compared to the relevant results of triaxial laboratory tests published by Jefferies and Been, 2006 but still further investigation need to be done in order to calibrate the model performance.

Phillips et al. (2010) modeled ice gouging in clay using three numerical techniques and compared the results with the PRISE centrifuge test data. The authors used the CEL and ALE methods of ABAQUS/Explicit and ALE method offered by LS-Dyna software to do finite element analysis of ice gouging. The soil was adopted to be in undrained condition and was modeled as an elastic-perfectly plastic material obeying von Mises failure criteria. The model predictions of three different finite element procedures were consistent. Although the results were in general agreement with PRISE test data and the proposed engineering model but the authors confirmed that the soil constitutive models need to be improved to account the effective stress behaviour within a single phase continuum including the shear induced dilatancy and drained versus undrained behaviour. They also suggested that using finer mesh might help to accurately capture the high strain gradients developed in soil particles located right under the moving keel. Phillips et al. (2010) pointed that due to the inability of the soil model to predict accurate clearing mechanism for soil in front called frontal mound, the ice gouge model never completely reached to the steady state condition.

Banneyake et al. (2011) conducted a series of 3D ice gouging simulations using CEL method of ABAQUS software. The normally consolidated clay soil was modeled using

von Mises material law. The authors confirmed that the clay under ice gouging as a fast enough loading process could be considered in undrained condition and there was no need to use an effective stress soil model such as Cam Clay. They suggested a pressure independent von Mises, Tresca or Mohr Coulomb plastic model with appropriate shear strain hardening could be selected. The authors reported that the result of horizontal subgouge soil deformation was compared to the relevant PRISE centrifuge test data and matched well with that but the results of vertical subgouge soil displacement showed some disagreement.

Lele et al. (2011) used ABAQUS CEL approach to analyse ice gouging process. The authors noted that seabed could not geometrically be modeled in real-field condition because the infinite elements are not available in the ABAQUS/Explicit CEL technique. The clay soil was modeled as an elastic-plastic material obeying von Mises failure criterion. Undrained condition was assumed for clay under ice gouging event. Their model underestimated the subgouge soil deformation when compared with the curve proposed by PRISE engineering model. The authors confirmed that this underestimation was due to possible conservatism and simplifying assumptions included in the PRISE engineering equations. Lele et al. (2011) mentioned that their model need to be validated against a real large scale field test data before going to be used in design.

Pike et al. (2011) conducted finite element analysis of free-field ice gouging in clay soil using the Coupled Eulerian Lagrangian (CEL) approach within ABAQUS/Explicit. Strength behaviour of clay soil was defined following the simple elasto-plastic von Mises plasticity theory. Soil under gouging was assumed to remain in undrained condition. The results of horizontal subgouge soil deformation compared favourably with the relevant

PRISE centrifuge test data. The author confirmed that there was a divergence in shallower depth which was probably due to inability of the von Mises criteria to accurate simulating failure and clearing mechanism (e.g. tension cracking and adhesion release) of soil in front and two sides of gouge. The vertical subgouge deformation showed disagreement in results. The authors confirmed that the disagreement might be due to the experimental errors came up from the inspection of the instruments used to measure the displacements (Lach, 1996). They also mentioned that PRISE engineering equation might originate residual errors due to not incorporating the effect of ice keel geometry, keel attack angle and soil strength characteristics in the proposed equation. Pike et al. (2011) concluded that further investigation have to be carried out to resolve such the discrepancy in results of subgouge deformation when compared to test data.

El-Gebaly et al. (2012) used ABAQUS/Explicit CEL to model ice gouging in soft clay. In order to define the clay soil behaviour under gouging process, they used an elastic-perfectly plastic constitutive model for the baseline analyses and added the Mohr Coulomb model with softening for the soil model sensitivity analysis. Their baseline model predicted smaller horizontal and vertical reaction forces when the results of the free-field analysis were compared to PRISE test data. Smaller horizontal subgouge soil deformation in shallow depth was predicted when the soil was modeled following Mohr Coulomb criteria with softening behaviour compared to ones predicted by baseline model. The authors concluded that post-yield soil behaviour could be more accurately captured by Mohr Coulomb constitutive model with softening compared with simple elastic-perfectly plastic model. El-Gebaly et al. (2012) also noted the inability of recently used numerical methods

to predict accurate failure and clearing mechanism under gouging (e.g. developed frontal mound with larger height and side berms with almost vertical outside angles).

Eskandari et al. (2012) discussed more about the results of their developed numerical model such as subgouge soil deformation, keel reaction forces, quality of soil formation and the soil failure mechanism. The authors concluded that the greater the gouge depth and the more the relative density of the sand, the more effective the role of critical stress ratio. They noted that combination of a state parameter and critical stress ratio can significantly affect the results of subgouge soil deformation compared with when they considered just the effect of critical stress ratio. The authors also proposed an equation to estimate the horizontal reaction forces.

Panico et al. (2012) simulated ice gouging in sand in order to investigate the effect of sand frictional properties on gouging performance. According to the defined soil model, the friction of the sand was assumed to be constant and varying. The results showed that the critical state behaviour of the sand could significantly have effect on the response rather than the effect of the peak friction angle of the sand. Although there were some uncertainties associated with test preparation, their continuum model's capability in predicting the keel reaction forces was reasonably approved when the results compared to the relevant centrifuge tests. Also the capability of their continuum model predicting the pipe strain demand was approved when the results compared to both test data and the results of decoupled analysis, idealized beam-spring model. As it was expected, the beam-spring model overstimated the pipe strains, so the authors noted that their model could reliably improve the cost effectiveness of the results.

Peek and Nobahar (2012) carried out coupled and decoupled analysis of ice-soil-pipe interaction following the ALE method offered in Abaqus/Explicit and Winkler beam-spring model respectively. The authors investigated the pipeline response under those two different approches, coupled and decoupled. They concluded that getting the subgouge soil deformation as a result of a continuum model and applying that as the soil displacement for Winkler model could produce superposition errors. The authors noted that the effectiveness of such this superposition errors on the results is more than that the other directional load decoupling error originated from directional coupling of Winkler springs in axial, lateral, and vertical directions.

Pike and Kenny (2012) conducted 3D finite element analysis of ice gouging in clay following the CEL formulation available in ABAQUS/Explicit. They developed a prototype numerical model of Test 5 of centrifuge ice gouging tests conducted by Lach (1996). The clay soil was modeled as an elastic-perfect plastic material obeying von Mises criteria. The authors mentioned that heavily reworked soils can be expected to be in the critical state, which has no tendency to dilate and that's why it is reasonable to idealized cohesive soils as perfectly-plastic non-dilate materials (Palmer et al. 1990). In their model the undrained elastic modulus of soil was varied through soil depth as a function of OCR profile, undrained shear strength profile and soil plasticity index based on the formulation proposed by Mayne (2007). Numerical prediction of the horizontal subgouge soil deformation showed good agreement when compared to Lach (1996) test data. The results sowed disagreement when compared with the PRISE engineering model data in shallow depth. The authors mentioned that the resulted disagreement might be related to this fact

that the element formulation with constant strain through each element was not able to accurate capture the sharp strain gradients.

Rossiter (2012) investigated the validity of the current finite element approaches, ABAQUS ALE and CEL formulation, to simulate keel-soil interaction under gouging process in clay. The author concluded that the CEL approach might not be able to properly account for the defined shear stress limit at the contact interface. In their CEL model, lower value of shear stress was developed in the keel-soil contact interface compared to the maximum value which was defined as the shear stress limit. The author mentioned that this inability led to develop greater clearing and subduction of the soil and incorrect prediction of the keel reaction forces. The results of horizontal subgouge soil deformation in shallow depths obtained from the free-field analysis using ALE method did not match well with the relevant Lach (1996) test data. The authors suggested that stiffer soil parameters might be required to be defined for clay soil in shallow depths.

Peek et al. (2013) calibrated their numerical work by conducting large scale ice gouging physical tests in clay. They used CEL approach provided by ABAQUS software to perform 3D finite element analysis of ice gouging. In their model ice keel was free to move up or down or rotate during gouging and was not constraint to just displace horizontally as what is most popular in the current ice gouge simulation. The total stress response of the clay under gouging was predicted by using an elastic-perfect plastic material obeying the von Mises failure criteria with isotropic strain hardening and the strength curve obtained from unconfined compression tests. The tension capacity was considered as well as the compression capacity for soil under shearing. Although it was concluded before by the author researcher (Rice, 1975) that the loss of tension capacity might happen when yielding

under tension due to the strain localization with local drainage in saturated material. The author reported some discrepancies in the predicted pulling force when compared to the related test results which was due to neglecting the strain rate effect in the soil behaviour. The soil model was not able to simulate the disintegration of the clay soil particles collected in both sides of ice keel called side berms so the berms were predicted too high and without any tendency to collapse and flow around the keel. Peek et al. (2013) pointed the reason that the cracking and air entrainment might prevent the development of tensile strength by pore water suction.

Fadaifard and Tassoulas (2014) conducted 2D finite element analysis of ice gouging in clay using ALE approach offered by a computational-fluid-dynamics (CFD) software. The authors modeled soil as a strain-rate dependent fluid following the Herschel-Bulkley model in order to reproduce the viscous non-Newtonian behaviour of the soil. They calibrated their numerical work against the Lach (1996) centrifuge test data. Although the analysis never reached to the steady state condition but the results of horizontal subgouge soil deformation was overall in good agreement with the test data. The authors confirmed that the results of reaction forces was also in excellent agreement with the test data while their model was unable to develop the clearing mechanism due to the 2D dimensional approach. Fadaifard and Tassoulas (2014) reported that it was seen a continuous increase of frontal mound during ice gouging analysis due to lack of a clearing mechanism for soil in front.

Liferov et al. (2014) conducted 3D finite element analysis of ice gouging in clay using CEL approach of ABAQUS/Explicit. The soil behaviour under gouging was simulated following the Drucker-Prager/Cap model. To find the properties of the generic cap data, position of the initial Cap was determined. As what was common in the previous

researches, hardening with an exponential function was assumed. The associated flow rule followed by the soil model in ABAQUS/Explicit causes the plastic shear deformation to be dilatant. When the soil volume is increased, consequently the density will reduce and the stable time increment will be decreased. This problem was major for the soil particles located on the top surface which were experienced large deformation and low pressure. The author mentioned that by lowering the cap the dilatants flow could be avoided. The authors also mentioned that due to the low velocity of ice, the mass effects were not significant. Although the CEL approach does not allow to mass scaling be used for soil as the Eulerian material. Their results confirmed that steeper the keel attack angle resulted in smaller subgouge soil deformation.

Nematzadeh and Shiri (2019) conducted 3D numerical analysis of ice gouging in dense Sand using CEL method offered by Abaqus/Explicit. In their model ice was considered as a rigid body and pipe was not included in the model. The authors developed a modified Mohr Coulomb soil model (MMC) in order to account the shear strength of the dense sand for the non-linear peak hardening and post-peak softening which is not included in the convensional Mohr Coulomb model. The capability of their model was approved when the results compared with the ones from the relevant experimental and numerical studies. The authors concluded that by incorporating the non-linear stress-strain behaviour of dense sand in the model, the results of subgouge soil deformation were estimated smaller values in comparison with those from the classical Mohr Coulomb model.

In recent years, the machine learning (ML) application has witnessed significant growth in multifarious areas because the ML advancement is adequately accurate, fast, confident, and inexpensive to simulate different non-linear and linear problems.

Kioka et al. (2003) and (2004) hybrid the neural network (NN) method with a mechanical approach to approximate the sub-gauge soil depth. The bottom shape of the ridge and the ice condition surrounding the ridge was detected as the most significant parameters affecting an ice-scouring problem. The NN demonstrated a high degree of precision and the authors claimed that this methodology was able to use instead the nonlinear multiple-regression approaches.

Azimi and Shiri (2020a) applied gene expression programming (GEP) for the simulation of the horizontal sub-gauge soil deformations in the sand. The authors estimated the horizontal deformations using the bearing pressure, the maximum vertical extent of sub-gouge deformation, the attack angle, dilation index, and soil depth. By performing different analyses, the soil depth and the dilation index were recognized as the most important input parameter to model the horizontal deformations.

Azimi and Shiri (2020b) introduced the parameters governing the iceberg-seabed interaction process by means of Buckingham's theorem. They developed some linear regression (LR) models to estimate the maximum horizontal and vertical sub-gouge soil displacements in sand and clay seabed. The study concluded that the LR model had better performance compared to the empirical models to estimate the ice-induced deformations in the sandy seabed.

Azimi and Shiri (2021a) modeled the ice-scoured soil deformations in the sand by the extreme learning machine (ELM). Nine ELM models were defined utilizing the parameters

affecting the ice-seabed interaction mechanism. The optimal number of neurons within the hidden layer and the best activation function has opted for the ELM algorithm. The author provided two ELM-based equations for calculating the horizontal and vertical displacements.

Azimi and Shiri (2021b) employed the Multiplayer Perceptron Neural Network (MLPNN) for the simulation of the horizontal sub-gouge soil deformations in the sand. Six neurons were embedded in the hidden neurons and the sigmoid activation function was selected for the MLPNN. The investigation highlighted that the MLPNN algorithm predicted the large displacements with higher accuracy although a few discrepancies were reported for the small deformations.

The ice-induced soil displacements and the reaction forces in the sand were simulated using a self-adaptive evolutionary extreme learning machine (SaE-ELM) algorithm by Azimi and Shiri (2021c). Regarding the input parameters, seventeen SaE-ELM models were developed to estimate both the deformations and forces. The conducted sensitivity analysis indicated that the soil depth and berm height were the most effective input factors. A set of SaE-ELM-based matrices were suggested to calculate the sub-gouge soil characteristics.

Azimi et al. (2021) modeled the ice-seabed interaction process in clay through a non-tuned machine learning algorithm entitled self-adaptive extreme learning machine (SAELM). In this study, 70% of the dataset was allocated for the training of the SAELM algorithm, while 30% of the remaining was utilized for the testing of these models. The best SAELM model showed an overestimated and underestimated performance to model the reaction forces and deformations, respectively.

Azimi and Shiri (2021d) applied the ELM algorithm to model the sub-gouge soil displacements in clay seabed and the ice keel-seabed reaction forces. The ELM algorithm was able to estimate the ice-scoured features with a good performance, meaning that almost 2% of the simulation results had an error of less than 10%. The authors concluded that the vertical component of load and the attack angle possessed the highest degree of effectiveness to forecast the reaction forces.

Azimi et al. (2022a) evaluated the capability of the generalized structure of the group method of data handling (GS-GMDH) in the estimation of the horizontal and vertical sub-gauge soil deformations in clay. The comparison between the GS-GMDH, the group method of data handling (GMDH), artificial neural network (ANN), and empirical models proved that the GS-GMDH had better performance.

Azimi et al. (2022b) employed three machine learning algorithms including the decision tree regression (DTR), random forest regression (RFR), and extra tree regression (ETR) to model the ice-scoured deformations in the sandy seabed. The simulation revealed that the ETR model had the highest level of precision and correlation along with the lowest level of complexity.

2.2.2. Progress in physical modelling

Lach (1996) performed centrifuge tests of ice gouging in clay on the beam centrifuge at the University of Cambridge Geotechnical Centrifuge Centre in Cambridge, England. The tests were carried out at a nominal acceleration level of 100 g. The author mentioned that the ice gouging model was regarded as an approximation to the case of a dynamic event in an impermeable soil. The velocity of ice keel during gouging, approximately 0.1 m/s, was considered fast enough for undrained condition of clay to prevail. A series of nine tests

with different conditions of clay soil and ice keel were performed. Reconstituted saturated Speswhite kaolin clay was selected as the soil type for the tests. The stress history of the soil was prescribed to establish the stress state and conditions of clay seabed in Beaufort Sea regions well known for ice gouging. The clay samples were uniformly consolidated in the laboratory from slurry. The undrained shear strength profile of the clay specimen was estimated by performing an in-flight vane shear test. The surface level of the clay soil strata was in overconsolidated state and with an undrained shear strength measured between 10 to 25 KPa. Subgouge soil deformation were evaluated by placing grids constructed of easily deformable materials both parallel and perpendicular to the gouging axis. As the main results the horizontal and vertical reaction forces and subgouge soil deformations were reported for every single test.

Woodworth-Lynas et al. (1996) conducted a series of 20 centrifuge tests modeling of ice gouging with scales of 75 g and 150 g in silty clay, sand, sand over clay and clay over sand soil strata under the Phase 3a of the Pressure Ridge Ice Scour Experiments (PRISE), a jointly-funded, international, multi-phase program. The soils were selected to approximate the real seabed in the offshore gouged areas including the Canadian and U.S. Beaufort Sea, and the Russian Arctic, especially offshore Sakhalin Island. The effects of soil type, soil condition, attack angle, gouge depth and gouge width on the gouging performance were assessed. Spaghetti marker were placed within the soil sample in order to capture the subgouge displacement during gouging. In order to measure the undrained shear strength of the soil samples, an in-flight con penetrometer test was conducted between the gouge events and a Torvane and/or handvane tests were conducted to estimate the post-test surface shear strength of the clay sample. Based on the test results, test keel horizontal

reaction force increased by increasing the gouge depth and gouge width and decreased by increasing the keel attack angle. As expected, keel horizontal reaction force increased by increasing the undrained shear strength of the clay soil. The authors pointed that the results of ice gouging from the layered seabed could be very useful in pipelines design process but more centrifuge tests have to done due to complexity of the problem.

Allersma and Schoonbeek (2005) carried out some ice gouging centrifuge tests in clay in the geotechnical centrifuge of University of Delft. They studied the effects of different parameters such as, test scale, gouging speed, keel angle, roughness of the keel surface, gouge depth, undrained shear strength of the soil, remoulded layer, multiple gouging event and gouging in layered soft over stiff clay, on the performance of ice gouging. Image processing technique and in placed grids were utilized in order to effectively capture the subgouge soil deformation. The tests were performed in 100 g scale. The undrained shear strength of each clay soil sample was measured with the in situ vane shear test in different depth in order to make sure the soil sample is homogeneous. The authors concluded that the resulted soil deformation was more sensitive for the change in rate of displacement, keel angle, surface roughness and specially the undrained shear strength of the clay sample.

References

Azimi, H., & Shiri, H. (2020a). Ice-Seabed interaction analysis in sand using a gene expression programming-based approach. Applied Ocean Research, 98, 102120.

Azimi, H., & Shiri, H. (2020b). Dimensionless groups of parameters governing the ice-seabed interaction process. Journal of Offshore Mechanics and Arctic Engineering, 142(5), 051601.

Azimi, H., & Shiri, H. (2021a). Sensitivity analysis of parameters influencing the ice–seabed interaction in sand by using extreme learning machine. Natural Hazards, 106(3), 2307-2335.

Azimi, H., & Shiri, H. (2021b). Modeling subgouge sand deformations by using multi-layer perceptron neural network. In The 31st International Ocean and Polar Engineering Conference. OnePetro.

Azimi, H., & Shiri, H. (2021c). Evaluation of ice-seabed interaction mechanism in sand by using self-adaptive evolutionary extreme learning machine. Ocean Engineering, 239, 109795.

Azimi, H., Shiri, H., & Malta, E. R. (2021). A non-tuned machine learning method to simulate ice-seabed interaction process in clay. Journal of Pipeline Science and Engineering.

Azimi, H., & Shiri, H. (2021d). Assessment of Ice-Seabed Interaction Process in Clay Using Extreme Learning Machine. International Journal of Offshore and Polar Engineering, 31(04), 411-420.

Azimi, H., Shiri, H., & Zendehboudi, S. (2022a). Ice-seabed interaction modeling in clay by using evolutionary design of generalized group method of data handling. Cold Regions Science and Technology, 193, 103426.

Azimi, H., Shiri, H., & Mahdianpari, M. (2022b). Simulation of Subgouge Sand Deformations Using Robust Machine Learning Algorithms. In Offshore Technology Conference. OnePetro.

Abdalla, B., Pike, K., Eltaher, A., Jukes, P. & Duron, B. 2009, "Development and Validation of a Coupled Eulerian Lagrangian Finite Element Ice Scour Model", *Proceedings of the 28th International Conference on Ocean, Offshore and Arctic Engineering (ISOPE)*, May 31 – June 5, 2009, 6p.

Banneyake, R., Hossain, M. K., Eltaher, A., Nguyen, T., Jukes, P., 2011. Ice-soil pipeline interactions using coupled eulerian-lagrangian (CEL) ice gouge simulations extracts from ice pipe JIP. Paper presented at the OTC Arctic Technology Conference.

El-Gebaly, S., Paulin, M., Lanan, G. & Cooper, P. 2012, "Ice gouge interaction with buried pipelines assessment using advanced coupled eulerian lagrangian", *Proceedings of the Arctic Technology Conference,* December 3 - 5, 2012, 12p.

Eskandari, F., Phillips, R., and Hawlader, B. (2010). A State Parameter Modified Drucker–Prager Cap Model. Canadian Geotechnical Conference.

Eskandari, Farzad, Ryan Phillips, and Bipul Hawlader.(2011) Ice Gouging Analysis Using NorSand Critical State Soil Model. 2011 Pan–Am CGS Geotechnical Conference, paper# 995.

Eskandari, F., Phillips, R., and Hawlader, B. (2012) Finite Element Analyses of Seabed Response to Ice Keel Gouging, Proc. 65th Canadian Geotechnical Conference Winnipeg, Manitoba, 2012.

Fadaifard, H., Tassoulas, J.L., 2014. Numerical modeling of coupled seabed scour and pipe interaction. Int. J. Solids Struct. 51 (19–20), 3449–3460.

Kenny, S., Barrett, J., Phillips, R. & Popescu, R. 2007, "Integrating geohazard demand and structural capacity modelling within a probabilistic design framework for offshore arctic pipelines", *17th International Offshore and Polar Engineering Conference*, July 1 - 6, 2007, pp. 3057-3064.

Konuk, I., Yu, S. & Fredj, A. 2006, "Do winkler models work: A case study for ICE scour problem", Proceedings of OMAE06 25th International Conference on Offshore Mechanics and Arctic Engineering, June 4 - 9, 2006, 7p.

Konuk, I., Yu, S. & Gracie, S. 2005, "An ALE FEM Model of Ice Scour", *11th International Conference of the International Association of Computer Methods and Advances in Geomechanics*., June 19 – 21, 2005, 8p.

Konuk, I.S., Fredj, A. (2004b). A FEM model for pipeline analysis of ice scour. Proc., OMAE, OMAE2004–51477.

Konuk, IS., Gracie, R., 2004. A 3-dimensional Eulerian FE model for ice scour. IPC04-0075, pp.1911-1918.

Kioka, S. D., Kubouchi, A., & Saeki, H. (2003). Training and generalization of experimental values of ice scour event by a neural-network. In The Thirteenth International Offshore and Polar Engineering Conference. OnePetro.

Kioka, S., Kubouchi, A., Ishikawa, R., & Saeki, H. (2004). Application of the mechanical model for ice scour to a field site and simulation method of scour depths. In The Fourteenth International Offshore and Polar Engineering Conference. OnePetro.

Lach, P.R. 1996, Centrifuge modelling of large soil deformation due to ice scour, Ph.D., Memorial University of Newfoundland (Canada).

Lele, S., Hamilton, J., Panico, M., Arslan, H., Minnaar, K., 2011. 3D continuum simulations to determine pipeline strain demand due to ice-gouge hazards. Arctic Technology Conference, ATC.

Liferov, P., Nes, H., Asklund, J., Shkhinek, K. & Jilenkov, A. 2014, "Ice Gouging and its Effect on Pipelines", *Proceedings of the Arctic Technology Conference*, February 10 - 12, 2014, 15p.

Mayne, P.W. 2007, *Cone Penetration Testing State-of-Practice: Final Report*. Available: http://geosystems.ce.gatech.edu/Faculty/Mayne/papers/NCHRP%20CPT%20Synthesis%20(2007)%20color.pdf

Nematzadeh, A. Shiri, H., 2019. The influence of non-linear stress-strain behavior of dense sand on seabed response to ice gouging, Cold Regions Science and Technology, Vol. 170, No. 102929, ISSN 0165-232X, Oct. 2019.

Nobahar, A., Kenny, S., and Phillips, R. (2007). Buried Pipelines Subject To Sub–Gouge Deformations. ASCE International Journal of Geomechanics GM/2005/000235, Vol. 7, No. 3, pp.206–216.Palmer, A.C., Konuk, I., Comfort, G., and Been, K. (1990). Ice gouging and the safety of marine pipelines. Proc., OTC, 3, OTC 6371, pp.235-244.

Panico, M., Lele, S. P., Hamilton, J. M., Arslan, H., and Cheng, W. (2012). Advanced Ice Gouging Continuum Models: Comparison With Centrifuge Test Results. International Society of Offshore and Polar Engineers.

Phillips, R., Barrett, J.A. & Al-Showaiter, A. 2010, "Ice keel-seabed interaction: Numerical modelling validation", *Proceedings of the Offshore Technology Conference*, May 3 - 6, 2010, 13p.

Peek, R., Been, K., Bouwman, V., Nobahar, A., Sancio, R. & Van Schalkwijk, R. 2013, "Buried pipeline response to ice gouging on a clay seabed large scale tests and finite element analysis", *22nd International Conference on Port and Ocean Engineering under Arctic Conditions (POAC)*, June 9 - 13, 2013, 10p.

Peek, R., Nobahar, A., (2012). Ice Gouging over a Buried Pipeline: Superposition Error of Simple Beam–And–Spring Models. Int. J. Geomech. 12 (4), 508–516.

Pike, K.P. & Kenny, S.P. 2012, "Advanced continuum modeling of the ice gouge process: Assessment of keel shape effect and geotechnical data", *22nd International Offshore and Polar Engineering Conference,* Rhodes, Greece, June 17 – 22, 2012, pp. 1287-1292.

Pike, K., Kenny, S. & Hawlader, B. 2011, "Advanced Numerical Simulations of Ice Gouge Events and Implications for Engineering Design", *International Conference on Port and Ocean Engineering Under Arctic Conditions (POAC)*, July 10 - 14, 2011, 10p.

Rice, J.R., (1975), "On the Stability of Dilatant Hardening for Saturated Rock Masses," Journal of Geophysical Research, Vol. 80, No. 11, pp. 1531-1536, April 10, 1975.

Rossiter, C. 2012, Assessment of Ice keel/Soil and Pipeline/Soil Interactions: Continum Modelling in Clay, Ph.D., Memorial University of Newfoundland (Canada).

Sayed, M. and Timco, G., (2009). A Numerical Model of Iceberg Scour. Cold Regions Sci. Tech., 55(1):103–110.

Woodworth-Lynas, C., Nixon, D., Phillips, R., Palmer, A., 1996. Subgouge Deformations and the Security of Arctic Marine Pipelines. Proc. 28th OTC, Vol. 4, Paper No. 8222, pp. 657–664.

Chapter 3

Numerical Modeling of Ice-seabed Interaction in Clay by Incorporation of the Strain Rate and Strain-Softening Effects

Seyedhossein Hashemi, as the main author, is credited for the methodology, modeling, data curation, visualization, investigation, validation and writing-original draft. Hodjat Shiri is credited for conceptualization, supervision, writing-review and editing and funding acquisition

This chapter was published as a paper in Journal of Offshore Mechanics and Arctic Engineering (ASME).

.

Abstract

Ice gouging is one of the main threats to the safety of the subsea pipelines buried in Arctic coastal regions. Determining the best pipeline burial depth relies on free-field ice gouging analysis and obtaining the resultant subgouge soil deformations. Therefore, improving the accuracy and efficiency of the free-field ice gouging analysis is a key demand in daily engineering practice. The pressure-induced by ice keel through the ice gouging process causes the seabed soil to undergo large localized plastic deformation, where the classical Lagrangian method confronts mesh instability challenges. Also, the conventional Mohr-Coulomb soil model is not able to account for the strain rate dependency and strain softening effects which are significant in ice gouging event. In this study, free-field ice gouging in clay was simulated using a Coupled Eulerian-Lagrangian approach. The strain rate dependency and strain-softening effects were incorporated by developing a user-defined subroutine and incremental updating of the undrained shear strength in ABAQUS. The comparison of the model predictions with published numerical and experimental studies showed a significant improvement of accuracy. A comprehensive parametric study was also conducted to investigate the effect of various model parameters on the seabed response to ice gouging.

Keywords: Ice gouging, Subgouge soil deformation, Soft clay, Numerical simulation, Strain rate and strain-softening effects

3.1. Introduction

Ice gouging is a significant threat to the structural integrity of the Arctic offshore pipelines. Pipelines are usually buried in trenches sufficiently deep for physical protection against the large subgouge soil deformation (see Figure 3-1). Soft cohesive seabed material is broadly observed in Canadian offshore territories (e.g., Beaufort Sea (Clark and Guigné, 1988), Grand Bank (Clark and Landva, 1988), etc.) and elsewhere in the Arctic Circle (e.g., Chukchi Sea (Winters and Lee, 1984)), where the ice gouge incidents are regularly recorded.

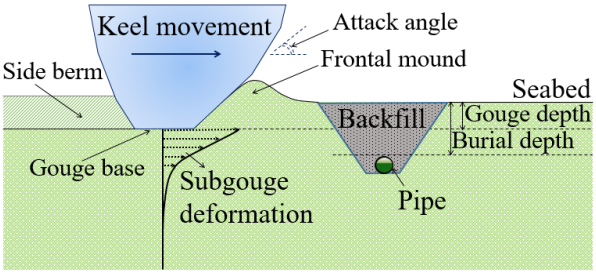

Figure 3-1. The main components in an ice gouging process

Determining the minimum trench depth as a compromise between the project cost and safety indexes is a challenging design aspect. The ice-seabed interaction problem has been widely investigated in the literature through numerical (e.g., Pike and Kenny, 2012; Babaei and Sudom, 2014; Liferov et al., 2007; Eskandari et al., 2012; Rossiter and Kenny, 2012b; Phillips and Barrett, 2011; Phillips et al., 2010; Abdalla et al., 2009; Sayed and Timco, 2009; Konuk et al., 2007; Kenny et al., 2007; Kenny et al., 2005; Konuk and Gracie, 2004; Yang and Poorooshasb, 1997) and experimental (e.g., Allersma and Schoonbeek, 2005; Phillips et al., 2005; Barrette and Sudom, 2012) studies or both (e.g., Panico et al., 2012; Yang et al., 1996; Lach, 1996). Many of these studies have considered granular seabed material using standard MC, Drucker-Prager Cap and Nor-Sand constitutive soil models

(e.g., Liferov et al., 2007; Eskandari et al., 2007; Phillips and Barrett, 2011; Phillips et al., 2010; Sayed and Timco, 2009; Yang and Poorooshasb, 1997). The cohesive seabed material is less explored in ice gouging studies using conventional soil models that are usually used for modelling the cohesive material such as elasto-plastic obeying Tresca or von-Mises criterion, MC, Cam-Clay, CAP model (e.g., Pike and Kenny, 2012; Liferov et al., 2007; Rossiter and Kenny, 2012b; Abdalla et al., 2009; Konuk et al., 2007; Kenny et al., 2007; Kenny et al., 2005; Konuk and Gracie, 2004; Yang et al., 1996; Lach, 1996). In practice, a decoupled approach is undertaken to assess the ice gouging impact on buried pipelines, where a free-field ice gouging analysis (no pipe, no trench) is conducted using a continuum finite element analysis (FEA) to obtain the subgouge soil deformations. Then the soil displacements are transfer to a beam-spring pipeline model to assess the pipeline response to the ice attack (Woodworth-Lynas et al., 1996; Phillips and Barrett, 2012). Although, this approach suffers from two limitations in accounting for the realistic continuum soil behaviour, i.e., i) superposition errors (e.g., Kenny et al., 2000; Peek and Nobahar, 2012; Pike and Kenny, 2016), and ii) idealization of the directional load decoupling (e.g., Pike and Kenny, 2012; Nyman; 1984; Phillips et al., 2004a; Rossiter and Kenny, 2012b; Daiyan, 2013; Kenny and Jukes, 2015) resulting in a reduced axial soil resistance that allows for greater axial pipe feed-in (e.g., 15%, Pike and Kenny, 2016), the methodology is still an attractive solution in the Arctic pipeline industry due to the simplicity and acceptably conservative predictions. The built-in classical Mohr-Coulomb (MC) soil model is usually used with as a simple and fast approach in commercial software like ABAQUS to simulate the ice gouging event in clay. However, the MC model is not able to simulate the strain-rate dependency and strain-softening effects, both of which may

have a significant impact on the resultant subgouge soil deformations. By increasing the shear strain rate, the undrained shear strength is increased (e.g., Biscontin and Pestana, 2001; DeGroot et al., 2007; Lunne and Andersen, 2007; DeJong et al., 2012). On the other hand, large shear strains that occurred in the subgogue soil deformations cause a gradual loss of shear strength in a strain-softening episode (Hossain and Randolph, 2009). These aspects of plastic material response that affects the failure mechanisms, the mobilized soil resistance, and the resultant subgogue soil deformations have not been simultaneously considered in earlier ice gouging studies in the literature.

In this study, the accuracy of the free-field ice gouging analysis in clay as a crucial element of decoupled approach was improved by incorporation of the strain rate dependency and strain softening effects. This, in turn, can significantly benefit the assessment of the safe burial depth in beam-spring models that can significantly relocate the project budget borders.

For this purpose, a numerical ice gouge model was developed by the incorporation of both strain-softening and strain rate-dependency. ABAQUS/Explicit was used through a Coupled Eulerian-Lagrangian (CEL) LDFE analysis (Abaqus 2020). Using the solution proposed by Einav and Randolph (2005), a user subroutine (i.e., VUSDFLD) was coded to progressively update the undrained shear strength by the incremental values of accumulated absolute plastic shear strain and the calculated maximum shear strain rate. The performance of the model was compared with the results of a published centrifuge tests (Lach, 1996) and a numerical study (i.e., Fadaifard and Tassoulas, 2014). The developed model significantly improved the prediction of subgouge soil deformation and keel reactions compared with earlier studies (e.g., Fadaifard and Tassoulas, 2014). A

comprehensive parametric study was conducted to examine the effects of different ice features and soil model parameters on the resultant subgouge soil deformation, keel reaction forces, and soil heave formation in front and sides of the ice keel. The developed model was found to be a simple but robust tool that can be used in the daily engineering practice of Arctic pipeline design against ice gouging.

3.2. Numerical model

Owing to the recent advancements in computational capacities, large deformation analyses are conducted by using powerful techniques such as Coupled Eulerian-Lagrangian (CEL) and Arbitrary Lagrangian-Eulerian (ALE) analysis. These frameworks allow the Eulerian (soil) and Lagrangian (ice) domains to interact properly and flows the soil through the fixed mesh without mesh distortion and instability problems. The CEL and ALE techniques have been successfully employed in the literature for pipe and ice-seabed interaction analysis through large deformations (Phillips et al., 2010; Konuk and Gracie, 2004; Nematzadeh and Shiri, 2019). The Arbitrary Lagrangian-Eulerian (ALE) method has resolved some of the limitations of the conventional Lagrangian method, but the methodology still applies a limited allowable mesh distortion (Banneyake, 2011).

In this study, to simulate the free-field ice gouging in clay, a Coupled Eulerian-Lagrangian (CEL) model was developed using ABAQUS/Explicit and a VUSDFLD subroutine was coded to incorporate the strain rate dependency and strain-softening effects.

3.2.1. Constitutive soil model

The seabed scour by icebergs is a rapid process resulting in the seabed being loaded in an undrained condition where continued shear deformation of the seabed takes place without any change in void ratio or any increase in pore-water pressure (Lach, 1996; Palmer, 1997).

The undrained shear strength of soils is dependent on the strain rate past a critical strain rate value, sometimes referred to as the threshold strain rate (Díaz-Rodríguez et al., 2009). Past the threshold strain rate, a 5–20% increase in the strength for each order of magnitude increase in the strain rate is observed (see e.g. Vaid et al., 1979; Casacrande and Wilson, 1951; Lehane et al., 2009). The conventional soil models (e.g., elasto-plastic obeying Tresca or von-Mises criterion, MC, Cam-Clay, CAP) that are used for clay do not simultaneously account for the effects of strain rate and strain softening on the undrained shear strength (s_u) that are important in the ice gouging as a large deformation problem. The shear strength of clays is strain-rate dependent, typically increasing by 5%–20% for each order of magnitude increase in shear strain rate (Casacrande and Wilson, 1951; Graham et al., 1983). This can be significant in ice gouging events, where high-velocity gradients exist in particular shear zones underneath, in front, and sides of moving ice keel (Pike and Kenny, 2006; Schoonbeek and Allersma, 2006; Pike et al., 2011) The significance of considering strain rate dependency and strain softening effect has been proven in the literature through a wide range studies particularly in partially buried pipelines (e.g., Chatterjee et al., 2012a; Chatterjee et al., 2012b; Dutta et al., 2015; Ghorai and Chatterjee, 2017; Wang et al., 2010a; Zhou and Randolph, 2007; Zhou and Randolph, 2009a). However, the affected rate of plastic work in the shear zones formed in ice gouging process that results in strain-softening through the shear bands and also increasing the strength with strain rate has not been collectively accounted for in earlier ice gouging studies. Sayed and Timco (2009) conducted a numerical study on the iceberg seabed scour by employing a Particle-In-Cell (PIC) advection scheme, which is suited for modeling large displacements and discontinuities. The authors obtained the failure zones and the shear

layers (similar to the slip planes which are considered in plastic limit analyses, e.g. Schoonbeek et al., (2006)) by using a Mohr–Coulomb yield criterion, and a pressure-solids volume fraction relationship proposed by Johnson and Jackson (1987) allowing for strain-rate dependant plastic deformation of soil. Fadaeifard and Tassoulas (2014) incorporated a simple constitutive model for clay into an iceberg-seabed interaction analysis using an arbitrary Lagrangian-Eulerian (ALE) approach. The authors used a rheological simulation for the seabed by defining a simple viscous non-Newtonian model dependant solely on the strain rate of the soil. The model predicted the yielding of soil localized around the ice ridge with a good prediction of subgouge soil displacements in deeper areas down the ridge. However, for the shallow depths right underneath the ice keel, where the highest velocity gradient and shearing zones are created, the model prediction did not properly match the published experimental studies (Lach, 1996).

In this study, the seabed soil was modelled as an elastic-perfectly plastic clay obeying the Tresca criterion. The soil properties were adapted from the experimental study conducted by Lach (1996). The undrained conditions were satisfied by taking the highest possible Poisson's ratio (ν) of 0.499 to minimize the volumetric strains without any concerns about numerical instabilities. The friction and dilation angles were set to zero. The variation of undrained shear strength and elastic modulus with soil depth was modeled by using a dummy temperature field (i.e. pseudo-depth), where the temperature was initially distributed through the depth (from 0 to 18, maximum soil depth). Then, the soil located at any given depth (Z) was assigned by the dummy temperature equal to Z. Using temperature as a dummy variable is a versatile modelling approach that has been widely used in the literature (e.g., Nematzadeh and Shiri, 2019; Pike et al., 2011; Dutta et al., 2015) and is

relatively easy to implement in comparison with the development of a user subroutine. Furthermore, parameters related to depth such as the effective vertical stress (e.g. proxy parameter for confining stress) can be implemented to define the variation in state parameters (e.g. elastic modulus for granular materials). Assuming a Poisson's ratio of 0.5 for undrained soil condition, and substituting it in the fundamental equation relating the undrained modulus of elasticity (E_{u50}) to shear modulus (G_{50}) from theory of elasticity ($E=2G(1+v)$), the undrained modulus of elasticity (E_{u50}) vary with the soil depth can be expressed as follows:

$$E_{u50} \approx 3.0 \times G_{50} \tag{3-1}$$

where, G_{50} is the shear modulus at 50% mobilized strength. The parameter represents the average response of the engaged soil volume (Konrad and Law, 1987; Schnaid et al., 1997) and is more appropriate for over-consolidated clays (OC) (Schnaid et al., 1997). The shear modulus (G_{50}) can be written as follows:

$$G_{50} = I_R \times s_{ui} \tag{3-2}$$

where I_R is the rigidity index and was calculated by using the equation proposed by Mayne (2007):

$$I_R \approx \frac{e^{\left(\frac{(137-\mathrm{PI})}{23}\right)}}{\left[1+\ln\left(1+\frac{(\mathrm{OCR}-1)^{3.2}}{26}\right)\right]^{0.8}} \tag{3-3}$$

where PI is the plasticity index that was taken as 31% based on the soil properties given by Lach (1996). The OCR is the over-consolidation ratio that is varied by soil depth (see Figure 3-2 (b)). Keaveny and Mitchell (1986) showed that by increasing the value of OCR and PI (plasticity index), the I_R (rigidity index) tends to decrease and results in a lower magnitude of undrained modulus of elasticity.

In the elastic zone, the variation of undrained modulus of elasticity (E_{u50}) with soil depth was tabulated using the aforementioned dummy temperature field.

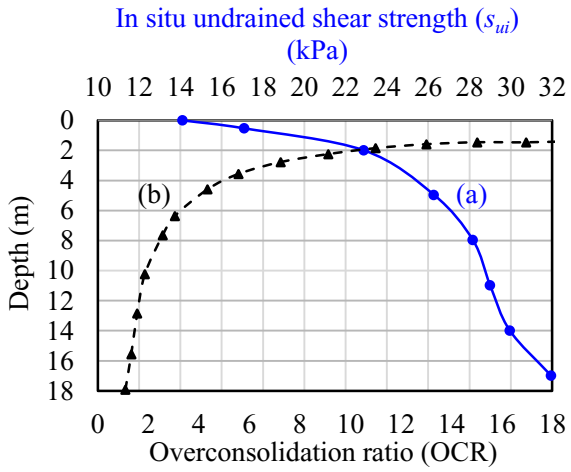

Figure 3-2. One dimensional consolidation test example.

As shown in Figure 3-2, the clay is over-consolidated near the surface with an untrained shear strength of about 10 kPa to 20 kPa.

3.2.1.1. Strain rate dependency and strain-softening

The strain rate dependency and strain-softening effects were modeled by coding an empirical equation proposed by Einav and Randolph (2005) into a VUSDFLD user subroutine in the ABAQUS. At each individual Gauss points of the soil elements, and in every time increment, the subroutine was called by the solver to update the undrained shear strength using the current values of the accumulated absolute plastic shear strain (ξ) and the calculated maximum shear strain rate ($\dot{\gamma}_{max}$), as proposed by Einav and Randolph (2005):

$$s_u = \left[1 + \mu \times log_{10}\left(\frac{max\left(\left(|\dot{\gamma}_{max}|, \dot{\gamma}_{ref}\right)\right)}{\dot{\gamma}_{ref}}\right)\right] \times \left[\delta_{rem} + (1 - \delta_{rem})e^{-3\xi/\,\xi_{95}}\right]s_{ui} \quad (3\text{-}4)$$

The first portion of the equation holds the effect of strain rate dependency, and the second portion incorporates the strain-softening effect, where μ is the increase rate of the shear strength per log cycle, $\dot{\gamma}_{ref}$ is the reference shear strain rate, δ_{rem} is the ratio of fully remoulded to initial shear strength or the inverse of the sensitivity (S_t), ξ_{95} is the relative ductility of the soil or the value of accumulated absolute plastic shear strain resulting in a 95% reduction in the remoulded shear strength, and s_{ui} is the in-situ undrained shear strength at the reference shear strain rate.

Table 3-1 shows the soil model parameters adopted from the corresponding references for the base case analysis in the current study. The basic soil parameters including the mass density, Poisson's ratio, and plasticity index have been taken from the experimental study conducted by Lach (1996) (Test No. 5). The other parameters related to strain rate and strain softening have been selected from the published studies in the literature, since Lach (1996) has not reported the values of these parameters.

Table 3-1. Soil mechanical properties used in FE analysis

Parameters	Values	Ref.
Mass density, ρ	1950 kg/m^3	(Lach, 1996)
Poisson's ratio, ν	0.499	(Lach, 1996)
Plasticity index, PI	31%	(Lach, 1996)
Rate of shear strength increase, μ	0.1	(Biscontin and Pestana, 2001; Graham et al., 1983; Dayal and Allen, 1975)
Reference shear strain rate, $\dot{\gamma}_{ref}$	0.024 S^{-1}	(Kim et al., 2015; Raie and Tassoulas, 2009)
Soil sensitivity, S_t	2.0	(Kvalstad et al., 2001; Andersen and Jostad, 2004; Randolph, 2004; Chen, 2005)
Ratio of fully remoulded to initial shear strength, δ_{rem}	0.5	(Kvalstad et al., 2001; Andersen and Jostad, 2004; Randolph, 2004; Chen, 2005)
Accumulated absolute plastic shear strain for 95% reduction in strength due to remoulding, ξ_{95}	12	(Randolph, 2004)

A μ value of 0.1 was assumed based on the values in a range of 0.05 to 0.2 suggested in the literature (Biscontin and Pestana, 2001; Graham et al., 1983; Dayal and Allen, 1975). The maximum shear strain rate ($\dot{\gamma}_{max}$) was obtained incrementally as follow:

$$\dot{\gamma}_{max} = \frac{(\Delta\varepsilon_1 - \Delta\varepsilon_3)}{\Delta t} \tag{3-5}$$

where $\Delta\varepsilon_1$ and $\Delta\varepsilon_3$ are the cumulative major and minor principal strains over the time increment, Δt. The reference shear strain rate ($\dot{\gamma}_{ref}$) may vary depending on the test conditions. The $\dot{\gamma}_{ref}$ is usually in the range of about (~0.00001 s^{-1}) for laboratory triaxial tests, (0.001–0.1 s^{-1}) for T-bar and ball penetrometer tests, (0.01–100 s^{-1}) for vane shear and viscometer tests, and (1– 10 s^{-1}) for fall cone test (Kim et al., 2015). Raie and Tassoulas (2009) has recommended a reference shear strain rate ($\dot{\gamma}_{ref}$) of 0.024 s^{-1} for vane shear tests

(Raie and Tassoulas, 2009), the same testing methodology that has been used by Lach (1996) in-flight for determining the undrained shear strength in ice gouging studies. Therefore, in this study, a reference shear strain rate of 0.024 was adopted in numerical simulations to compare the results with the test No. 5 conducted by Lach (1996).

For the ratio of fully remoulded to initial shear strength (δ_{rem}), the sensitivity (S_t) was taken as 2.0. A typical sensitivity of 2.0 to 2.8 has been reported in the literature for reconstituted kaolin clay that is usually used in centrifuge model tests (Kvalstad et al., 2001; Andersen and Jostad, 2004; Randolph, 2004; Chen, 2005). The value of ξ_{95} was assumed to be 12. For typical soft marine clays, a range of 10 to 25 (i.e., 1000% to 2500% cumulative plastic shear strain for a rapidly to gradually softening soil, respectively) is suggested by Randolph (2004).

3.2.2. FEA model configuration

The finite element model configuration was selected based on a published experimental study (Lach, 1996) to facilitate model verification. A half-space rigid ice keel with a base length of 5 m, a width of 10 m, and an attack angle of 15° were modelled as a Lagrangian body. In reality, the icebergs may have an endless different type of geometries but it doesn't significantly affect the area of investigation considered in the study. There are some iceberg shape characterization studies in the literature some of them with simplified concepts such as the MANICE designation (i.e. tabular, dome, drydock etc.). More comprehensive models usually include relationships for contact area (e.g. Fuglem et al., 1998; McKenna et al., 2001), keel shape (e.g. PERD, 2000; Croasdale et al., 2001), and for overall shape (e.g. McKenna et al., 1999). Most of these studies consider a portion of the iceberg for specific purposes in the ice-structure interaction process. In this study, since the ice

dynamics has not been explicitly modeled to further focus on ice-seabed interaction, same as all of the previously published research works the iceberg shape has been simplified with an upside-down trapezoidal pyramid with right angle sides as seen in Figure 3-3. The ice keel was moved horizontally, while the other five degrees of freedom were constrained. The gouge depth was considered to be 1.21 m in a seabed with dimensions of 70 × 20 × 18 m (length, width, depth) that was modelled as the Eulerian domain (see Figure 3-3). A void domain of 8 m high was considered to capture the front mound and side berm formations. The seabed soil was modelled by 3D Eulerian 8-node linear brick elements with reduced integration (a single integration point located in the middle of the element for a more accurate formulation of the uniform strain) (EC3D8R). This element is equipped with the capability of hourglass control (i.e., the spurious deformation mode of the mesh, resulting from the excitation of zero-energy degrees of freedom). Reduced-integration elements use one fewer integration point in each direction than the fully integrated elements. In linear reduced integration elements, only a single integration point located at the element's centroid. These elements tend to be too flexible because of hourglassing, i.e., a severe mesh distortion, with no stresses resisting the deformation. In ABAQUS a small amount of artificial “hourglass stiffness” is introduced in reduced-integration elements to limit the propagation of hourglass modes. Hourglass control tries to minimize this problem without introducing excessive constraints on the element's physical response. The element size was biased at the intersection of the void and soil space from minimum to maximum in the vertical upward and downward directions. The element size was kept constant in the horizontal gouge direction. The minimum element size varied from 1.0 m to 0.25 m, while the maximum element size was maintained at 1.0 m.

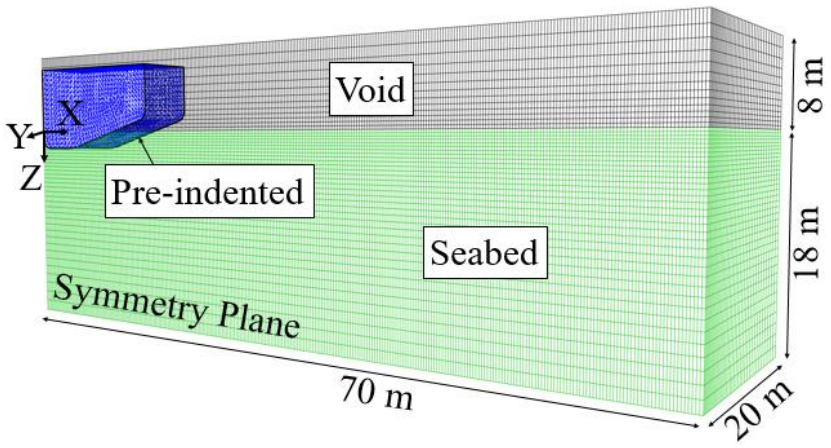

Figure 3-3. FEA model configuration

Velocity boundary conditions were defined to constrain the Eulerian soil movement in the normal direction to the model boundaries. A general contact was defined for interaction between the ice keel surface and the soil. The general contact algorithm enforces the contact between the Eulerian materials and Lagrangian surfaces to compensate the mesh size discrepancies and prevent penetration of the Eulerian material through the Lagrangian surface (Abaqus. 2020). A "hard" ice-soil interaction property was considered for the normal interaction between the ice keel and the seabed soil. For tangential behavior, following an isotropic Coulomb friction formulation, a friction coefficient of 0.1 was assigned and the maximum shear stress at the interface was set to a limit of $0.5s_{ui}$, where s_{ui} was the value of measured in situ undrained shear strength at the gouge depth.

The ice displacement velocity was set to a constant rate of 0.072 m/s throughout the steady-state gouging event. The velocity was selected as per Test 05 of the Lach (1996) to ensure the undrained conditions (with a transverse velocity to the hydraulic permeability ratio of about 7.2 × 107). The ice velocity in the Canadian Beaufort Sea is usually less than 0.1 m/s (Palmer et al., 2005). Typically, the reported icebergs drift speed based on the field surveys

are less than 1.5 m/s. For example, in the Labrador Sea a velocity range of 0.21-0.39 m/s with a maximum value of 1.69 m/s was reported on 1976, while a lower velocity of 0.03 m/s was reported for long term winter ice drift velocities in the Beaufort Sea. Palmer et al. (1989) suggested that clays in the field based on the history of moving ice speed, are always in undrained condition while a value larger than 1 m/s is required for sand to be adopted in undrained condition.

The vertical displacement of the ice keel was restrained during the ice gouging analysis. Same as the earlier studies focusing on subgouge soil deformations, this simplifying assumption helped to leave aside the iceberg dynamics and mitigate the complexity of the numerical model. It has been reported in real field surveys that a uniform gouge with constant depth has been regularly observed in leveled seabed along 10 km or more distances. The huge load exerted by the iceberg on the seabed easily develops the shearing planes under and in front of the ice without being affected by the seabed soil shear strength. On the other hand, the current study looks for the horizontal soil displacement under steady state gouging condition which is the main input for a beam-spring model. Therefore, a restrained ice keel in vertical direction with a pre-assumed gouge depth has no or minor impact on the objectives of the currents study.

3.2.2.1. Analysis procedure and mesh sensitivity

At the start of the analysis, the ice keel was set in a pre-indented position at a prescribed gouge depth (i.e., 1.21m) to minimize the analysis time for achieving the steady-state scour condition. The entire analysis was conducted in two steps. First, a geostatic step was run to initialize the soil in situ stress under gravity loads. Then the second step was started as a dynamic explicit analysis for about 600 seconds. In this step, the ice keel was horizontally

displaced through the soil domain with a constant velocity of 0.072 m/s (i.e., Lach, 1996). The subgouge soil deformations were monitored by using tracer particles distributed vertically through the soil depth.

Mesh sensitivity analysis was conducted for the full model to obtain the optimal mesh size and compromise the computational effort and accuracy. A uniform, cohesive soil with an in situ undrained shear strength distribution through soil depth, according to Figure 3-2 was examined in the mesh sensitivity study. The MC failure surface with yield stress criterion matching the Tresca yield stress was used in which the friction and dilation angle was set to zero. The cohesion yield stress (τ_y) was set equal to the in situ undrained shear strength, s_{ui}, and the elastic modulus was varied through soil depth according to Eq. 1, Eq. 2 and Eq. 3. The total unit weight of soil was assumed 19 kN/m^3. A limited allowable keel-soil interface shear stress (τ_{max}) was considered as half the undrained shear strength ($0.5s_{ui}$). The limit is to ensure that the interface shear stress does not exceed the strength of the underlying material due to high normal contact stresses. This also accounted for the remoulded strength of the clay due to shearing at the interface. The remoulded shear strength of clay is the product of δ_{rem} (i.e., 0.5 as discussed in previous section) and the initial shear strength (s_{ui}).

Three different meshes with fine, medium, and coarse densities were examined. A fine mesh size of 0.25 m, a medium-mesh size of 0.5, and a coarse mesh size of 1.0 was tested. Figure 3-4 compares the horizontal and vertical keel reaction forces obtained from mesh sensitivity analysis with the corresponding subgouge soil deformation.

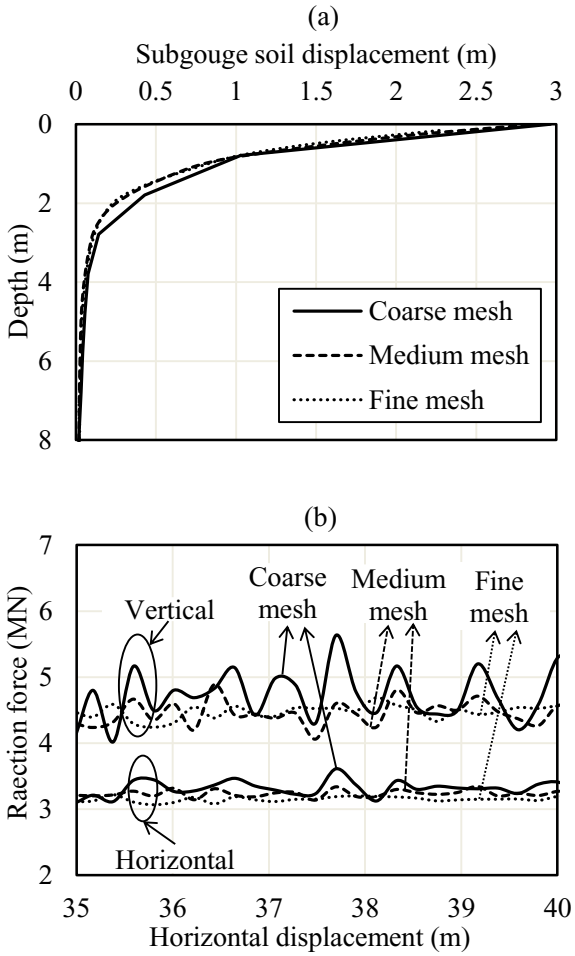

Figure 3-4. The Results of mesh sensitivity analysis

Table 3-2 shows the number of elements and corresponding run time in the conducted sensitivity analysis.

Table 3-2. Mesh convergence study for free-field ice gouge simulations.

Case	Min. Element Size (m)	Max. Element Size (m)	Number of Eulerian Elements	Run Time on 76 CPUs
1	1.0	1.0	36,400	3 hrs. 3 min.
2	0.5	1.0	141,120	7 hrs. 52 min.
3	0.25	1.0	497,280	29 hrs. 15 min.

Table 3-2 shows a nonlinear relationship between the solution run time and the mesh densities. As shown in Figure 3-4 (a), the coarse mesh (Case 1, Table 3-2) provided conservative predictions for the horizontal subgouge soil displacement. The medium and fine meshes (Case 2 and 3, Table 3-2) resulted in optimistic and converging predictions of the horizontal subgouge soil displacements. The comparison of the keel reaction forces in Figure 3-4 (b) indicates significant noise in the coarse mesh (Case 1) with a prediction of about 4% higher than medium and fine mesh cases (Case 2 and 3). A good correlation was also observed between the medium and fine mesh cases (Case 2 and 3).

Based on these observations, the medium mesh size (Case 2) was considered for the comprehensive parametric study to balance analysis run times and solution accuracy. The fine mesh (Case 3) was used for model verification analysis for a higher accuracy that will be discussed in the next section.

3.3. Benchmarking of the numerical model

To verify the model performance and validate the prediction of results, comparisons were made between the current study and three other sources including the experimental study published by Lach (1996) (Test 05), the numerical study conducted by Fadaifard and Tassoulas (2014), and the classical MC model predictions. Lach (1996) conducted a total of nine small-scale centrifuge tests of free-field ice gouging in Speswhite kaolin clay at 100 gravities (see the configuration in Figure 3-3). The Test 05 was selected for comparisons with the current study. The properties of this soil material has been sufficiently published in the literature (e.g., Airey, 1984; Al–Tabbaa, 1987). The soil stress history was practically prescribed to establish the seabed condition in the Canadian Beaufort Sea, which is an iceberg crossing region (Crooks et al., 1996). Lach (1996) used

a vane shear device to estimate the in-flight undrained shear strength and obtain the variation of overconsolidation ratio (OCR) through the soil depth.

Fadaifard and Tassoulas (2014) conducted a numerical study to simulate the Test 04 and Test 05 of Lach (1996) using a viscous non-Newtonian fluid to represent the seabed soil. The strain rate effect was accounted for by a rheological approach for soil flow, but the strain-softening effect was not incorporated. A soil mass density of 1400 kg/m^3 was adapted with a no-slip condition for ice-soil interaction. The authors considered a value of 0.0005 s^{-1} for the reference shear strain rate ($\dot{\gamma}_{ref}$) but did not provide any information about modulus of elasticity. The magnitude of $\dot{\gamma}_{ref}$ was taken between the assumption made by Raie and Tassoulas (2009) for numerical modelling of torpedo anchor installation, and the experimental results published by Rattley et al. (2008) for Kaolin clay.

Figure 3-5 and Figure 3-6 show the comparison of the reaction forces and subgouge soil deformations obtained from the current study with Lach (1996), Fadaifard and Tassoulas (2014), and classical MC soil model predictions. The results are compared in a steady-state region, where the reaction forces almost remain constant, and the frontal soil mound is no longer enlarged by the movement of the ice keel.

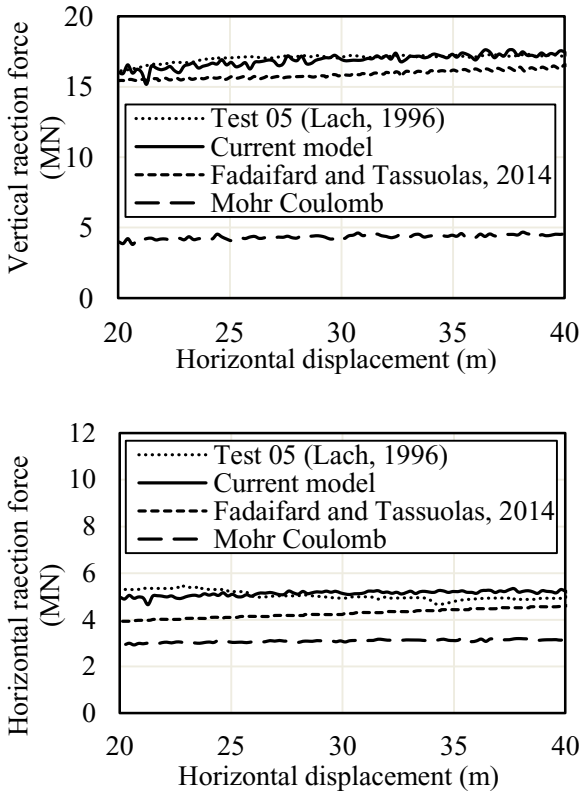

Figure 3-5. The Comparison of the vertical component of reaction force and horizontal one.

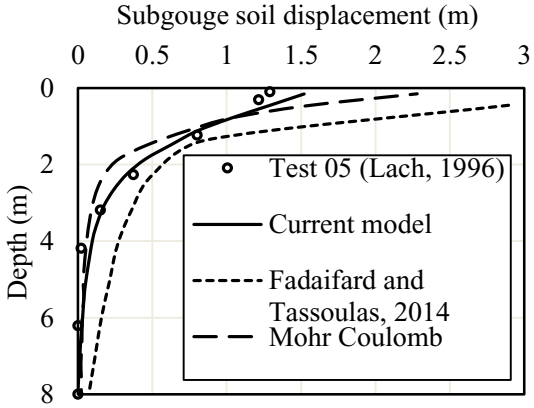

Figure 3-6. The Comparison of the tracked subgouge deformation.

The reaction forces and subgouge soil deformations obtained from the current study are in great agreement with experimental results (Lach, 1996). The developed model significantly

improved the prediction of these key parameters in comparison with earlier numerical models (Fadaifard and Tassoulas, 2014). The remarkable underestimation by the classical MC model shows the significance of the incorporation of strain rate dependency and strain-softening effects. These combined effects, i.e., the increasing by strain rate effect and decreasing by strain softening effect, resulted in an undrained shear strength (s_u) of 2.14 times greater than its in situ value (s_{ui}), in the areas with high shear strain rate. This, in turn, resulted in a stiffer soil response compared with the classical MC model. Figure 3-6 shows that the current model gives a much closer prediction of subgouge soil deformation to the test results within the depths closer to the ice keel as well. This area is the most crucial region for the prediction of soil and pipe displacements due to ice attack.

The dimensions of frontal mound and side berms created by the current and classical MC models for the modelled overconsolidated clay was compared in a half-space side-by-side illustration (see Figure 3-7).

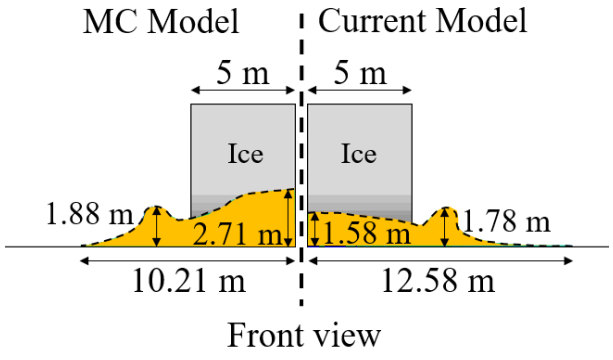

Figure 3-7. Comparison of the dimensions of frontal mound and side berms created by the current and the MC models.

The classical MC model overestimated the dimensions of the front and side soil heaves. Figure 3-8 illustrates the progressive plastic shear strains obtained from the current model

and the MC. Despite the classical MC predictions (Figure 3-8 (b)), the plastic shear strain in the current model has been less extended from the bottom of the keel towards the ice front (see Figure 3-8 (a)). This, in turn, has resulted in rising the contact pressure between the ice keel and the seabed soil, leading to increased values of reaction forces (Figure 3-5) and reduced magnitudes of subgouge soil deformations (Figure 3-6).

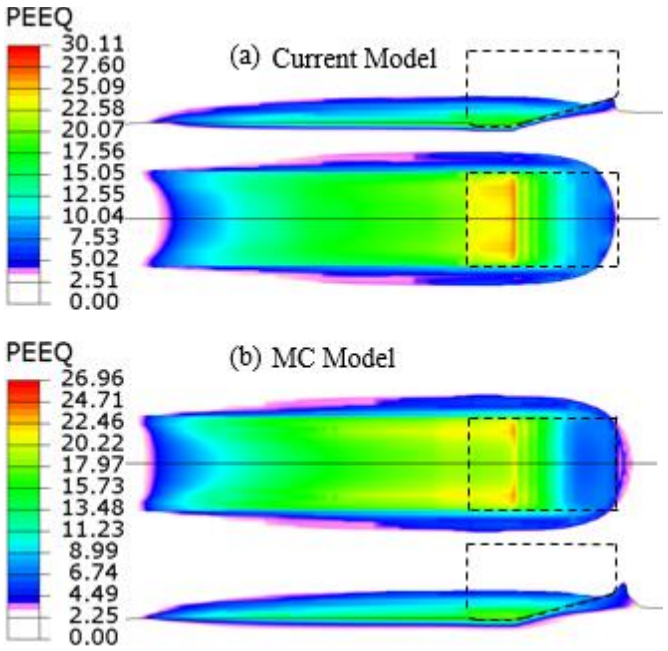

Figure 3-8. Comparison of the progressive developed equivalent plastic shear strains for the current and the MC models.

Analyses were conducted to study the individual and combined effects of strain rate dependency and the strain-softening. Figure 3-9 shows the comparison of the obtained results for reaction forces and subgouge soil deformation with predictions of the classical MC model.

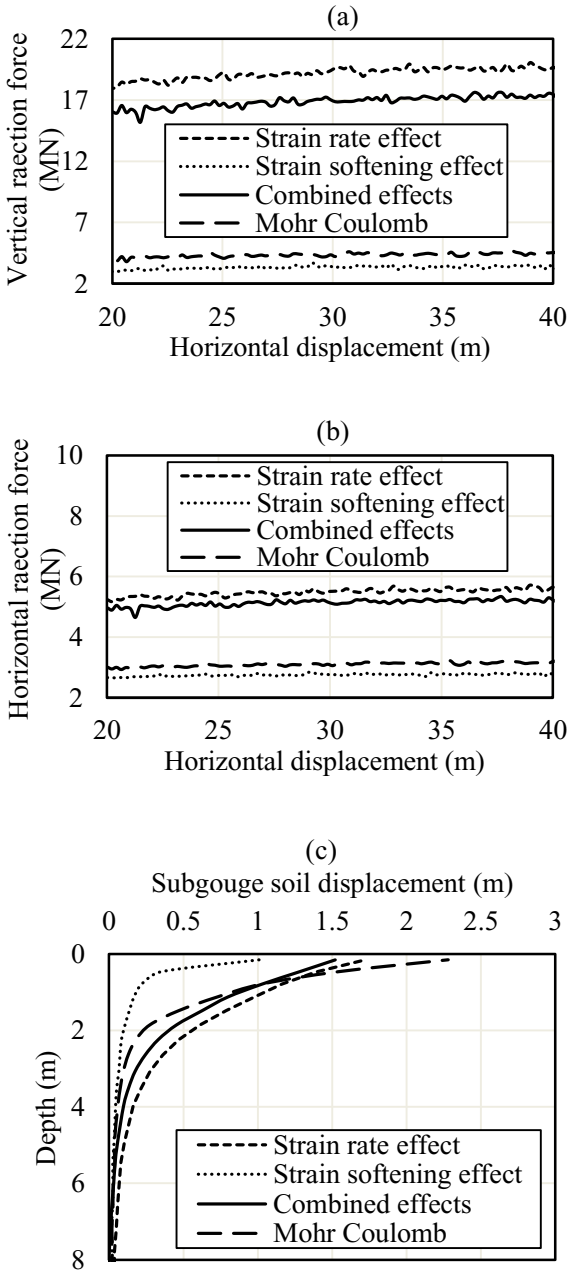

Figure 3-9. The individual and combined effects of strain rate and strain-softening.

It was observed that the strain rate effects result in a stiffer soil response by increasing the values of undrained shear strength. In an inverse fashion, a softer response closer to the MC model performance was observed by the incorporation of the individual effect of

strain-softening. However, the results produced by the combined effect of strain rate and strain-softening shows the dominance of strain rate dependency.

Figure 3-10 shows the difference in the developed undrained shear strength contours due to individual and combined effects of strain rate dependency and strain-softening.

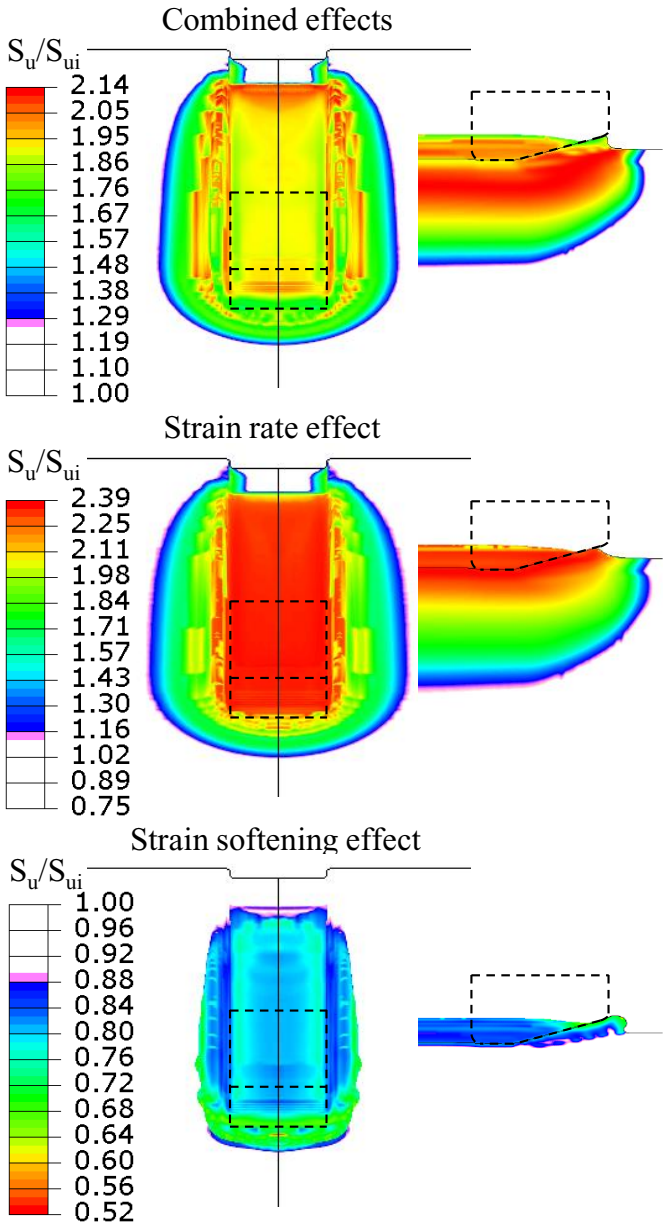

Figure 3-10. Comparison of the developed undrained shear strength contours by the current and MC models.

The strain-softening effect is well developed in the proximity of the ice keel front, where large plastic shear strains have occurred in soil heave formation process. However, the effect of strain-rate is dominant, as observed earlier in Figure 3-9.

3.4. Parametric case studies

A comprehensive parametric study was conducted through 30 case studies (CS-1 to CS-30) to investigate the influence of a broad range of key parameters from ice keel geometry, gouging configuration, and constitutive soil model. In all case studies, the magnitude of horizontal and vertical reaction forces in the steady-state, subgouge soil deformation, and the soil heave dimensions were extracted and compared. Table 3-3 shows the layout of a conducted parametric study and the summary of key parameters.

Table 3-3. Parametric study layout.

Case studies	Ice				Soil				
	Attack Angle (°)	Gouge Depth (m)	Keel Width (m)	Geometry of keel	μ	$\dot{\gamma}_{ref}$ (S^{-1})	δ_{rem}	ξ_{95}	s_{um}(kPa) (s_{ui}=s_{um}+kz) , k=1.0 kPa/m)
CS-1	10	1.2	10	Rectangular	0.1	0.024	0.5	12	14
CS-2	15	1.2	10	Rectangular	0.1	0.024	0.5	12	14
CS-3	30	1.2	10	Rectangular	0.1	0.024	0.5	12	14
CS-4	15	0.8	10	Rectangular	0.1	0.024	0.5	12	14
CS-5	15	1.2	10	Rectangular	0.1	0.024	0.5	12	14
CS-6	15	2.5	10	Rectangular	0.1	0.024	0.5	12	14
CS-7	15	1.2	5	Rectangular	0.1	0.024	0.5	12	14
CS-8	15	1.2	10	Rectangular	0.1	0.024	0.5	12	14
CS-9	15	1.2	20	Rectangular	0.1	0.024	0.5	12	14
CS-10	30	1.2	5	Conical	0.1	0.024	0.5	12	14
CS-11	15	1.2	10	Rectangular	0	0.024	0.5	12	14
CS-12	15	1.2	10	Rectangular	0.05	0.024	0.5	12	14
CS-13	15	1.2	10	Rectangular	0.1	0.024	0.5	12	14
CS-14	15	1.2	10	Rectangular	0.2	0.024	0.5	12	14
CS-15	15	1.2	10	Rectangular	0.1	0.000003	0.5	12	14
CS-16	15	1.2	10	Rectangular	0.1	0.0005	0.5	12	14
CS-17	15	1.2	10	Rectangular	0.1	0.024	0.5	12	14
CS-18	15	1.2	10	Rectangular	0.1	1	0.5	12	14
CS-19	15	1.2	10	Rectangular	0.1	0.024	0.2	12	14
CS-20	15	1.2	10	Rectangular	0.1	0.024	0.33	12	14
CS-21	15	1.2	10	Rectangular	0.1	0.024	0.5	12	14
CS-22	15	1.2	10	Rectangular	0.1	0.024	1.0	12	14
CS-23	15	1.2	10	Rectangular	0.1	0.024	0.5	10	14
CS-24	15	1.2	10	Rectangular	0.1	0.024	0.5	12	14
CS-25	15	1.2	10	Rectangular	0.1	0.024	0.5	15	14
CS-26	15	1.2	10	Rectangular	0.1	0.024	0.5	25	14
CS-27	15	1.2	10	Rectangular	0.1	0.024	0.5	12	2
CS-28	15	1.2	10	Rectangular	0.1	0.024	0.5	12	6
CS-29	15	1.2	10	Rectangular	0.1	0.024	0.5	12	14
CS-30	15	1.2	10	Rectangular	0.1	0.024	0.5	12	18

The parameters were investigated one-at-a-time, while the other parameters were set to default values given in Table 3-3.

3.4.1. Effect of ice keel features and gouging configuration

The effect of ice attack angle, ice width, and gouge depth was investigated through CS-1 to CS-9. A conical ice keel was also studied in CS-10 for comparison with a rectangular ice keel in the same condition (CS-EX) to observe the significance of global geometry. Figure 3-11 shows the reaction forces and subgouge soil deformations obtained from these case studies.

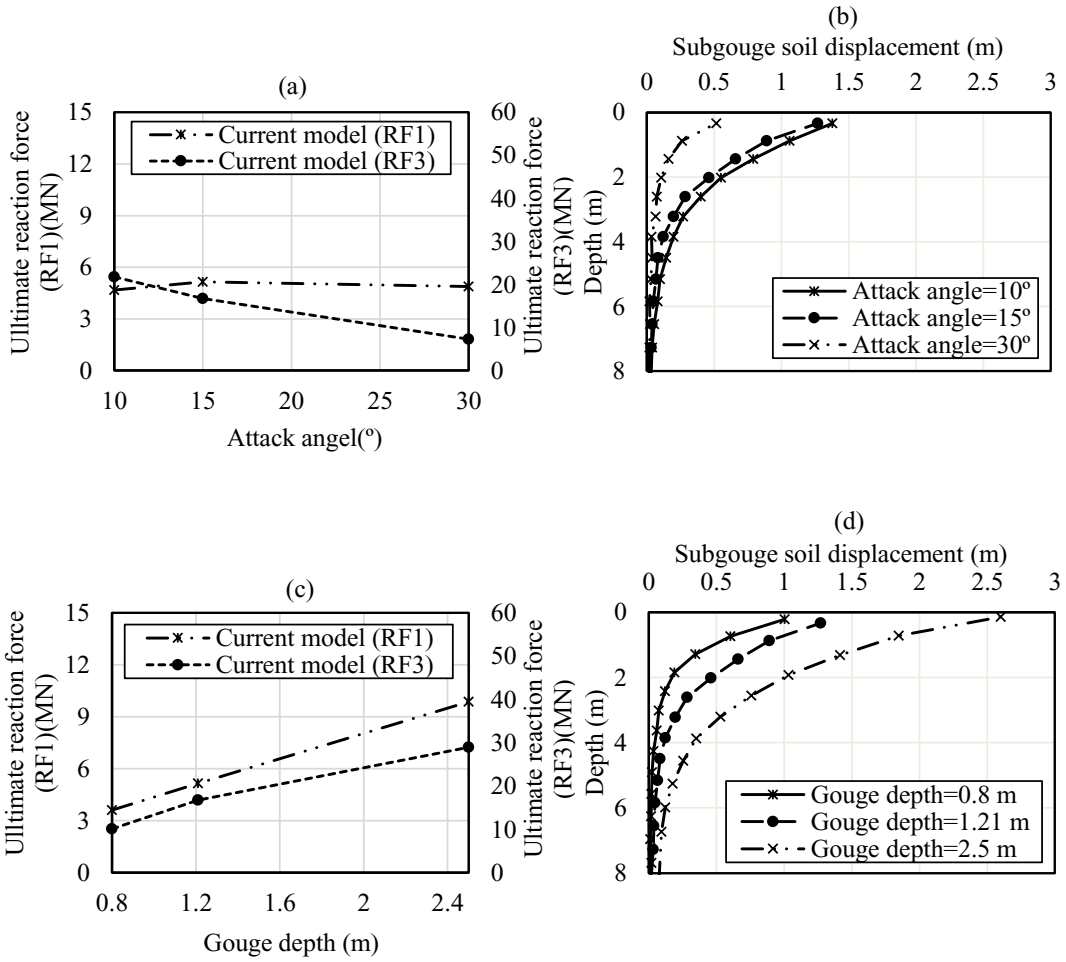

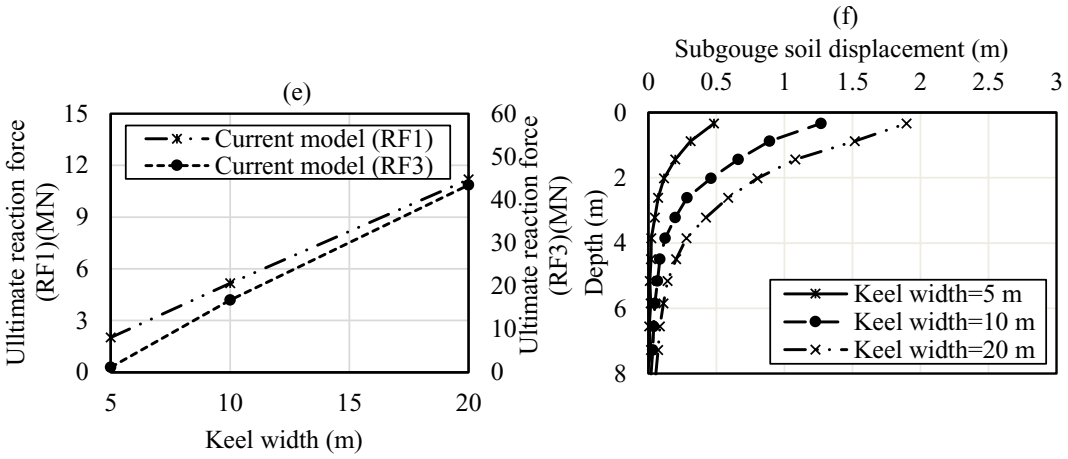

Figure 3-11. The effect of different attack angles, keel widths, and gouge depths on reaction forces and subgouge soil deformations (CS-1 to CS-9).

The effect of these parameters on the dimensions of frontal soil mounds and side berms after achieving the steady-state condition (schematically shown in Figure 3-12) is illustrated in Figure 3-13.

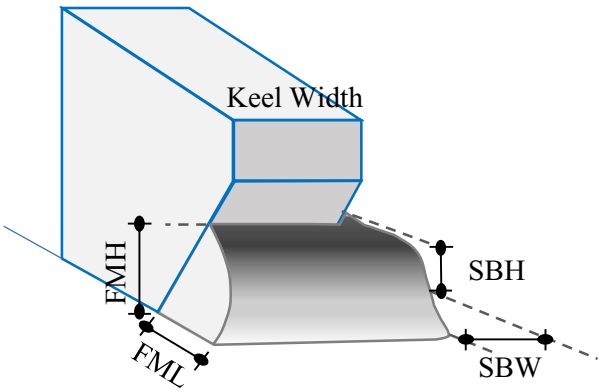

Figure 3-12. Dimensions of soil heaves in front and sides of ice keel.

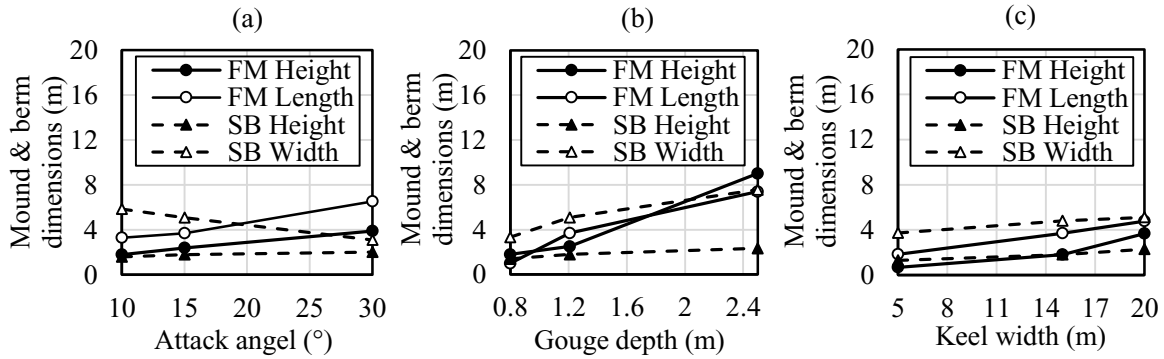

Figure 3-13. The effect of different attack angles, keel widths, and gouge depths on soil heave dimensions (CS-1 to CS-9).

Figure 3-11 (a) and (b), and Figure 3-13 (a) shows that by reducing the attack angle, the soil is more compressed between the ice keel and the seabed and this results in a smaller horizontal reaction force, smaller heave formation, larger vertical reaction force, and larger subgouge soil deformations. Figure 3-11 (c) and (d) and Figure 3-13 (b) shows that the reaction forces, subgouge soil deformation, and the dimensions of soil heave are increased for deeper ice gouges. The wider ice keel produces larger reaction forces, subgouge deformations, soil heave formations (Figure 3-11 (e) and (f) and Figure 3-13 (c)). Also, Figure 3-13 shows that when the dimensions of frontal mound increased, the dimensions of side berms are increased or slightly increased. This is related to the continuous flow of the soil material from the keel front to the sides through the steady-state gouging process. The effect of global ice keel geometry was investigated through conical and rectangular ice keels (CS-10 and CS-EX), while the key parameters remained identical by default values. Figure 3-14 shows the resultant subgouge soil deformations with the reaction forces and soil heave dimensions summarized in Table 3-4.

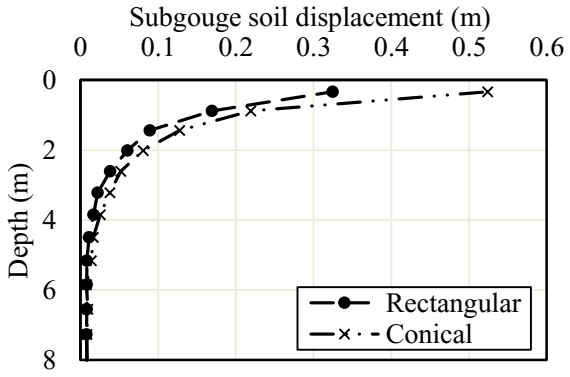

Figure 3-14: Comparison of the subgouge soil deformation from analyses with different keel shapes (CS-10 and CS-EX)

Table 3-4. Soil formation characteristics developed by ice keel with different shapes (CS-10 and CS-EX).

	Rectangular		Conical	
Frontal mound height (FMH) (m)	1.97	±0.0%	1.44	-27%
Frontal mound length (FML) (m)	4.56	±0.0%	0.78	-83%
Side berms height (SBH) (m)	1.31	±0.0%	1.62	+24%
Side berms width (SBW) (m)	2.87	±0.0%	4.45	+55%
Ultimate RF3 (MN)	-2.24	±0.0%	0.25	+111%
Ultimate RF1 (MN)	2.03	±0.0%	2.53	+25%

Figure 3-14 and Table 3-4 show that the conical keel produces smaller soil heave and larger subgouge soil deformations. The reason behind these trends is that the conical keel facilitates flowing of the soil material from the front to the keel sides. This can be observed in Table 3-4 as well, where the dimensions of the frontal mound in the conical keel are smaller and the side berms are larger compared to rectangular keels. This, in turn, reduces

the mobilized soil resistance against the moving ice keel but increases the subgouge soil deformations.

3.4.2. Effect of soil model parameters

3.4.2.1. Effect of soil strain rate

The influence of μ and $\dot{\gamma}_{ref}$ on ice keel-seabed interaction was examined as the key parameters governing the strain rate dependency. Eight different case studies (CS-11 to CS-18) were conducted with four different values for μ and $\dot{\gamma}_{ref}$. The rate of shear strength increase, μ, was varied between 0 and 0.2 and the reference shear strain rate, $\dot{\gamma}_{ref}$ was varied between 0.000003 S^{-1} to 1 S^{-1}. Figure 3-15 shows the results obtained from CS-11 to CS-18, including the reaction forces, subgouge soil deformations, and soil heave dimensions.

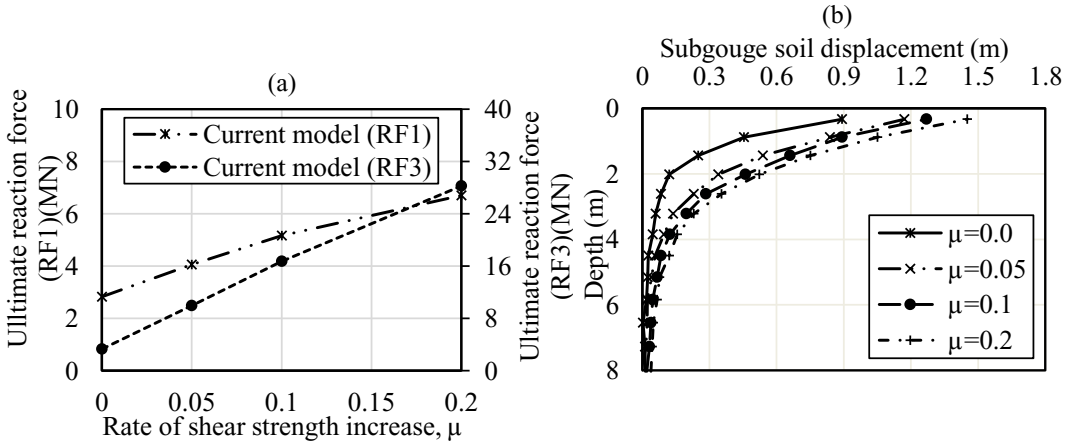

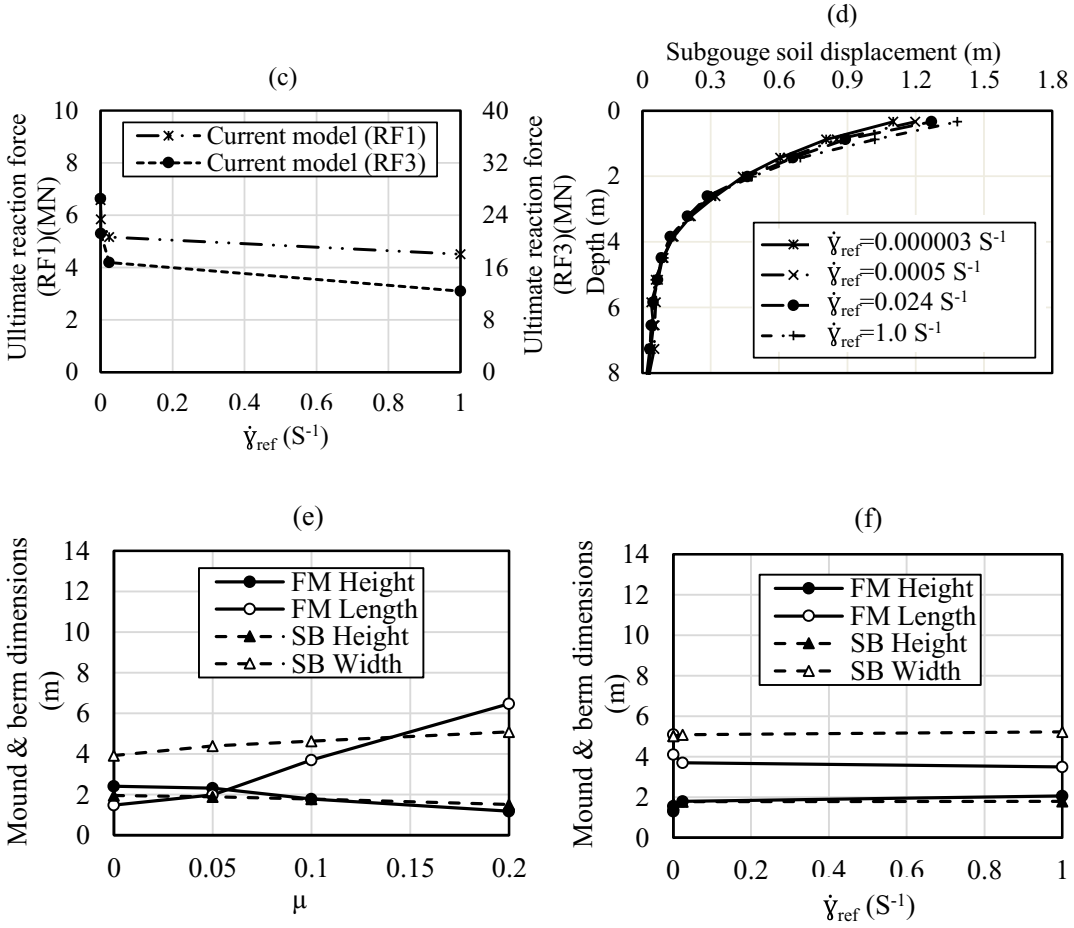

Figure 3-15: The effect of different strain rate parameters (CS-11 to CS-18)

Figure 3-15 (a) and (b) shows that by increasing the rate of shear strength increase, $\boldsymbol{\mu}$, the reaction forces and subgouge soil deformations are increased. This happens by increasing the mobilized undrained shear strength that results in stiffer seabed response to ice gouging. Figure 3-15 (e) shows that the length of the frontal mound and the width of side berms are increased, while the height of both was decreased. As shown in Figure 3-15 (c) and (d) the higher values of reference shear strain rate, $\dot{\gamma}_{ref}$, results in a smaller reaction forces but larger subgouge soil deformations. Also, the frontal mound height is increased, but its length is decreased, while the dimensions of the side berms show negligible dependence on the strain rate parameter, $\dot{\gamma}_{ref}$ (see Figure 3-15 (f)).

3.4.2.2. Effect of soil strain-softening

Analyses were conducted to investigate the effect of δ_{rem} and ξ_{95} on ice keel-seabed interaction, as the key parameters governing the strain-softening effect. Four different values from each parameter were examined totalling eight case studies (CS-19 to CS-26). The values of δ_{rem}, i.e., the ratio of fully remoulded to virgin shear strength, was varied between 0.2 and 1.0. The soil ductility (ξ_{95}) or the accumulated absolute plastic shear strain required to cause a 95% reduction in strength due to remoulding was varied between 10 and 25. Figure 3-16 presents a summary of conducted case studies.

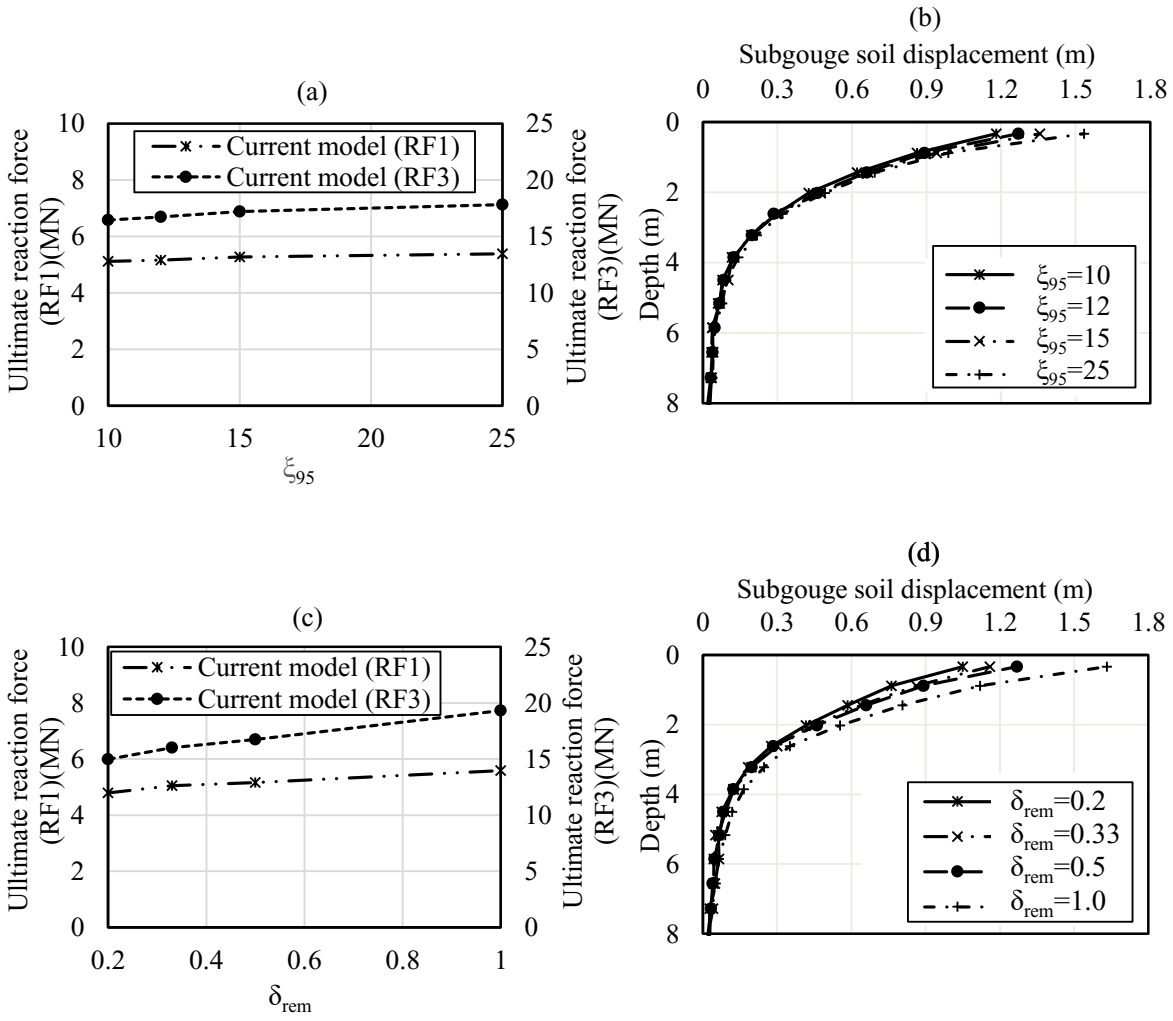

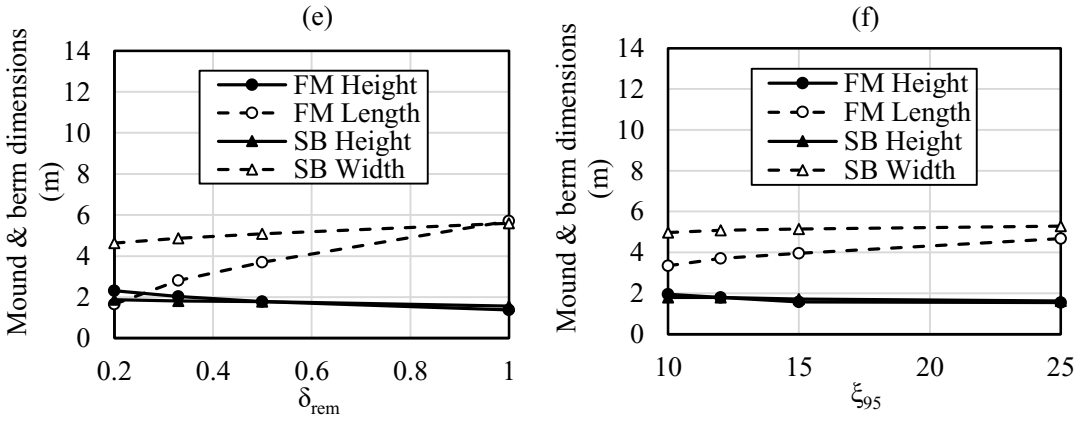

Figure 3-16: The effect of different strain-softening parameters (CS-19 to CS-26)

Overall, ξ_{95} was found to have a negligible influence on the results. Decreasing the soil sensitivity as a result of increasing the δ_{rem}, led to a slight increase in the reaction forces and subgouge soil deformations. By increasing this parameter, the frontal mound length and soil berms width were slightly increased, but their heights were almost remained unchanged.

3.4.2.3. Effect of undrained shear strength

The influence of undrained shear strength on ice keel-seabed interaction was examined by assuming a linear profile for variation of undrained shear strength with depth. The intercept values in the mudline (s_{um}) were varied between 2 kPa and 18 kPa, and a constant gradient of 1 kPa/m was considered (Minerals Management Service, 2008). This resulted in four case studies (CS27-CS30) with the results presented in Figure 3-17 and Table 3-5.

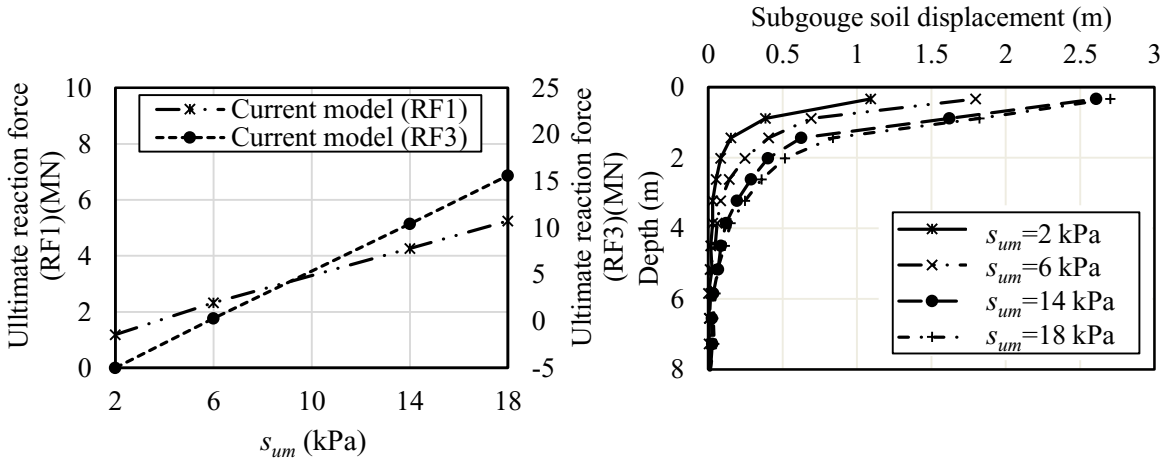

Figure 3-17: The effect of different undrained shear strength (s_{um}) intercept at mudline, (CS-27 to CS-30)

Table 3-5. Soil heave dimensions with different undrained shear strength (s_{um}) intercept at mudline.

	s_{um}= 2 kPa		s_{um}= 6 kPa		s_{um}= 14 kPa		s_{um}= 18 kPa	
Frontal mound height (FMH) (m)	2.05	±0.0%	1.56	-24%	1.52	-26%	1.45	-29%
Frontal mound length (FML) (m)	3.56	±0.0%	4.04	+13%	5.26	+48%	5.64	+58%
Side berms height (SBH) (m)	1.39	±0.0%	1.59	+14%	1.60	+15%	1.60	+15%
Side berms width (SBW) (m)	5.02	±0.0%	5.30	+6%	5.39	+7%	5.46	+9%

It was observed that the reaction forces and subgouge soil deformation were increased by increasing the mudline undrained shear strength, s_{um}. Table 3-5 shows that a higher undrained shear strength results in increased soil heave dimensions, except the height of the frontal mound that is decreased.

3.5. Conclusions

A numerical model was developed to incorporate the strain rate dependency and strain-softening effects in large deformation analysis of ice gouging in clay. Coupled Eulerian-Lagrangian (CEL) approach was employed, and the ideal elastic perfectly plastic Tresca soil model was modified by coding a VUSDFLD user subroutine in ABAQUS to account for the incremental strain rate and softening effects. The results produced by the developed model were compared with the published experimental and numerical studies and the predictions made by MC model. A comprehensive parametric study was conducted to investigate the effect of a broad range of key parameters governing the ice keel geometry, gouge depth, and seabed soil model parameters. The key findings of the current study are as follows:

- The developed model with incorporation of the strain rate dependency and strain-softening effects was found to be a simple but robust tool for simulation of free-field ice gouging process in clay. Compared with earlier numerical and the MC model, the developed model achieved a significantly improved agreement with the published test results.
- The incorporation of strain rate and strain-softening effects resulted in reaction forces higher than MC model and subgouge soil deformation smaller than MC model. The strain rate and strain-softening produced higher values of undrained shear strength around the scour area and a stiffer seabed response with high localized plastic shear strain in the proximity of the ice keel. The study showed the dominance of the strain rate effects compared with strain-softening effects. The strain-softening contributed to a broader extend of plastic shear strain under and in the front of the ice keel. This,

in turn, resulted in a larger frontal mound and also a smaller subgouge soil deformation. Eventually, the strain rate effects governed the ice keel-seabed interaction. The parametric study revealed several interesting trends of the influence of various parameters on the ice keel-seabed interaction.

Overall, the study provided a valuable insight into the numerical modelling of free-field ice gouging in clay. More specifically the significant effect of incorporation of the strain rate dependency and strain-softening effects in to the constitutive soil model. These effects are more visible on the keel reaction forces, subgouge soil deformations, and the dimensions of soil heaves in front and sides of the ice keel. These results can improve the accuracy of free-field ice gouging analysis and the resultant subgouge soil displacements. Consequently, by improving the input values to the beam-spring models, the overall prediction of these simplified models can be also enhanced.

3.6. Acknowledgments

The authors gratefully acknowledge the financial support of this research by Wood PLC via establishing the Wood Group Chair in Arctic and harsh environment engineering at Memorial University, the NL Tourism, Culture, Industry and Innovation (TCII) via CRD collaborative funding program, the Natural Sciences and Engineering Research Council of Canada (NSERC) via CRD funding program, the Memorial University of Newfoundland through the school of graduate studies (SGS) baseline fund.

References

Abaqus. 2020. Analysis user manual. Abaqus 6.2. Simulia Inc., Dassault Systemes.

Abdalla, B., Pike, K., Eltaher, A., Jukes, P. & Duron, B. 2009, "Development and Validation of a Coupled Eulerian Lagrangian Finite Element Ice Scour Model", Proceedings of the 28th International Conference on Ocean, Offshore and Arctic Engineering (ISOPE), May 31 – June 5, 2009, 6p.

Airey, D.W., 1984. Clays in Circular Simple Shear Apparatus. Ph.D. Thesis, University of Cambridge. Cambridge. U.K.

Al–Tabbaa, A., 1987. Permeability and Siress - Strain Response of Speswhile Kaolin. Ph.D. Thesis. University of Cambridge, Cambridge. U.K., 133 p.

Allersma, H.G.B., and Schoonbeek, I.S.S. (2005). Centrifuge modelling of scouring ice keels in clay. Int. Conference on Offshore and Polar Engineering, ISOPE2005, Seoul, June 19-24, paper 2005-JSC-427, pp.404-409.

Andersen, K. H., Jostad, H. P., 2004. Shear strength along inside of suction anchor skirt wall in clay. Proc., Offshore Technology Conf., Houston, OTC 16844.

Babaei, H., and Sudom, D. 2014. Ice-seabed gouging database: review and analysis of available numerical models. In Proceedings, Offshore Technology Conference. Paper No. OTC-24603. doi:10.4043/24603-MS.

Banneyake, R., Hossain, M. K., Eltaher, A., Nguyen, T., Jukes, P., 2011. Ice-soil pipeline interactions using coupled eulerian-lagrangian (CEL) ice gouge simulations extracts from ice pipe JIP. Paper presented at the OTC Arctic Technology Conference.

Barrette, P. & Sudom, D. 2012, "Physical simulations of seabed scouring by ice: Review and database", Proceedings of the 22nd International Offshore and Polar Engineering Conference, ISOPE, Rhodes, Greece, June 17 - 22, 2012, pp. 381-388.

Biscontin, G., Pestana, J.M., 2001. Influence of peripheral velocity on vane shear strength of an artificial clay. Geotech. Test.J. 24(4), 423–429.

Casacrande, A., Wilson, S., 1951. Effect of rate of loading on the strength of clays and shales at constant water content. Géotechnique 2 (3), 251–263.

Chatterjee, S., Randolph, M. F., and White, D. J. (2012a). The effects of penetration rate and strain softening on the vertical penetration resistance of seabed pipelines. Géotechnique, 62(7), 573-582, http://dx.doi.org/10.1680/geot.10.P.075.

Chatterjee, S., Randolph, M. F., and White, D. J. (2012b). Numerical simulations of pipe-soil interaction during large lateral movements on clay. Géotechnique, 62(8), 693-705, http://doi: 10.1680/geot.10. P.107.

Chen, W., 2005. Uniaxial behaviour of suction caissons in soft deposits in deepwater. Ph.D. thesis, The Univ. of Western Australia, Perth, Australia.

Clark J. I., Guigné J. Y., 1988. Twenty-fifth anniversary special paper: Marine geotechnical engineering in Canada. Canadian Geotechnical Journal, 1988, 25(2): 179-198.

Clark, J. I., Landva, J., 1988. Geotechnical aspects of seabed pits in the Grand Banks area. Canadian Geotechnical Journal 25:448-454.

Crooks, J. H. A., Jefferies, M. G. Becker, D. E., Been, K., 1996. Geotechnical properties of Beaufort Sea clays. Proc. 3rd Canadian Conf. on Marine Geotechnical Engineering, St. John's, Newfoundland, pp. 329-343.

Croasdale, K., Brown, R., Campbell, P., Crocker, G., Jordaan, I., King, A., McKenna, R. and Myers, R. (2001) Iceberg risk to seabed installations on the Grand Banks, in Proc. POAC'01, Vol. 2, pp 1019-1028, Ottawa, Canada, 2001.

Daiyan, N. 2013. Investigating soil/pipeline interaction during oblique relative movements. Ph.D. thesis, Memorial University of Newfoundland.

Dayal, U., Allen, J. H., 1975. The effect of penetration rate on the strength of remolded clay and sand samples. Can. Geotech. J., 12(3),336–348.

DeGroot, D. J., DeJong, J. T., Yafrate, N. J., Landon, M. M., Sheahan, T. C., 2007. Application of recent developments in terrestrial soft sediment characterization methods to offshore environments. Proc., Offshore Technology Conf., Houston, OTC 18737.

DeJong, J., DeGroot, D., Yafrate, N., 2012. Evaluation of undrained shear strength using full-flow penetrometers. J. Geotech. Geoenviron. Eng.138(6),765–767.

Díaz-Rodríguez, J.A., Martínez-Vasquez, J.J., Santamarina, J.C., 2009. Strain-rate effects in Mexico city soil. J. Geotech. Geoenviron. Eng. 135 (2), 300–305.

Dutta, S., Hawlader, B., and Phillips, R. (2015). Finite element modeling of partially embedded pipelines in clay seabed using Coupled Eulerian-Lagrangian method. Canadian Geotechnical Journal, 52(1), 58-72, http://dx. doi.org/10.1139/cgj-2014-0045.

Einav, I., Randolph, M. F., 2005. Combining Upper Bound and Strain Path Methods for Evaluating Penetration Ristance. International Journal for Numerical Methods in Engineering, Vol. 63, No. 14, pp. 1991-2016.

Eskandari, F., Phillips, R. & Hawlader, B. 2012, "Finite Element Analyses of Seabed Response to Ice Keel Gouging", Proceedings of the 65th Canadian Geotechnical Conference (GeoManitoba), September 30 - October 3, 2012, 8p.

Fadaifard, H., Tassoulas, J.L., 2014. Numerical modeling of coupled seabed scour and pipe interaction. Int. J. Solids Struct. 51 (19–20), 3449–3460.

Fuglem, M., Muggeridge, K., and Jordaan, I.J. (1998) Design load calculations for iceberg impacts, in Proc. ISOPE Conference, Montreal, Vol. 2, pp. 460-467.

Ghorai, B., and Chatterjee, S. (2017). Influences of strain rate and soil remoulding on initial break-out resistance of deepwater on-bottom pipelines. Computers and Geotechnics, (91), 82-92, doi: 10.1016/j.compgeo.2017.07.006.

Graham, J., Crooks, J. H. A., Bell, A. L., 1983. Time effects on the stress-strain behaviour of natural soft clays. Geotechnique, 33(3), 327–340.

Hossain, MS, Randolph, MF, 2009. Effect of Strain Rate and Strain Softening on the Penetration Resistance of Spudcan Foundations on Clay. International Journal of Geomechanics, Vol 9, No 3, pp 122-132.

Johnson, P.C., Jackson, R., 1987. Frictional–collisional constitutive relations for granular materials with application to plane shearing. J. Fluid Mech. 176, 67–93.

Keaveny, J., Mitchell, J.K., 1986. Strength of fine-grained soils using the piezocone. Use of In-Situ Tests in Geotechnical Engineering, GSP 6, ASCE, Reston/VA, 668-685.

Kenny, S., and Jukes, P. 2015. Pipeline/soil interaction modelling in support of pipeline engineering design and integrity. In Oil and gas pipelines: integrity and safety handbook. Edited by R.W. Revie. John Wiley and Sons Ltd. ISBN 978-1-118-21671-2.

Kenny, S., Barrett, J., Phillips, R. & Popescu, R. 2007, "Integrating geohazard demand and structural capacity modelling within a probabilistic design framework for offshore arctic pipelines", 17th International Offshore and Polar Engineering Conference, July 1 - 6, 2007, pp. 3057-3064.

Kenny, S., Phillips, R., McKenna, R.F. and Clark, J.I. (2000). Response of buried arctic marine pipelines to ice gouge events. Proc., OMAE, OMAE00-5001.

Kenny, S., Phillips, R. & Nobahar, A. 2005, "PRISE Numerical Studies on subgouge deformations and pipeline/soil interaction analysis", Proceedings of the International Conference on Port and Ocean Engineering Under Arctic Conditions (POAC), June 26 - 30, 2005, 10p.

Kim, Y.H., Hossain, M.S., Wang, D., 2015. Effect of strain rate and strain softening on embedment depth of a torpedo anchor in clay. Ocean Engineering, Volume 108, Pages 704-715.

Kvalstad, T. J., Nadim, F., Harbitz, C. B., 2001. Deepwater geohazards: Geotechnical concerns and solutions. Proc., Offshore Technology Conf., Houston, OTC 12958.

Konrad, J.M., Law, K.T., 1987. Undrained shear strength from piezocone tests. Can. Geotech. J., 24, 392- 405.

Konuk, I., Liferov, P. & Loset, S. 2007, "Challenges in modelling ice gouge and pipeline response", Proceedings of the 19th International POAC Conference, June 27 - 30, 2007, pp. 760-773.

Konuk, I. & Gracie, R. 2004, "A 3-Dimensional Eulerian Finite Element Model for Ice Scour", Proceedings of the 5th International Pipeline Conference, October 4 - 8, 2004, pp. 1911-1918.

Lach, P.R. 1996, Centrifuge modelling of large soil deformation due to ice scour, Ph.D., Memorial University of Newfoundland (Canada).

Lehane, B., O'Loughlin, C., Gaudin, C., Randolph, M., 2009. Rate effects on penetrometer resistance in kaolin. Géotechnique 59 (1), 41–52.

Liferov, P., Shkhinek, K.N., Vitali, L. And Serre, N., 2007. Ice gouging study-actions and action effects. Proc. 19th International Conference on Port and Ocean Engineering under Arctic Conditions, Dalian, China.

Lunne, T., Andersen, K. H., 2007. Soft clay shear strength parameters for deepwater geotechnical design. Proc., 6th Int. Offshore Site Investigation and Geotechnics Conf.: Confronting New Challenges and Sharing Knowledge, Vol. 1, Society for Underwater Technology, London, 151–176.

Mayne, P.W. 2007, *Cone Penetration Testing State-of-Practice: Final Report*. Available: http://geosystems.ce.gatech.edu/Faculty/Mayne/papers/NCHRP%20CPT%20Synthesis%20(2007)%20color.pdf

McKenna, R.F., Crocker, G.B. and Paulin, M.J. (1999) Modelling iceberg scour processes on the northeast Grand Banks, in Proc. 17th International Conference on Offshore Mechanics and Arctic Engineering (OMAE), St. John's.

McKenna, R., Crocker, G., King, T., Brown, R. (2001) Efficient characterization of iceberg shape, in Proc. CANCAM, St. John's.

Minerals Management Service (2008). Design Options for Offshore Pipelines in the US Beaufort and Chukchi Seas, Report R–07–078–519.

Nematzadeh, A., & Shiri, H., 2019. The influence of non-linear stress-strain behavior of dense sand on seabed response to ice gouging. Cold Reg. Sci. Technol. 170 (2019) 102929.

Nyman, K. 1984. Soil response against oblique motion of pipes. Journal of Transportation Engineering, 110(2): 190–202. doi:10.1061/(ASCE)0733-947X(1984) 110:2(190).

Palmer, A.C. 1997. Geotechnical Evidence as a guide to pipeline burail depth.Can. Geotech. J. 34: 1002–1003.

Palmer, A. C., Konuk, I., Niedoroda, A.W., Been, K., Croasdale, K. R., 2005. Arctic Seabed Ice Gouging and Large Sub-Gouge Deformations. 1st International Symposium on Frontiers in Offshore Geotechnic., Perth, Australia, 645-650.

Panico, M., Lele, S.P., Hamilton, J.M., Arslan, H. & Cheng, W. 2012, "Advanced ice gouging continuum models: Comparison with centrifuge test results", Proceedings of the 22nd International Offshore and Polar Engineering ConferenceInternational Society of Offshore and Polar Engineers, Rhodes, Greece, June 17 - 22, 2012, pp. 504-510.

Peek, R. & Nobahar, A., 2012. Ice Gouging over a Buried Pipeline: Superposition Error of Simple Beam-and-Spring Models. ASCE International Journal of Geomechanics, 12(4), pp.508–516.

PERD (2000) Study of iceberg scour & risk in the Grand Banks region, PERD/CHC Report 31-26 by K.R Croasdale & Associates Ltd., Ballicater Consulting Ltd., Canadian Seabed Research Ltd., C-CORE, and Ian Jordaan & Associates Inc.

Pike, K., and Kenny, S. 2012. Advanced continuum modelling of the ice gouge process: Assessment of keel shape effect and geotechnical data. In Proceedings, Twenty-second International Offshore and Polar Engineering Conference. Paper No. ISOPE-12-TPC-0464.

Pike, K., Kenny, S., 2016. Offshore pipelines and ice gouge geohazards: Comparative performance assessment of decoupled structural and coupled continuum models. Canadian Geotechnical Journal, 53(11), 1866-1881.

Pike, K., Seo, D., and Kenny, S. 2011. Continuum modelling of ice gouge events: observations and assessment. In Proceedings, Offshore Technology Conference. Paper No. OTC-22097. doi:10.4043/22097-MS.

Phillips, R., Barrett, J.A. & Al-Showaiter, A. 2010, "Ice keel-seabed interaction: Numerical modelling validation", Proceedings of the Offshore Technology Conference, May 3 - 6, 2010, 13p.

Phillips, R., Barrett, J., 2012. PIRAM: Pipeline Response to Ice Gouging. Proceedings of the Arctic Technology Conference, December 3 - 5, 2012, 6p.

Phillips, R. & Barrett, J. 2011, "Ice Keel-Seabed Interaction: Numerical Modelling for Sands", Port and Ocean Engineering under Arctic Conditions (POAC), July 10 - 14, 2011, 10p.

Phillips, R., Clark, J.I. & Kenny, S. 2005, "PRISE studies on gouge forces and subgouge deformations", Proceedings of the International Conference on Port and Ocean Engineering Under Arctic Conditions (POAC), June 26 - 30, 2005, 10p.

Phillips, R., Nobahar, A., and Zhou, J. 2004a. Combined axial and lateral pipe-soil interaction relationships. In Proceedings, International Pipeline Conference. Paper No. IPC-0144. doi:10.1115/IPC2004-0144.

Raie, M., Tassoulas, J., 2009. Installation of torpedo anchors: numerical modeling. J. Geotech. Geoenviron. Eng. 135 (12), 1805–1813.

Randolph, M. F., 2004. Characterization of soft sediments for offshore applications. Keynote Lecture, Proc., 2nd Int. Conf. on Site Characterization, Porto, Portugal, Vol. 1, Millpress Science Publishers, Rotterdam, 209–231.

Rattley, M., Richards, D., Lehane, B., 2008. Uplift performance of transmission tower foundations embedded in clay. J. Geotech. Geoenviron. Eng. 134 (4), 531-540.

Rossiter, C., and Kenny, S. 2012a. Evaluation of lateral-vertical pipe/soil interaction in clay. In Proceedings, Offshore Technology Conference. Paper No. OTC- 23735.

Rossiter, C., and Kenny, S. 2012b. Assessment of ice-soil interactions: continuum modelling in clays. In Proceedings, Twenty-second International Offshore and Polar Engineering Conference. Paper No. ISOPE-12-TPC-0304.

Sayed, M., Timco, G.W., 2009. A numerical model of iceberg scour. Cold Regions Science and Technology 55, 103–110.

Schnaid, F., Sills, G.C., Soares, J. M., Nyirenda, Z., 1997. Predictions of the coefficient of consolidation from piezocone tests. Can. Geotech. J., 34, 315-327.

Schoonbeek, I.S.S., and Allersma, H.G.B. 2006. Centrifuge modelling of scouring ice keels in clay. In Proceedings, 8th International Conference on Physical Modelling in Geotechnics, ICPMG. pp. 1291–1296.

Schoonbeek, I.S.S., Xin, M.X., Van Kesteren,W.G.M., Been, K., 2006. Slip line field solutions as an approach to understand ice subgouge deformation patterns. Proceedings of the 16th International Offshore and Polar Engineering Conference. The International Society of Offshore and Polar Engineers (ISOPE), San Francisco, pp. 628–633.

Vaid, Y.P., Robertson, P.K., Campanella, R.G., 1979. Strain rate behaviour of Saint-Jean-Vianney clay. Can. Geotech. J. 16 (1), 34–42.

Wang, D., White, D. J., and Randolph, M. F. (2010a). Large-deformation finite element analysis of pipe penetration and large-amplitude lateral displacement. Canadian Geotechnical Journal, 47(8), 842-856, http://dx.doi.org/10.1139/T09-147.

Winters, W. J., Lee, H. J., 1984. Geotechnical properties of samples from borings obtained in the Chukchi Sea. Alaska. USGS Report 85-23.

Woodworth-Lynas, C., Nixon, D., Phillips, R., Palmer, A., 1996. Subgouge Deformations and the Security of Arctic Marine Pipelines. Proc. 28th OTC, Vol. 4, Paper No. 8222, pp. 657–664.

Yang, Q. S., Poorooshasb, H. B., & Lach, P. R. (1996). Centrifuge Modeling and Numerical Simulation of Ice Scour. Soils and foundations., 36(1), 85.

Yang, Q.S. & Poorooshasb, H.B. 1997, "Numerical modeling of seabed ice scour", Computers and Geotechnics, vol. 21, no. 1, pp. 1-20.

Zhou, H., and Randolph, M. F. (2007). Computational techniques and shear band development for cylindrical and spherical penetrometers in strain-softening clay. International Journal of Geomechanics, 7(4), 287-295, http://dx.doi.org/10.1061/(ASCE)1532-3641(2007)7: 4(287).

Zhou, H., and Randolph, M. F. (2009a). Resistance of full-flow penetrometers in rate-dependent and strain-softening clay. Géotechnique, 59(2), 79-86, http://dx.doi.org/10.1680/geot. 2007.00164.

Chapter 4

The Influence of Layered Soil on Ice-seabed Interaction: Soft over Stiff Clay

Seyedhossein Hashemi, as the main author is credited for the methodology, modeling, data curation, visualization, investigation, validation and writing-original draft. Hodjat Shiri is credited for conceptualization, supervision, writing-review and editing and funding acquisition. Xiaoyu Dong is credited for writing-review and editing.

This chapter was published as a journal paper in Applied Ocean Research (Elsevier).

Abstract

Ice gouging is one of the main threats for the structural integrity of the offshore pipelines in the territories that floating icebergs can reach. The safe and cost-effective burial depth of pipelines for protection against the iceberg attack depends on accurate assessment of the subgouge soil deformation and the ice keel-seabed contact forces. Layered seabed soil strata that are found in many geographical locations adds to the complexity of assessing the ice keel-seabed interaction process by signifying the effect of strain rate dependence and strain softening in the soil layers interaction areas and ice-seabed contact zone. The existing design codes simplify the seabed condition by assuming a uniform soil strata. This in turn affects the accuracy and cost-effectiveness of the design. In this paper, large deformation finite element (LDFE) analysis was conducted using Coupled Eulerian Lagrangian (CEL) approach to investigate the free-field ice gouging in layered (soft over stiff clay) cohesive seabed. A modified Tresca soil model was coded in a user subroutine to account for the effects of strain rate and strain-softening on the mobilised undrained shear strength. A comprehensive parametric study was conducted to examine the effect of gouging features and soil shear strength profiles on the subgouge soil deformation, developed plastic shear strains and the resultant ice keel reaction forces. The analysis results showed that the seabed response to ice gouging is heavily dependent on the soil strata, where the layers interaction effects can override the usual response expected from a uniform seabed. Practical solutions were proposed to improve the pipeline design in layered seabed soils.

Keywords: Ice gouging, Subgouge soil deformation, Layered seabed, Numerical simulation, Strain rate and strain-softening effects

4.1. Introduction

Floating icebergs threaten the structural integrity of subsea pipelines and structures by scouring the seabed that is called ice gouging. Protection of the subsea pipelines against ice gouging is a challenging design and construction aspect. Trenching and backfilling of the pipelines with pre-excavated material is the most common and economic method for physical protection of subsea pipelines against the large subgouge soil deformation caused by the ice gouging. Determining the minimum trench depth is a key aspect both in terms of the pipeline structural health and construction costs. The current state-of-practice to analyze the pipeline response to ice gouging is to transfer the subgouge soil deformation extracted from a free-field finite element analysis (FEA) to a beam-spring pipeline model as the initial displacement (Woodworth-Lynas et al., 1996; Phillips and Barrett, 2012). Although the accuracy of this approach is affected by the superposition of idealization and directional load decoupling as two sources of errors (Konuk and Gracie, 2004; Nobahar et al., 2007b; Lele et al., 2011; Peek and Nobahar, 2012; Phillips and Barrett, 2012; Eltaher, 2014; Pike and Kenny, 2016), it is still a cost-effective approach that is undertaken by the pipeline industry.

All of the solutions developed based on this approach have considered uniform soil strata, while complex layered seabed with non-uniform strata have been broadly observed in offshore areas scoured by icebergs (e.g., Chukchi Sea (Winters and Lee, 1984; C-CORE, 2008), Alaskan Beaufort Shelf (C-CORE, 2008), Russian Sakhalin Island (C-CORE,

1995e), etc.). The significance of the impact of layered seabed soil on ice gouging process has been highlighted in the literature as an existing knowledge gap (NRC-PERD, 2014; BSEE-WGK, 2015; Winters and Lee, 1984; Babaei and Sudom, 2014; Alba, 2015). In case of a layered seabed (see Figure 4-1), the subgouge soil deformation is significantly influenced by strength properties of the soil layers and their interaction that affects the failure mechanisms and seabed reaction forces on the ice keel.

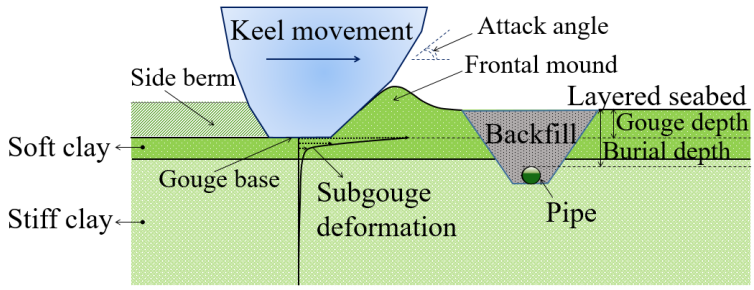

Figure 4-1: Schematic view of ice gouging process in layered cohesive seabed

The current study investigates the effect of layered seabed soil strata on the seabed response to the free-field ice gouging process using large deformation finite element analysis (LDFE). The study has focused on the soft over stiff clay soil strata that has been observed in the western Chukchi Sea (Winters and Lee, 1984).

Conventional FEA analysis of a rate-independent elastoplastic continuum model affected by strain localization, inherently suffer from mesh dependency. The reason is the loss of mathematical well-posedness of initial or boundary value problems that result in the solution uniqueness and dependency on the boundary data. To overcome these limitations, Coupled Eulerian-Lagrangian (CEL) and Arbitrary Lagrangian-Eulerian (ALE) approaches have been used in the past for the large deformation analysis of the ice gouging process (Konuk and Gracie, 2004; Babaei and Sudom, 2014; Pike and Kenny, 2016).

Although the Arbitrary Lagrangian-Eulerian (ALE) method has resolved some of the limitations of the conventional Lagrangian method, but still suffers from a limited mesh distortion (Banneyake et al., 2011). In these LDFE approaches, the Eulerian body (e.g., soil) can easily interact with Lagrangian domain (e.g., ice) and flow through the fixed meshes without any concern about the mesh over-distortion and instability problems.

The soil in ice gouging analysis is usually modeled as an elastic perfectly plastic material which is a fast and simple approach (e.g., Pike and Kenny, 2016). However, it is known today that the undrained shear strength of soil actually increases with increasing the shear strain rate, and decreases in the area with the large plastic shear strain (e.g., Biscontin and Pestana, 2001; DeGroot et al., 2007; Lunne and Andersen, 2007; Hossain and Randolph, 2009; DeJong et al., 2012). This can significantly influence the failure mechanisms, the mobilized soil resistance and the resultant subgouge soil deformation in ice gouging analysis. Therefore, it is important to incorporate these effects in the soil plastic behaviour.

In this study, based on the layered seabed configuration reported by Winters and Lee (1984), a numerical ice gouge model was developed using the Coupled Eulerian Lagrangian (CEL) method in ABAQUS/Explicit. The friction angle was set as zero in the classical Mohr Coulomb and the strain rate and strain-softening effects were incorporated by coding the solution proposed by Einav and Randolph (2005) into a user subroutine (i.e., VUSDFLD). The developed model was verified against the published centrifuge test results (Allersma and Schoonbeek, 2005). A comprehensive parametric study was conducted to examine the effects of key parameters on the ice gouging, including ice features (i.e., keel width, gouge depth, and attack angle) and layered soil features (soil layer

thickness and strength). The influence of the parameters was evaluated based on the resultant subgouge soil deformation, keel reaction forces, progressive plastic shear strains distribution, and the interaction intensity between two soil layers (e.g., the sliding tendency between the soil layers). The developed model was proven to be an efficient and robust approach in engineering practice. The study provided a good insight into the assessing the response of complex layered seabed to the ice gouging event.

4.2. Numerical model

4.2.1. CEL model configuration

In order to be able to verify the model performance against the published experimental test results, the geometry and parameters of the CEL model were set according to the centrifuge tests conducted by Allersma and Schoonbeek (2005) on layered soil. A symmetric model with overall dimensions of the Eulerian domain as 40 × 20 × 15 m (length, width, depth, respectively) was used to mitigate the computational effort. . The soil and ice were modelled as Eulerian and Lagrangian domains, respectively to enable flowing the material through the fixed mesh. The Eulerian domain was discretized using the 8-node linear Eulerian brick elements with reduced integration and hourglass control (EC3D8R). A constant element size was considered that was refined in the areas with large soil deformation. The element size were gradually increased to its maximum value in the vertical upward and downward directions. The ice keel was modelled as using 8-node linear brick elements with reduced integration and hourglass control (C3D8R) with a base length of 10.8 m, a width of 6 m, and an attack angle of 27° which was initially pre-indented into the seabed at a depth of 2.2 m (see Figure 4-2).

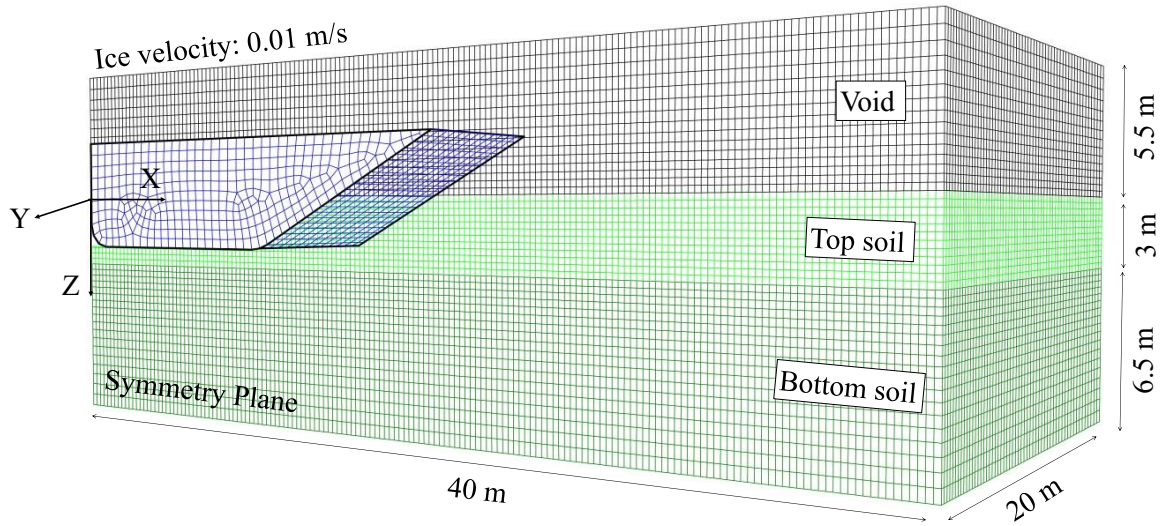

Figure 4-2**:** FEA model configuration

An Eulerian part was created representing the space to enable the layered soil to deform and interact with the ice keel. Reference parts were used to separate the domains. The volume fraction tool was used to assign the material to the layered soil (e.g., 3 m soft clay overlaying a 6.5 m stiff clay in the base analysis). A void domain of 5.5 m height was left to accommodate the soil front mound and side berm formations during the gouging process.

Velocity boundary conditions were considered to displace the ice keel and control the model boundaries. The velocity in the direction normal to the boundary surfaces was restricted for the Eulerian domain to avoid material flowing out of the model. Two analysis steps were conducted including a geostatic step and a dynamic explicit step. During the initial geostatic step, the in situ geostatic stress was distributed through soil depth. In the second dynamic explicit step, the ice keel was horizontally displaced at a constant velocity of 0.01 m/s for a duration of 800 seconds.

General contact algorithm was defined between the ice keel and the seabed soil. A "hard" behaviour was used for the normal interaction, and an isotropic coulomb friction formulation was set for the tangential interaction. The soil layers were defined as a single continuum domain with varying geomechanical properties through the layers. A friction coefficient of 0.3 and 0.4 was used for the contact surfaces in ice keel-soft soil interaction and ice keel-stiff soil interaction, respectively. The maximum allowable interface shear stress was controlled by setting the interface shear stress limit to be 0.5 s_{ui} (s_{ui} was the value of measured in situ undrained shear strength in gouge depth) (Pike and Kenny, 2016).

4.2.2. Constitutive soil model

Soil properties were set according to the experimental Test No. 9 (soft clay layer over the stiff over-consolidated clay layer) reported by Allersma & Schoonbeek (2005). The loading process was fast enough to ensure the undrained condition of soil. The seabed soil was modelled as elastic-perfectly plastic clay obeying the Tresca criterion. Both friction and dilation angles were set as zero, and the Poisson's ratio was assumed to be 0.499. The icebergs are usually separated from the glaciers in the Arctic areas in the warm seasons, travel far away, and arrive in the subsea pipelines in the areas with seawater and seabed soil temperature above the zero. This justify assuming a zero friction and dilation angle for clay. The in situ undrained shear strength (s_{ui}) was taken as 25 kPa and 110 kPa respectively for soft and stiff layer. These values were constant through the depth as reported by Allersma & Schoonbeek (2005). The Young's modulus was assumed as 500 s_{ui} and constant throughout each soil layer.

4.2.2.1. Strain rate dependency and strain-softening effects

The effect of strain rate dependency and strain softening were incorporated in constitutive soil model by coding the user subroutine VUSDFLD in ABAQUS and using the empirical equation (see equation (4-1)) proposed by Einav and Randolph (2005). At each time increment in the analysis, the subroutine was called by the solver and equation (4-1) was used to update the undrained shear strength (s_u) based on the current accumulated absolute plastic shear strain (ξ) and the average rate of maximum shear strain ($\dot{\gamma}_{max}$) in the previous time step.

$$s_u = \left[1 + \mu \times log\left(\frac{max\left(\left(|\dot{\gamma}_{max}|, \dot{\gamma}_{ref}\right)\right)}{\dot{\gamma}_{ref}}\right)\right] \times \left[\delta_{rem} + (1 - \delta_{rem})e^{-3\xi/\,\xi_{95}}\right]s_{ui} \quad (4\text{-}1)$$

Both sections in the square brackets include two constants and one variable. The increase rate of the shear strength per log cycle (μ) and the reference shear strain rate ($\dot{\gamma}_{ref}$) are constant, while the maximum shear strain rate ($\dot{\gamma}_{max}$) is a variable. The ratio of fully remoulded to initial shear strength (or the inverse of the sensitivity) (δ_{rem}) and the value of accumulated absolute plastic shear strain resulting in 95% reduction in the remoulded shear strength (ξ_{95}) are constant while the incremental value of the current accumulated absolute plastic shear strain (ξ) is varying. The parameter s_{ui} is the undrained shear strength measured at the reference shear strain rate before making changes according to the effects.

The constant parameters for the soil model used in the benchmark analysis are shown in Table 4-1.

Table 4-1: Soil mechanical properties used in FE analysis

Parameter	Value
Mass density, ρ	2065 kg/m^3
Poisson's ratio, ν	0.499
Rate of shear strength increase, μ	0.1
Reference shear strain rate, $\dot{\gamma}_{ref}$	0.024 s^{-1}
Soil sensitivity, S_t	2.0
Ratio of fully remoulded to initial shear strength, δ_{rem}	0.5
Accumulated absolute plastic shear strain for 95% reduction in strength due to remoulding, ξ_{95}	12

As shown in Table 4-1, the value of μ was taken as 0.1 that is in a range of 0.05 to 0.2 as suggested in the literature (Dayal and Allen, 1975; Graham et al., 1983; Biscontin and Pestana, 2001). The reference shear strain rate $\dot{\gamma}_{ref}$ was assumed to be 0.024 s^{-1} as suggested by the numerical study conducted by Raie and Tassoulas (2009). The variable parameter $\dot{\gamma}_{max}$ was calculated incrementally using equation (4-2) during the analysis:

$$\dot{\gamma}_{max} = \frac{(\Delta\varepsilon_1 - \Delta\varepsilon_3)}{\Delta t} \tag{4-2}$$

where $\Delta\varepsilon_1$ and $\Delta\varepsilon_3$ are the cumulative major and minor principal strains over the time increment, Δt.

For typical soft marine clays the value of ξ_{95} was set to be 12, which is in a range of 10 to 25 as suggested by Randolph (2004) (for soil from rapidly softening soil to gradually softening). The δ_{rem} was taken as 0.5 as the inverse of the assumed soil sensitivity.

The target is to find the incremental ratio of the mobilized undrained shear strength to the in situ values (FV= s_u /s_{ui}) at every individual Gaussian points for each soil element in

different depths. Therefore, FV, is the field variable that is incrementally calculated in VUSDFLD subroutine and used to update the shear strength and fed into the solver. Figure 4-3 shows the flowchart of the main solver calling the subroutine VUSDFLD.

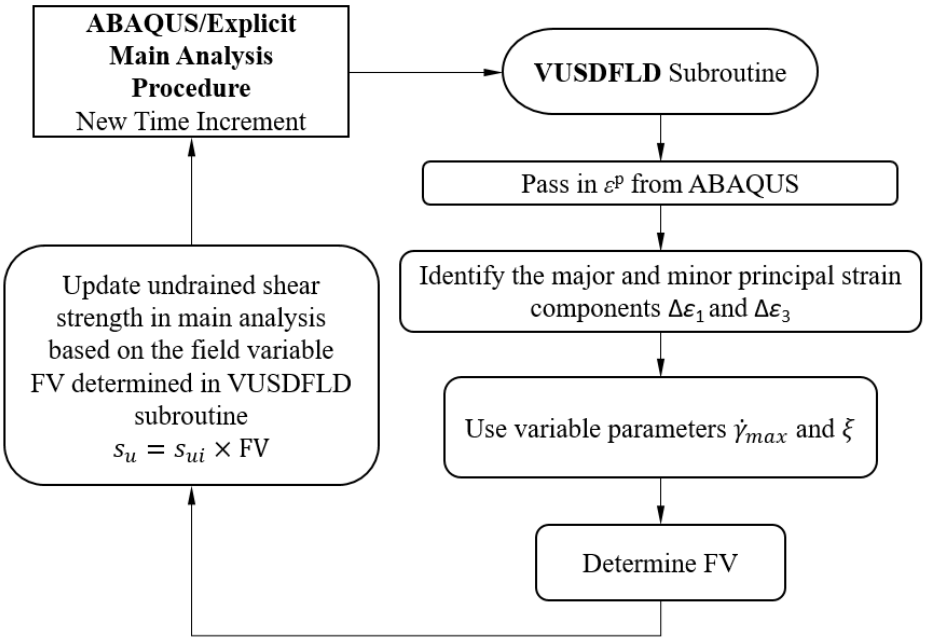

Figure 4-3: Flowchart declaring the interaction between the solver and the user subroutine, VUSDFLD

4.2.2.2. Mesh sensitivity analysis

To find the optimal mesh size in terms of accuracy and computational effort, a mesh sensitivity study was conducted. The model's geometrical configuration and the parameters were provided in Section 4.2.1, and soil properties were given in Section 4.2.2. Three different mesh sizes were examined, including a fine mesh size of 0.15 m, a medium mesh size of 0.25 m, and a coarse mesh size of 0.5 m. The reaction forces and subgouge soil deformation were obtained from the analyses using different mesh sizes and plotted in Figure 4-4.

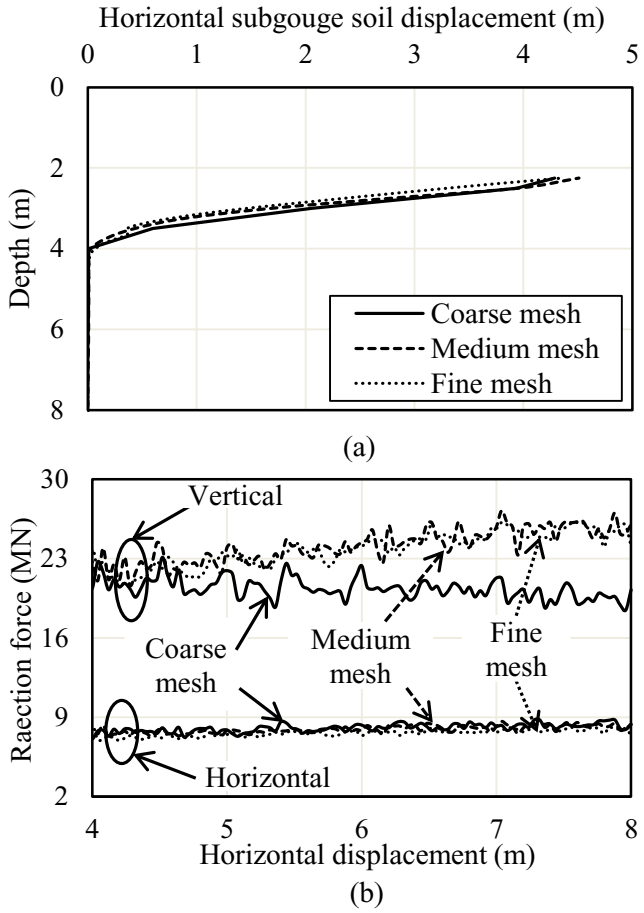

Figure 4-4**:** The results of mesh sensitivity analysis

The number of elements and the corresponding run time showing the computational efforts required for analysis are summarized in Table 4-2.

Table 4-2: Mesh convergence analysis for free-field ice gouge simulations

Case	Min. Element Size (m)	Max. Element Size (m)	Number of Eulerian Elements	Run Time on 76 CPUs
1	0.5	0.5	96,000	0 hrs. 11 min.
2	0.25	0.5	396,000	0 hrs. 57 min.
3	0.15	0.5	1,123,803	4 hrs. 18 min.

As shown in Figure 4-4 (a), slight differences could be observed in the subgouge soil deformation for different mesh sizes, while the coarse mesh (Case 1) provided a slightly conservative prediction. A similar trend could be observed in Figure 4-4 (b) for the horizontal reaction force of the ice keel. However, for the vertical reaction forces (see Figure 4-4 (b), a noisy response was obtained by the coarse mesh (Case 1) and remarkably differed from the responses obtained by the medium and fine mesh cases (Case 2 and 3). A good match was also observed in Figure 4-4 (b) between the responses obtained from the medium and fine mesh cases (Case 2 and 3). Comparing the results obtained in the Figure 4-4 (a) and the solution run time in Table 4-2, the medium mesh size (Case 2) was selected for the model verification analysis and the comprehensive parametric study to achieve an optimal balance between the computation efficiency and solution accuracy.

4.3. Model verification

The developed model was verified through comparing the results with the classical Mohr-Coulomb (MC) model predictions and the published experimental study results (i.e., Test 9 conducted by Allersma & Schoonbeek (2005)). Figure 4-5 shows the comparison of the predicted and tested soil deformations.

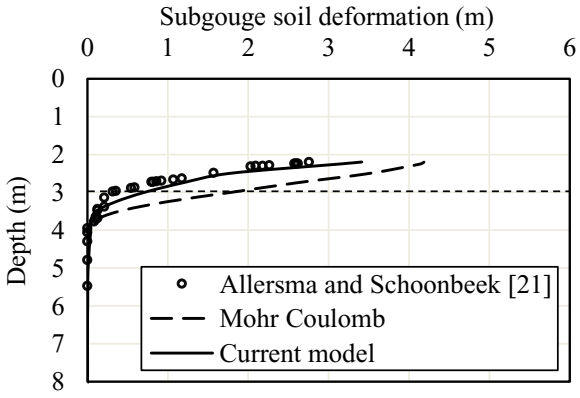

Figure 4-5**:** The Comparison of the tracked soil deformation

The subgouge soil deformations obtained from the current study match well with the experimental results in (Allersma and Schoonbeek, 2005). The remarkable overestimation of subgouge soil deformation by the classical MC model emphasized the significance and importance of incorporating the strain rate dependency and strain-softening effects into the modified Tresca model. By accounting these effects in the modified Tresca model, the in situ undrained shear strength (s_{ui}) increased by a factor of 2.14 in the areas with high shear strain rate and resulted in a stiffer soil response compared with the classical MC model. In the depths closer to base of the ice keel, the magnitude of subgouge soil deformation computed by the modified Tresca model was significantly closer to the published experimental results than the classical MC model. This area is the most crucial region for the prediction of soil and pipe displacements due to ice attack. It should be noted that based on the test condition, ice gouging never reached to the steady-state condition.

4.4. Parametric study

A comprehensive parametric study was conducted through 24 case studies (CS-1 to CS-24) to investigate the influence of the key parameters of the free-field ice gouging model,

including the geometry of the ice keel (attach angle and keel width), gouge depth of the ice keel, the thickness and strength of the layered-soil. The parametric study map is illustrated in Table 4-3.

Table 4-3: Parametric study layout

	Ice			**Soil**	
	Attack angle (°)	Gouge depth (m)	Keel width (m)	Soil layer thicknesses (m/m)	Soil strength conditions
CS-1	27	0.5	12	3/15	Soft/Stiff
CS-2	27	1.5	12	3/15	Soft/Stiff
CS-3	27	2.2	12	3/15	Soft/Stiff
CS-4	27	3.5	12	3/15	Soft/Stiff
CS-5	27	5	12	3/15	Soft/Stiff
CS-6	15	2.2	12	3/15	Soft/Stiff
CS-7	27	2.2	12	3/15	Soft/Stiff
CS-8	45	2.2	12	3/15	Soft/Stiff
CS-9	27	2.2	5	3/15	Soft/Stiff
CS-10	27	2.2	12	3/15	Soft/Stiff
CS-11	27	2.2	20	3/15	Soft/Stiff
CS-12	27	0.5	12	1/17	Soft/Stiff
CS-13	27	1.5	12	1/17	Soft/Stiff
CS-14	27	2.2	12	1/17	Soft/Stiff
CS-15	27	3.5	12	1/17	Soft/Stiff
CS-16	27	5	12	1/17	Soft/Stiff
CS-17	27	2.2	12	3/15	Uniform soft
CS-18	27	2.2	12	3/15	Uniform stiff
CS-19	27	5	12	3/15	$s_{ui\ \mathrm{Stiff}}$ doubled
CS-20	27	5	12	3/15	$s_{ui\ \mathrm{Stiff}}$ halved
CS-21	27	5	12	3/15	$s_{ui\ \mathrm{Soft}}$ doubled
CS-22	27	5	12	3/15	$s_{ui\ \mathrm{Soft}}$ halved
CS-23	27	3.5	12	3/15	Uniform soft
CS-24	27	3.5	12	3/15	Uniform stiff

The undrained shear strength profile of the layered soil for the base analyses (CS-1 to CS-11) in the parametric study map was adopted from the data collected in Chukchi Sea by Winters and Lee (1984) (see Figure 4-6).

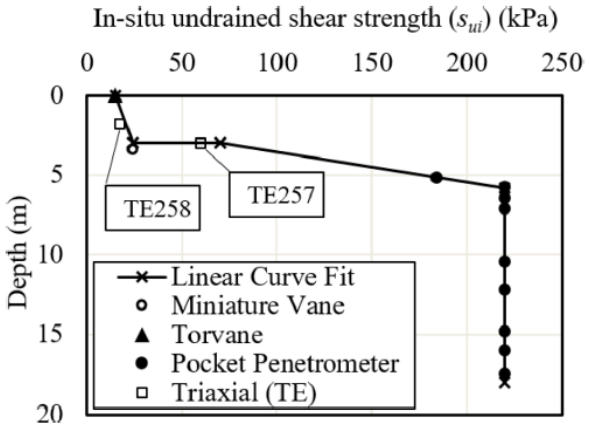

Figure 4-6**:** Undrained shear strength (s_{ui}) profile of the layered soil

In section 4.4.1 and section 4.4.2, the results obtained on the effects of ice keel features and layered soil properties are presented.

4.4.1. Effect of ice keel features and gouging configuration

The effect of ice attack angle, gouge depth and keel width were investigated respectively through CS-1 to CS-11. The reaction forces and subgouge soil deformations obtained in these case studies are plotted in Figure 4-7. The RF1 and RF3 refer to the horizontal and vertical reaction forces, respectively.

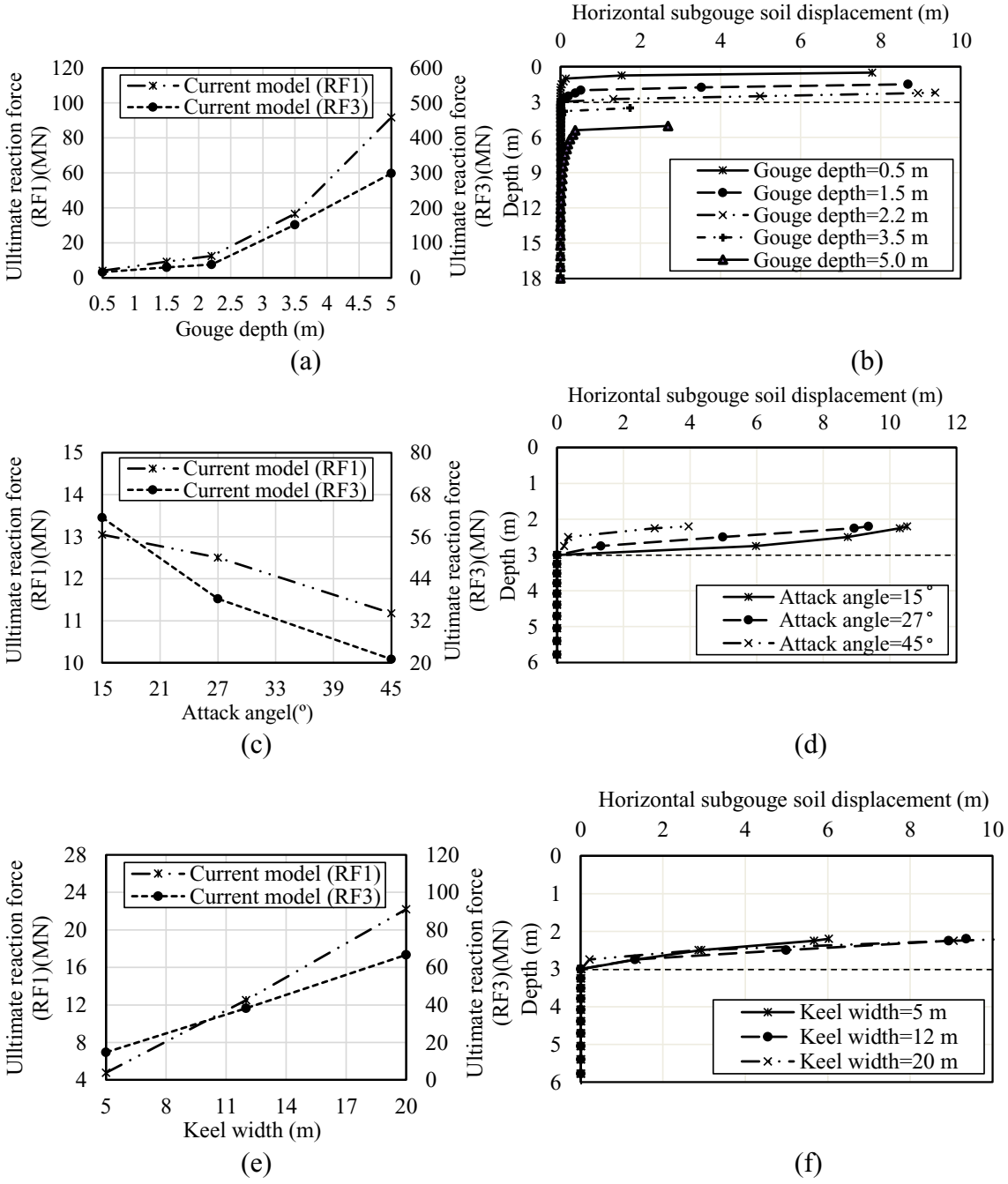

Figure 4-7: The effect of different attack angles, keel widths, and gouge depths on reaction forces and subgouge soil deformations (CS-1 to CS-11)

Given the gouge depth of ice keel used in the case studies (CS-6 to CS-11) was less than the thickness of the upper layer of the soil (soft clay), the ice keel bottom was initially in contact with the upper soft clay layer only. Figure 4-7 (a) and (b) show that for the gouge depths less than the thickness of soft layer (i.e., 3m) the subgougue soil displacements are truncated in the bottom of soft layer and the deformations are not transferred to the stiff layer. This truncation of deformations causes the reaction forces to be solely generated from the ice keel contact with the soft layer. When the gouge depth is less than the thickness of soft layer, a direct shear happens in the border of soft and stiff layers, and the soft soil is somehow slides on the surface of stiff layer. The industry can take the advantage of this interesting observation for design and construction of subsea pipelines in the proximity of Arctic areas. In other words, if the ultimate potential gouge depth in a given geographical location that is determined based on probabilistic and statistical studies, is less than the thickness of the upper soft layer, then it would be safe to bury the pipeline right below the soft layer inside the stiff layer. Because, the current study shows that the subgouge soil displacements are stopped in the border of layers and not transferred to the stiff layer. This is in agreement with the study conducted by Palmer et al. (1990) and Palmer (1997). As the gouge depth increases from 0.5 m (in CS-1) to 5 m (in CS-5), the lower stiff layer starts to contribute and significantly rise the magnitude of reaction forces. Also, the subgouge soil deformation increases in the stiff layer. However, the increasing rate is less for the gouge depth closer to the border of layers (i.e., 3.5m).

Figure 4-7 (c) and d show that in both horizontal and vertical direction, the reaction forces of the ice keel are decreased with increasing the attack angle, which is in agreement with all of the earlier studies. The effect of attack angle was observed only in soft layer due to

truncation in the border of layers; the shallower the attack angle, the larger the subgouge soil displacement. The larger keel width resulted in a higher reaction forces (see Figure 4-7 (e)) and a larger subgouge soil deformation (see Figure 4-7 (f)).

The effect of different gouge depths on the progressive plastic shear strains and the quality of soil formations is illustrated in Figure 4-8.

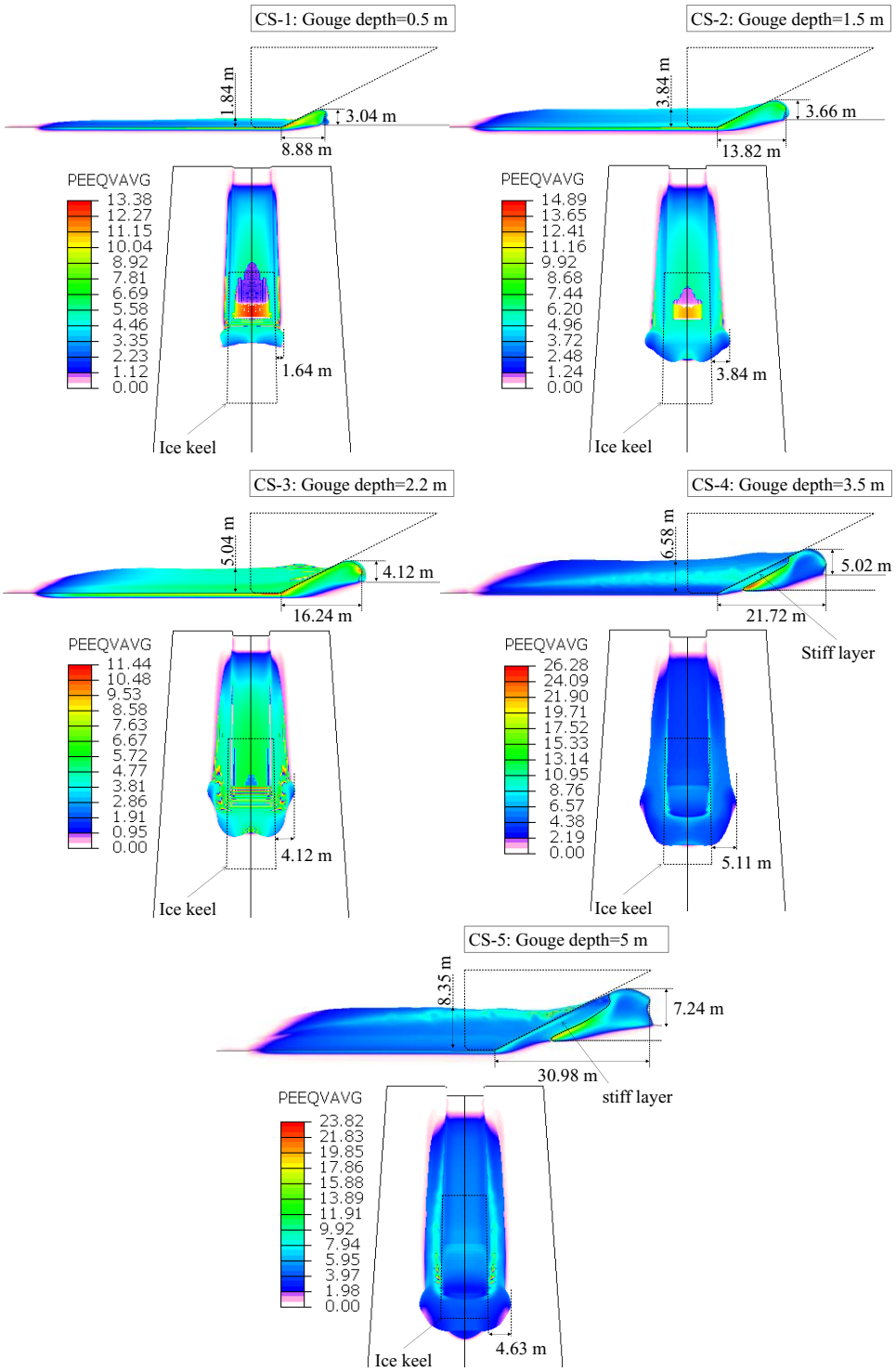

Figure 4-8: The effect of gouging with different depths on progressive plastic shear strain and quality of soil formation

Figure 4-8 shows that by increasing the gouge depth, the size of frontal mound and side berms are increased. In the case studies with a gouge depth less than 3 m (CS-1, CS-2 & CS-3) the maximum plastic shear strain occurs in the contact areas between the keel chest and frontal mound, and the keel base and the underneath soft soil. In the case studies with the ice keel initially located in the stiff soil at a gouge depth larger than 3 m (CS-4 & CS-5) the soft soil experienced the maximum plastic shear strain in the border of layers, where the soft soil is pushed by the stiff soil behind it. Also, the magnitude of produced plastic shear strain was almost twice the cases with the gouge depth less than 3 m. These trends show that the layered soil condition magnifies the plastic shear strains in the border of layers. This, in turn, shows the significance of incorporating the strain rate and softening effects on the undrained shear strength and the resultant reaction forces and subgouge soil deformation.

4.4.2. Effect of layered soil strata

Analyses were conducted to investigate the effect of layering seabed on ice keel-seabed interaction. The key output were compared from uniform soft (CS-17 & CS-23), uniform stiff (CS-18 & CS-24), and soft over stiff layers (CS-3 & CS-4). Figure 4-9 shows the soil in situ undrained shear strength profile adopted for these case studies.

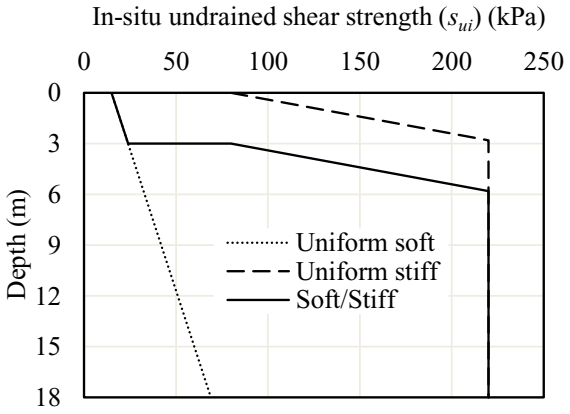

Figure 4-9: In situ undrained shear strength (s_{ui}) profile

Different gouge depths were considered with the ice keel tip inside the soft and stiff layers, respectively. Figure 4-10 compares the reaction forces and subgouge soil displacements for the soft, stiff, and soft over stiff layers.

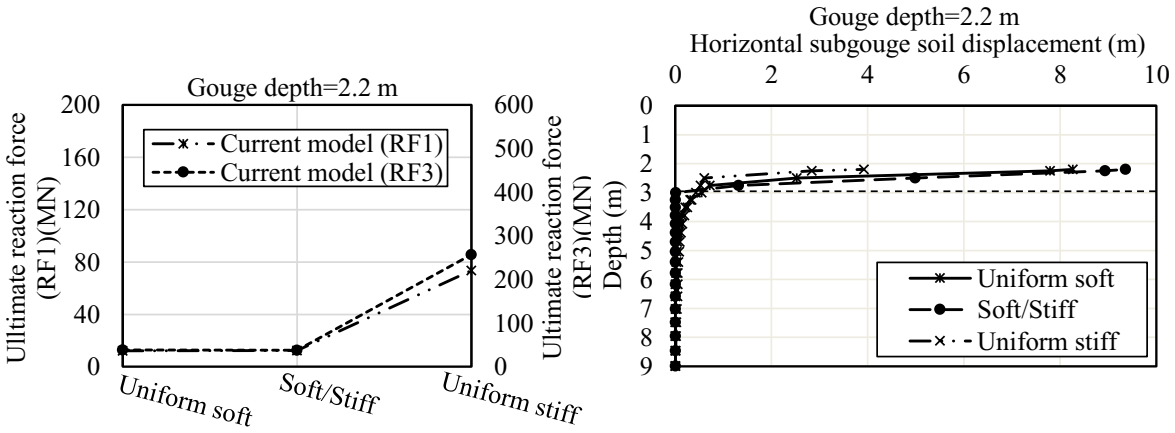

(a) (b)

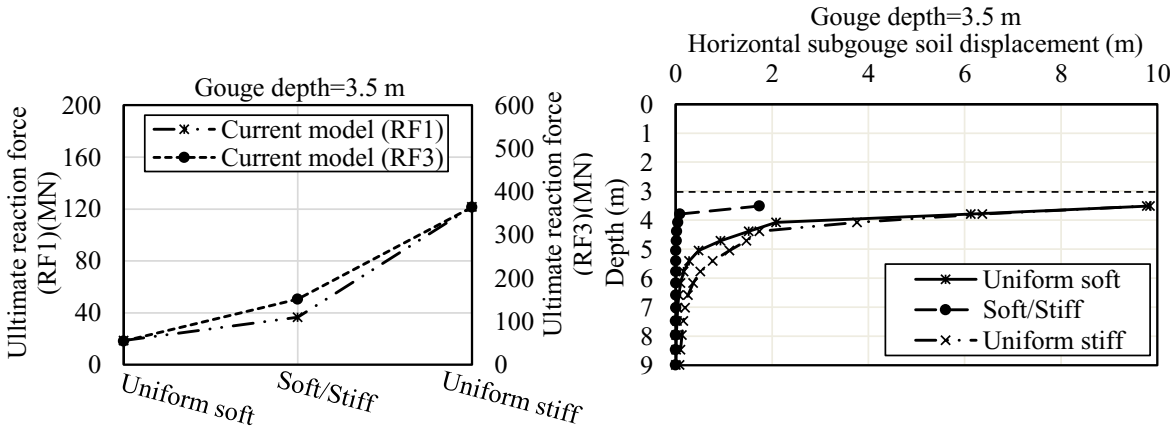

(c) (d)

Figure 4-10: The effect of gouging in different layered soil strata on reaction forces and subgouge soil deformation

Figure 4-10 (a) shows identical reaction forces for uniform soft and soft over stiff strata, where the bottom of ice keel in shallow gouge depth condition was in pure contact with the soft clay. The uniform stiff soil shows higher reaction forces. Figure 4-10 (c) shows that the reaction forces are higher for deeper gouge in uniform soft and stiff layers. For deeper gouge, the reaction forces in soft over stiff layers are no longer identical to uniform soft seabed because the bottom of ice keel is in contact with both soft and stiff layers. Figure 4-10 (c) shows that the reaction forces in soft over stiff seabed is less than uniform stiff layer. This shows the significance of incorporation of layered seabed in engineering design practice that can result in considerable cost reduction in this case. Figure 4-10 (b) shows that the subgouge soil displacement in layered seabed is smaller in deeper areas compared with uniform soft soil. However, their magnitudes are almost identical right underneath the ice keel. These interesting results show the significance of soil layer interaction and its dominance in the subgouge soil deformation. The engineering practice can take the

advantage of these observations to improve the safety and cost-effectiveness of pipeline design against ice gouging. Figure 4-10 (b) shows larger subgouge soil deformations in uniform stiff seabed. The results presented in Figure 4-10 (d) interestingly show that the subgouge soil deformation in layered seabed is less than the uniform soft clay in the proximity of layers interaction line. This again shows the dominance of layers interaction effect that overrides the individual strengths of uniform soil layers.

Figure 4-11 compares the equivalent plastic shear strains (PEEQVAVG) along with frontal mound, side berm formation, and the layers interaction in uniform and layered seabeds.

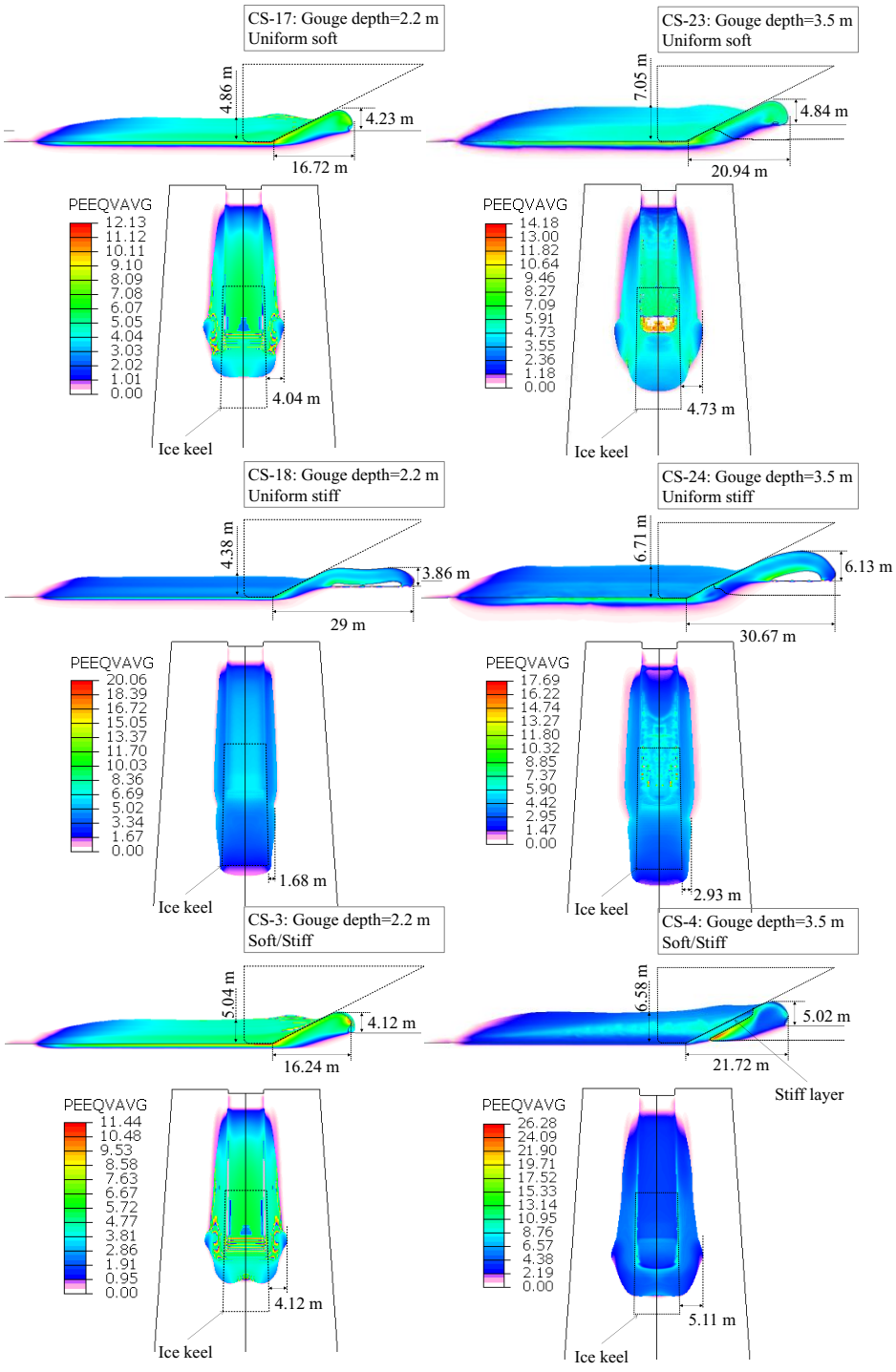

Figure 4-11: The effect of gouging in different layered soil strata on progressive plastic shear strain and quality of soil formation

Figure 4-11 shows that distribution of maximum plastic shear strain follow the same approach for uniform soft and soft over stiff layer soil in ice gouging with a gouge depth less than 3 meter (CS-17 & CS-3). In those cases, plastic shear strain globally developed the maximum values in the contact areas between the keel chest and frontal mound, and the keel base and the underneath soft soil. The produced frontal mound and side berms are almost in the same dimensions as well. The frontal mound developed in the uniform stiff clay (CS-18) showing a high integrity and in a consistency action jumped in front of the ice keel. The maximum plastic shear strain in this case, was localized in the borders of frontal mound with air and ice keel and also the contact surface between the keel base and the soil on the bottom. Also the magnitude of the developed plastic shear strain was almost twice the values for uniform soft and soft over stiff clay. In the case studies with the gouge depth larger than 3 meter (CS-23 & CS-4) the plastic shear strain was more locally developed in front of the ice keel comparing with the cases by shallower gouging. For the soft over stiff layer case study (CS-4), the front soft soil was pushed by the stiff layer on behind and resulted the maximum plastic shear strain to be localized in the narrow area of contact between two kind of soils.

4.4.3. Effect of different soil layer thicknesses

Analyses were conducted to investigate the effect of considering soil with different layer thicknesses on gouging performance. Ice gouging in two layered soil strata, 1 m soft over 17 m stiff and 3 m soft over 15 m stiff, were examined. Analyses were conducted for ice gouging in three different gouge depths, 0.5 m, 2.2 m and 3.5 m. The result of reaction forces and subgouge soil deformation is illustrated in Figure 4-12.

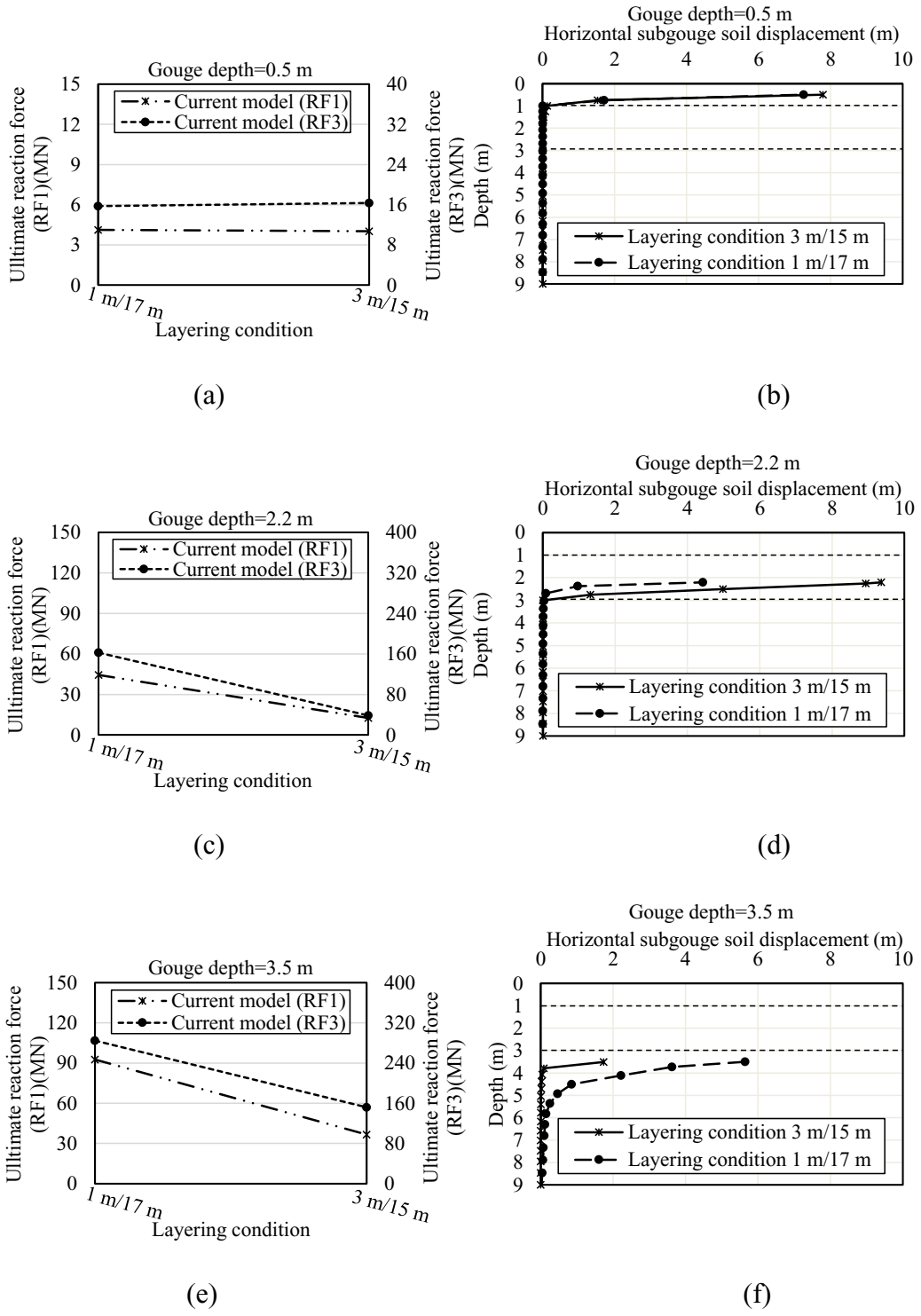

Figure 4-12: The effect of gouging in soils with different layered thicknesses on reaction forces and subgouge soil deformation

Figure 4-12 (a) and (b) show almost identical results for two different soil layering condition, 1 m over 17 m and 3 m over 15 m, where the keel base never touched the stiff layer (CS-12 & CS-1). Figure 4-12 (c) and (e) confirms that the larger amounts of stiff soil carried by keel, the larger developed the keel reaction forces. Figure 4-12 (d) shows the subgouge soil deformation is larger when the keel base was gouging in a soft layer that was located on top of a stiff layer (CS-3) comparing when the keel base was in touch with a stiff layer (CS-14). Figure 4-12 (f) shows although the keel base was in touch with stiff layer for two cases (CS-15 & CS-3) but the subgouge soil deformation was larger when the keel was start gouging in deeper depth in stiff layer (CS-15).

Figure 4-13 compares the equivalent plastic shear strains (PEEQVAVG) along with frontal mound, side berm formation, and the layers interaction in soils with different layer thicknesses.

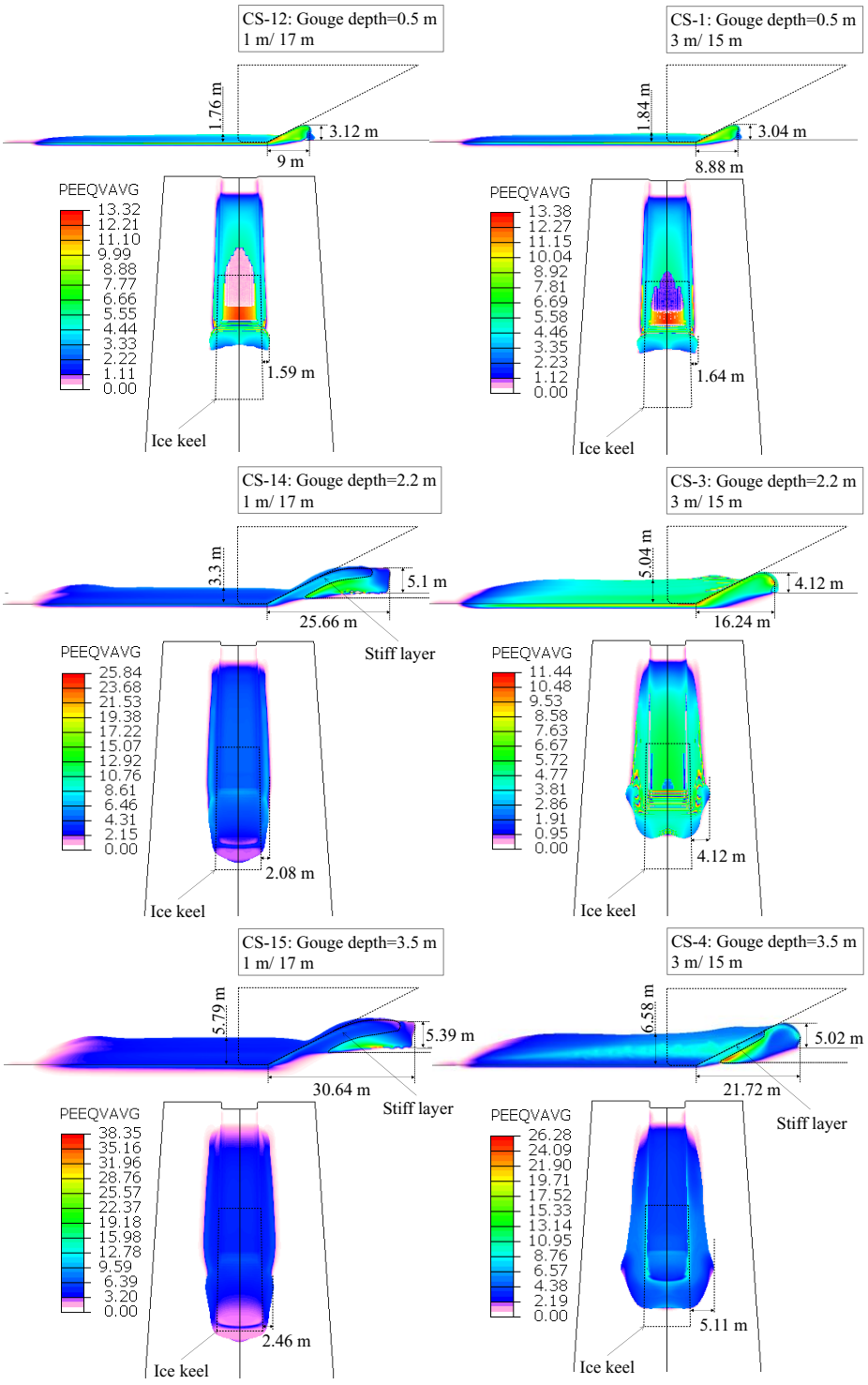

Figure 4-13: The effect of gouging in soils with different layered thicknesses on progressive plastic shear strain and quality of soil formation

Figure 4-13 shows the same trend in the quality of the distribution of equivalent plastic shear strain for two cases with gouge depth less than 1 m (CS-12 & CS-1). Maximum values of plastic shear strain was developed right at the bottom of keel base. A global distribution of plastic shear strain was showed for frontal mound. Plastic shear strain was localized in the soft soil particles located right beneath the integrated stiff layer pushing the soft layer on front. In that cases (CS-14, CS-15 & CS-4) keel base was located at the stiff layer at the start of gouging. The more volume of stiff layer gouged by keel, the less extension of maximum plastic shear strain towards the frontal mound (Comparing CS-14 & CS-15 with CS-4). A narrow localized plastic shear strain distributed from behind the stiff soil extended towards the top of frontal mound was seen in CS-4. Again a global distribution of plastic shear strain was seen in the case study, CS-3, in which the keel base didn't touch the stiff layer.

4.4.4. Effect of layers' strength ratio

Analyses were conducted to investigate the effect of different strength ratios between two layers of the soil strata on ice keel-seabed interaction. Four new case studies were defined (CS-19 to CS-22) and the results were compared with the base soft over stiff case study with gouge depth equal to 5 m (CS-5). Following the base soft over stiff soil layer strength condition, the intercept undrained shear strength magnitude of soft and stiff layer increased and decreased by the coefficients of 2 and 0.5 (Doubled and halved) and made our 4 new cases (See Figure 4-14 and Table 4-4).

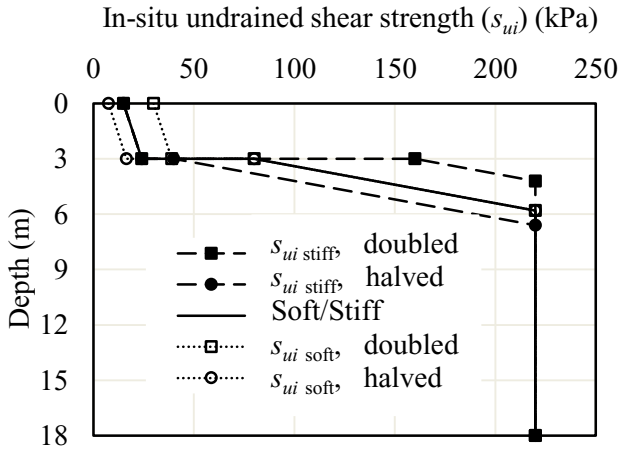

Figure 4-14: In situ undrained shear strength (s_{ui}) profile (CS-19 to CS-22)

Table 4-4: The intercepts of undrained shear strength magnitude of the soil layer

s_{ui} soft / s_{ui} stiff		Case studies				
		CS-5	CS-19	CS-20	CS-21	CS-22
		Base	s_{ui} stiff, doubled	s_{ui} stiff, halved	s_{ui} soft, doubled	s_{ui} soft, halved
Intercept undrained shear strength magnitude (kPa)	Soft	15	15	15	30	7.5
	Stiff	80	160	40	80	80

Figure 4-15 compares the reaction forces and subgouge soil displacements for the defined case studies (CS-5 & CS-19 to CS-22).

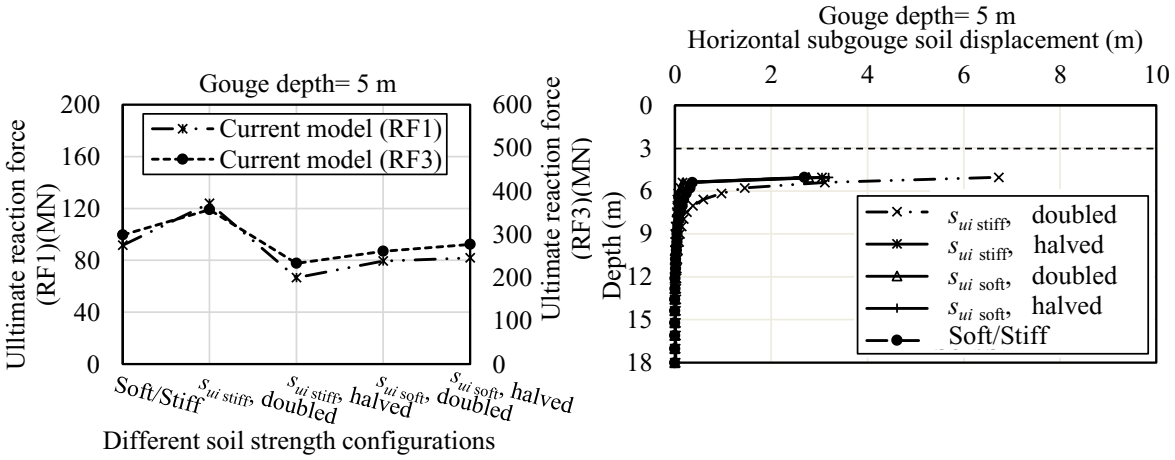

(a) (b)

Figure 4-15: The effect of different soil undrained shear strength profiles on reaction forces and subgouge soil deformations (CS-5 & CS-19 to CS-22)

Comparing with the base case (CS-5) results, by increasing the strength of stiff layer (CS-19) the magnitude of reaction forces were increased and by decreasing of that (CS-20) the magnitude of reaction forces were decreased. By increasing the strength of soft layer (CS-21) the reaction forces were lightly decreased comparing with the base values. Also by doubling the magnitude of shear strength of soft layer (CS-21) the reaction forces decreased comparing with the results got from halving the magnitude of shear strength of soft layer (CS-22). The reason for such this surprising results could be figured out by exploring the quality of the soil formation in front of ice keel including the pushing stiff layer and the carrying soft layer. Figure 4-15 (b) shows that doubling the strength of the bottom stiff layer (CS-19) could make a significant increase in subgouge soil deformation. The

subgouge soil deformation was increased when the strength of soft soil was halved (CS-22) comparing by the case when the strength of soft soil was doubled (CS-21).

Figure 4-16 compares the equivalent plastic shear strains (PEEQVAVG) along with frontal mound, side berm formation, and the layers interaction in soils with different undrained shear strength profile.

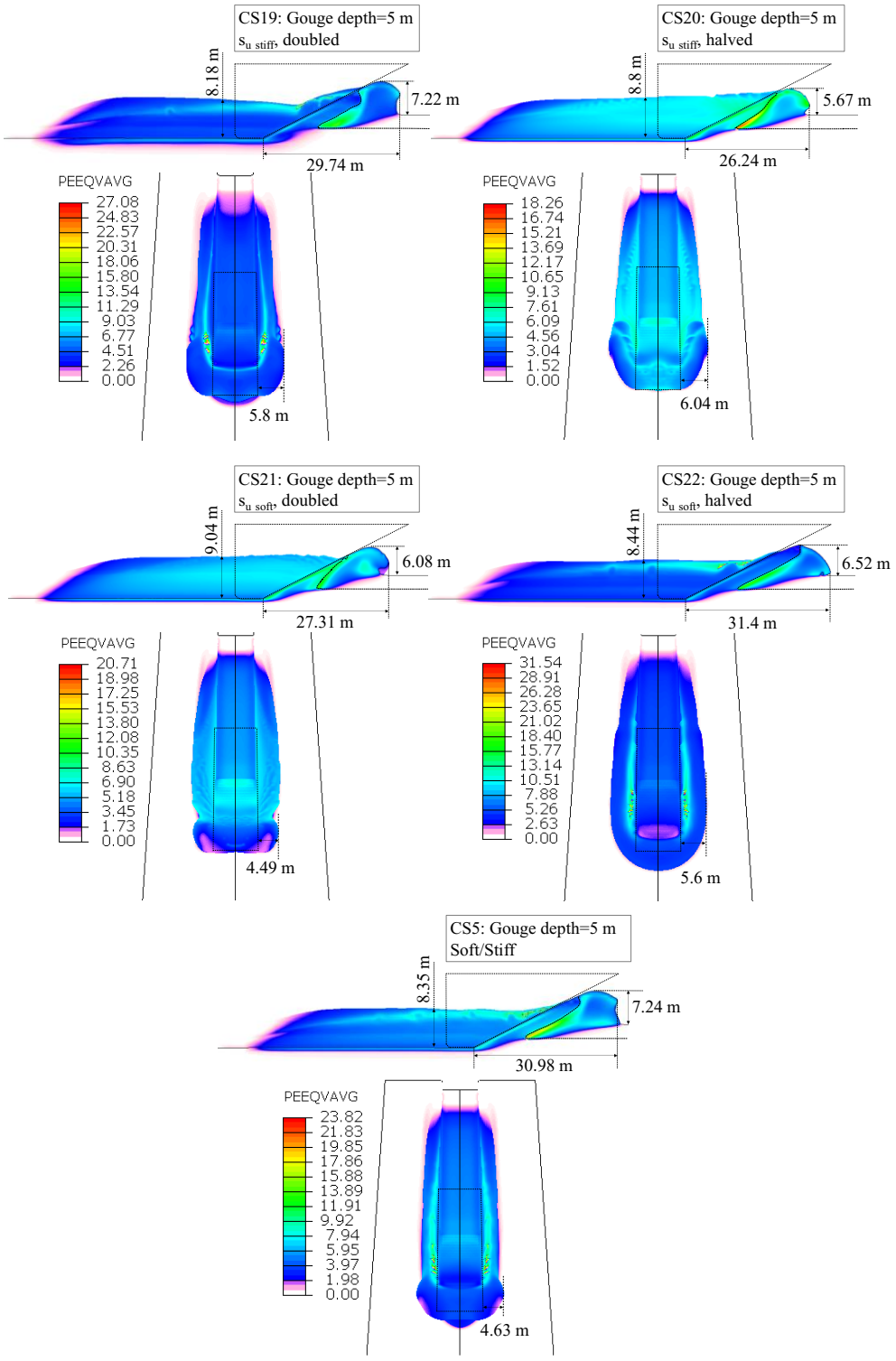

Figure 4-16: The effect of soil with different strength ratios on the progressive plastic shear strain and the quality of soil formation

Comparing with the base case results (CS-5), Figure 4-16 shows that by increasing the strength of stiff layer (CS-19), the less amount of stiff soil were developed to push the soft soil in front. Also the volume of soft soil collected in frontal mound was at highest level among the other three cases and was almost equal to the amount collected in base case. The quality of stiff soil formation was different for the case when the strength of stiff layer was decreased (CS-20). A sharp deformation was seen at top of the stiff soil and the dimensions of frontal mound was also decreased. Maximum plastic shear strain in this case was developed more locally and was extended from the border of contact between two soils in soft soil to top of soft soil in frontal mound. Also the dimensions of the frontal mound and the volume of mixed soils in front of ice keel were at the lowest level.

A sharp formation of stiff soil was also seen in the case when the strength of soft soil was increased (CS-21) similar to what was seen in the results when the strength of stiff soil was decreased (CS-20). Also the volume of stiff soil developed in this case study was at the lowest level. By decreasing the shear strength of soft soil (CS-22) the highest amount of stiff soil was developed in front of ice keel.

4.5. Conclusions

In this paper, the ice gouging process in layered seabed including soft over stiff clay was comprehensively investigated using CEL modeling approach. A modified Tresca model was coded in a user-subroutine in ABAQUS to incorporate the rate dependence and strain softening effect. The developed numerical model was verified against published experimental results and the classical MC soil model predictions. A parametric study was

conducted to investigate the effects of ice keel and layered soil characteristics. The key findings of the study can be summarized as follows:

- The interactions between the soil layers with different strengths could significantly override the usual seabed response to ice gouging in a uniform soil. In the soft over stiff clay, for the gouge depths less than the thickness of the soft layer, the subgouge soil deformation was truncated in the interface of the soil layers. This suggests that the trench depth can be safely limited to thickness of soft layer, and the pipeline buried in stiff layer with its crown touching the soft layer. This in turn would need new trenching technics to excavate an opening in the trench bed to locate the pipe. Overall, it is highly recommended to consider the effect of soil layering, where applicable.
- The effects of strain rate dependency and strain softening were found to be significant in the loading area with high developed plastic shear strain. These areas include the interface of different soil layers, and the proximity of ice keel soil contact zone. It was observed that the conventional soil models may overestimate the subgouge soil deformation and reaction forces.
- The seabed reaction forces in layered soil is in between the ones from uniform layers, i.e., lower than uniform stiff clay and higher than uniform soft clay. The magnitude of difference depends on the thickness and shear strength of each layer, and also the gouge depth. This shows the significance of modeling layers seabed soil strata where applicable.

- The study showed that the same as the uniform soil, the intensity of the ice gouging could be influenced by the by the geometry of the ice keel. In both horizontal and vertical direction, the reaction force of the ice keel decreased with the increase in keel attack angle, and increased with the increasing keel width.

4.6. Acknowledgments

The authors gratefully acknowledge the financial support of this research by Wood PLC via establishing the Wood Group Chair in Arctic and harsh environment engineering at Memorial University, the NL Tourism, Culture, Industry and Innovation (TCII) via CRD collaborative funding program, the Natural Sciences and Engineering Research Council of Canada (NSERC) via CRD funding program, the Memorial University of Newfoundland through the school of graduate studies (SGS) baseline fund.

References

Alba, J. L. , 2015, Ice Scour and Gouging Effects With Respect to Pipeline and Wellhead Placement and Design, Bureau of Safety and Environmental Enforcement (BSEE), Wood Group Kenny, Report No. 100100.01.PL.REP.004, Houston, TX.

Allersma, H.G.B., and Schoonbeek, I.S.S. (2005). Centrifuge modelling of scouring ice keels in clay. Int. Conference on Offshore and Polar Engineering, ISOPE2005, Seoul, June 19-24, paper 2005-JSC-427, pp.404-409

Babaei, M. H., & Sudom, D. (2014). Ice-seabed gouging database: review and analysis of available numerical models. In *OTC Arctic Technology Conference*. Offshore Technology Conference.

Banneyake, R., Hossain, M. K., Eltaher, A., Nguyen, T., Jukes, P., 2011. Ice-soil pipeline interactions using coupled eulerian-lagrangian (CEL) ice gouge simulations extracts from ice pipe JIP. Paper presented at the OTC Arctic Technology Conference.

Biscontin, G., Pestana, J.M., 2001. Influence of peripheral velocity on vane shear strength of an artificial clay. Geotech. Test.J. 24(4), 423–429.

BSEE-WGK (2015). Ice Scour and Gouging Effects with Respect to Pipeline and Wellhead, Final Report, 100100.01.PL.REP.004, Rev0.

C-CORE. (1995e). Pressure Ridge Ice Scour Experiment, PRISE: Phase 3-Centrifuge Modelling of Ice Keel Scour: Draft Final Report. April 1995. Publication 95-C12, 52p.

C-CORE. (2008). Design Options for Offshore Pipelines in the US Beaufort and Chukchi Seas. April 2008. Report R-07-078-519.

Dayal, U., Allen, J. H., 1975. The effect of penetration rate on the strength of remolded clay and sand samples. Can. Geotech. J., 12(3),336–348.

DeGroot, D. J., DeJong, J. T., Yafrate, N. J., Landon, M. M., Sheahan, T. C., 2007. Application of recent developments in terrestrial soft sediment characterization methods to offshore environments. Proc., Offshore Technology Conf., Houston, OTC 18737.

DeJong, J., DeGroot, D., Yafrate, N., 2012. Evaluation of undrained shear strength using full-flow penetrometers. J. Geotech. Geoenviron. Eng.138(6),765–767.

Einav, I., Randolph, M. F., 2005. Combining Upper Bound and Strain Path Methods for Evaluating Penetration Resistance. International Journal for Numerical Methods in Engineering, Vol. 63, No. 14, pp. 1991-2016.

Eltaher, A., 2014. Gaps in Knowledge and Analysis Technology of Ice Gouge Pipeline Interaction. Proceedings of the Arctic Technology Conference, February 10 - 12, 2014, 10p.

Graham, J., Crooks, J. H. A., Bell, A. L., 1983. Time effects on the stress-strain behaviour of natural soft clays. Geotechnique, 33(3), 327–340.

Hossain, MS, Randolph, MF, 2009. Effect of Strain Rate and Strain Softening on the Penetration Resistance of Spudcan Foundations on Clay. International Journal of Geomechanics, Vol 9, No 3, pp 122-132.

Konuk, IS., Gracie, R., 2004. A 3-dimensional Eulerian FE model for ice scour. IPC04-0075, pp.1911-1918.

Lele, S., Hamilton, J., Panico, M., Arslan, H., Minnaar, K., 2011. 3D continuum simulations to determine pipeline strain demand due to ice-gouge hazards. Arctic Technology Conference, ATC.

Lunne, T., Andersen, K. H., 2007. Soft clay shear strength parameters for deepwater geotechnical design. Proc., 6th Int. Offshore Site Investigation and Geotechnics Conf.: Confronting New Challenges and Sharing Knowledge, Vol. 1, Society for Underwater Technology, London, 151–176.

Nobahar, A., Kenny, S., Phillips, R., 2007b. Buried pipelines subject to subgouge deformations. International Journal of Geomechanics, vol. 7, no. 3, pp. 206-216.

NRC-PERD (2014), Ice-Seabed Gouging Database: Review & Analysis of Available Numerical Models (Babae, M.H. and Sudom, D. (2014)); Physical Simulations of Seabed Scouring by Ice: Review and Database (Barrette, P. and Sudom, D. (2014)).

Palmer, A., 1997. Geotechnical evidence of ice scour as a guide to pipeline burial depth. Can. Geotech. J. 34 (6), 1002–1003.

Palmer, A.C., Konuk, I., Comfort, G., and Been, K. (1990). Ice gouging and the safety of marine pipelines. Proc., OTC, 3, OTC 6371, pp.235-244.

Peek, R., Nobahar, A., 2012. Ice gouging over a buried pipeline: Superposition error of simple beam-and-spring models. International Journal of Geomechanics, vol. 12, no. 4, pp. 508-516.

Pike, K., Kenny, S., 2016. Offshore pipelines and ice gouge geohazards: Comparative performance assessment of decoupled structural and coupled continuum models. Canadian Geotechnical Journal, 53(11), 1866-1881.

Phillips, R., Barrett, J., 2012. PIRAM: Pipeline Response to Ice Gouging. Proceedings of the Arctic Technology Conference, December 3 - 5, 2012, 6p.

Raie, M., Tassoulas, J., 2009. Installation of torpedo anchors: numerical modeling. J. Geotech. Geoenviron. Eng. 135 (12), 1805–1813.

Randolph, M. F., 2004. Characterization of soft sediments for offshore applications. Keynote Lecture, Proc., 2nd Int. Conf. on Site Characterization, Porto, Portugal, Vol. 1, Millpress Science Publishers, Rotterdam, 209–231.

Winters, W. J. and Lee, H. J. (1984). Geotechnical properties of samples from borings obtained in the Chukchi Sea, Alaska. USGS Report 85-23.

Woodworth-Lynas, C., Nixon, D., Phillips, R., Palmer, A., 1996. Subgouge Deformations and the Security of Arctic Marine Pipelines. Proc. 28th OTC, Vol. 4, Paper No. 8222, pp. 657–664.

Chapter 5

Numerical Modeling of Ice-seabed Interaction in Layered Soil: Stiff over Soft Clay

Seyedhossein Hashemi, as the main author, is credited for the methodology, modeling, data curation, visualization, investigation, validation and writing-original draft. Hodjat Shiri is credited for conceptualization, supervision, writing-review and editing and funding acquisition

This chapter is submitted as a journal manuscript to Applied Ocean Research.

.

Abstract

The current study presents the numerical investigation of free field ice gouging in layered cohesive seabed comprising stiff over soft clay. Three dimensional, half-space, dynamic large deformation finite element (LDFE) analysis was conducted using the Coupled Eulerian Lagrangian (CEL) approach. A Tresca soil model along with the strain rate and strain-softening effects was coded into a user subroutine to simulate the seabed. The model was verified through comparison with published experimental studies. A comprehensive parametric study was conducted to examine the effect of different ice gouging scenarios and seabed soil parameters on the subgouge soil deformation and the ice keel reaction forces. The study showed an interactive response in between the soil layers and the ice keel that may cause the peak subgouge soil deformation and keel reaction magnitudes to be significantly different from the uniform soil condition. The developed model was found to be an efficient tool for modelling free field ice gouging analysis in cohesive layered seabed.

Keywords: Ice gouging, Subgouge soil deformation, Stiff over soft clay, Numerical simulation, Strain rate and strain-softening effects

5.1. Introduction

In the Arctic offshore regions and neighbouring areas that are reached by traveling icebergs, the ice gouging (ice tip scouring the seabed) is known as a major threat to the structural integrity of subsea pipelines. Burying the pipelines below the highest potential gouge depths is a common method for physical protection of pipelines against the ice gouging (see Figure 5-1).

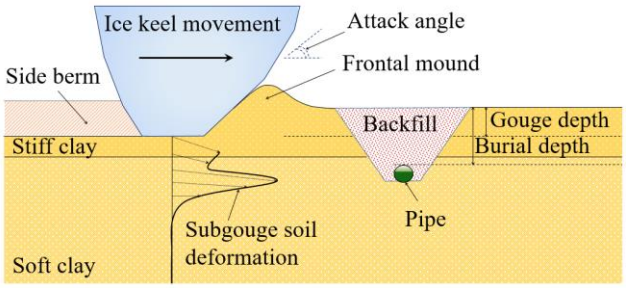

Figure 5-1**:** Schematic view of ice gouging process in layered cohesive seabed

The lateral and vertical soil displacement is not limited to the depth of the ice keel tip. The shear resistance of the seabed soil causes the subgouge soil deformation to extend much deeper than the ice keel tip. This, in turn, attacks the subsea pipelines and mandates achieving a sufficient burial depth to ensure the structural integrity of the pipeline. Finding the best burial depth satisfying the safety and economical consideration is a challenging aspect. In practice, a decoupled approach is usually undertaken by engineers, where, a continuum large deformation finite element analysis of free field ice gouging process is conducted. Then, the results of subgouge soil deformations are transferred to a simplified beam-spring model to obtain the structural response of the pipeline (Woodworth-Lynas et al., 1996; Phillips and Barrett, 2012). Therefore, the free field ice gouging analysis is a key

part of the design practice. However, the seabed is usually represented by a uniform material domain ignoring the complexities and implications that may arise from layered seabeds (e.g., Konuk and Gracie, 2004; Nobahar et al., 2007b; Lele et al., 2011; Peek and Nobahar, 2012; Phillips and Barrett, 2012; Eltaher, 2014; Pike and Kenny, 2016).

There exist a knowledge gap in the literature digging in to the ice gouging performance in non-uniform layered soil strata (Winters and Lee, 1984; Babaei and Sudom, 2014; Alba, 2015) while layered seabed has been broadly observed in Arctic offshore scoured areas with oil and gas activities ongoing (e.g., Chukchi Sea (Winters and Lee, 1984; C-CORE, 2008), Alaskan Beaufort Shelf (C-CORE, 2008), Russian Sakhalin Island (C-CORE, 1995e), etc.).

The very few published experimental and numerical studies investigating the ice gouging in layered seabed (e.g., Allersma and Schoonbeek, 2005; Hashemi and Shiri, 2022a) have shown that interactive mechanisms in between the soil layers may significantly affect the seabed response to ice gouging.

In this study, the response of a layered seabed comprising stiff over soft clay (e.g., Alaskan Beaufort Sea (Miller and Bruggers,1980)) to the ice gouging has been investigated by performing advanced large deformation finite element (LDFE) analysis using a Coupled Eulerian Lagrangian (CEL) in a fashion similar to earlier studies (e.g., Konuk and Gracie, 2004; Babaei and Sudom, 2014; Pike and Kenny, 2016), where the material could flow through the Eulerian fixed mesh surrounded by the defined velocity boundary conditions. However, despite these conventional studies that have typically considered uniform soil strata with an elastic perfect plastic seabed soil material obeying von Mises or Tresca

criterion, the current study incorporated the strain rate and strain softening effects as well, through coding a user-defined subroutine (VUSDFLD) and modifying the classical Mohr Coulomb soil model. Strain rate dependency and strain softening during shearing and remoulding are two natural behaviours of cohesive soils affecting the value of soil undrained shear strength. It is generally agreed that increasing shear strain rate leads to increase in undrained shear strength (e.g., Biscontin and Pestana, 2001; DeGroot et al., 2007; Lunne and Andersen, 2007; DeJong et al., 2012). Also, within large shear strains, the strain softening causes a gradual loss of shear strength (Hossain and Randolph, 2009). Including these effects in the current study improved the accuracy of simulating of ice gouging process in layered seabed as a high velocity geotechnical problem involving large deformations. During the analysis, the user subroutine is incrementally called by ABAQUS to update the undrained shear strength of the soil based on the incremental values of the currently accumulated absolute plastic shear strain and the calculated maximum shear strain rate with zero value adopted for friction and dilation angles. The performance of the model was earlier verified (Hashemi and Shiri, 2022a & b) through comparisons with published experimental studies (Allersma and Schoonbeek, 2005; Lach, 1996).

A comprehensive parametric study was conducted to examine the ice keel-seabed interaction in a layered seabed and the effect of a range of different input parameters including the ice keel geometry, gouge depth, seabed soil strength and layering condition on the keel reaction forces, subgouge soil deformation, quality of soil formation and progressive plastic shear strains distribution.

It was observed that replacing a stiff over soft clay with a uniform seabed for simplicity can be significantly misleading resulting in non-reliable subgouge soil deformation magnitudes and keel reaction forces. The study showed that an interactive mechanism between the stiff and soft layer may cause large subgouge deformation in soft layer even if the ice keel tip dose nor reach the soft soil under the stiff clay. This finding is quite significant and has never been reported in earlier studies. The study suggests performing accurate numerical and experimental studies of ice gouging in case of having stiff over soft clay seabed stratum.

5.2. Numerical model

5.2.1. CEL model configuration

Using a CEL algorithm in ABAQUS/Explicit, the rigid ice keel (the Lagrangian body) was initially pre-indented in to the soil (the Eulerian domain) to achieve the desired gouge depth. The ice keel was modeled using 8-node linear brick elements with reduced integration and hourglass control (C3D8R) which was constraint to displace in horizontal direction only. A half-space soil domain with overall dimensions of 95 × 25 × 30 m (length × width × depth) was modelled and discretized using 8-node linear Eulerian brick elements with reduced integration and hourglass control (EC3D8R). Appropriate mesh densities were considered for the area with different deformations. An stiff clay layer of 3 m was considered on top of a 15 m soft clay. A void domain of 12 m high was considered on top of the seabed to accommodate the seabed surface deformations during the ice gouging process (see Figure 5-2).

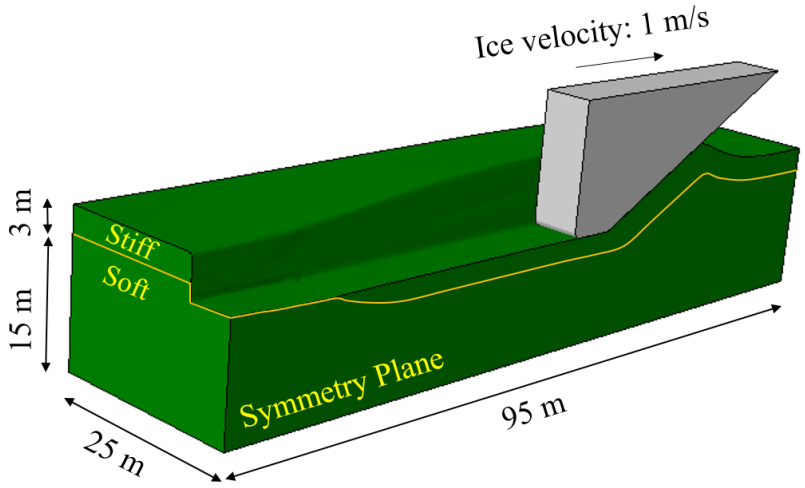

Figure 5-2**:** FEA model configuration

Two analysis steps were defined. First, an initial geostatic step was conducted to initialize the soil under in situ stress condition through the soil depth. Second, a dynamic explicit analysis was conducted to horizontally move the ice keel through the soil domain at a constant velocity of 1 m/s.

A general contact algorithm was adopted defining the interaction between ice keel and the seabed soil. The ice keel-soil interaction properties were modelled by defining "hard contact" in the normal direction and an isotropic coulomb friction theory for tangential direction. Friction coefficients (μ) of 0.4 and 0.3 were considered for the ice-stiff soil and ice-soft soil contact pairs, respectively. The maximum allowable shear stress at the interface was set to be limited to 0.5 s_{ui}, where s_{ui} is the value of measured in situ undrained shear strength in gouge depth (Pike and Kenny, 2016).

5.2.2. Constitutive soil model

The seabed soil was modeled as an elastic-perfectly plastic material obeying the Tresca failure criterion. Zero value was adopted for both friction and dilation angles. Ice gouging

process is sufficiently fast for clay to be considered undrained. In all of the analyses, undrained conditions of clay was approximately satisfied by taking the value of Poisson's ratio equal to 0.499, which is large enough to minimize the volumetric strains without any concerns about numerical instabilities. The in situ undrained shear strength of the layered soil was distributed through the depth based on the field data reported by Miller and Bruggers (1980) for the Alaskan Beaufort Sea. The stiffness ratio, E/s_{ui} (E, Young's modulus) was taken as 500.

5.2.2.1. Strain rate dependency and strain-softening effects

The effects of both strain rate and strain softening on the shear strength of the soil during undrained shearing in a large deformation process were incorporated into the constitutive soil model. Using the empirical formulation proposed by Einav and Randolph (2005) (see equation (5-1)), a user-defined subroutine (VUSDFLD) was coded in FORTRAN and linked to the main processor of the ABAQUS/Explicit. This equation incrementally updates the in situ undrained shear strength (s_{ui}) at each Gaussian point of the soil elements based on the current accumulated absolute plastic shear strain (ξ) and also the average rate of maximum shear strain ($\dot{\gamma}_{max}$) in previous time step:

$$s_u = \left[1 + \mu \times log\left(\frac{max\left(\left(|\dot{\gamma}_{max}|, \dot{\gamma}_{ref}\right)\right)}{\dot{\gamma}_{ref}}\right)\right] \times \left[\delta_{rem} + (1 - \delta_{rem})e^{-3\xi/\xi_{95}}\right] s_{ui} \tag{5-1}$$

The first part of this equation models the effect of strain rate and the second part implements the strain softening effect. The (s_{ui}) is the in situ undrained shear strength measured at the reference shear strain rate prior to any softening and rate effects. In the

first part, the reference shear strain rate ($\dot{\gamma}_{ref}$) and the increase rate of the shear strength per log cycle (μ) are two constant parameters. Also, the maximum shear strain rate ($\dot{\gamma}_{max}$) is an incrementally variable parameter. In the second part, two parameters (δ_{rem}), (ξ_{95}) representing the ratio of fully remoulded to initial shear strength (or the inverse of the sensitivity) and the value of accumulated absolute plastic shear strain resulting in 95% reduction in the remoulded shear strength are two constant parameters. The parameter (ξ) representing the incremental value of the current accumulated absolute plastic shear strain is also varying during the analysis.

Table 5-1 presents the mechanical properties of the seabed and the constant parameters adopted for the conducted parametric analysis.

Table 5-1: Soil mechanical properties used in FE analysis

Parameter	Value
Mass density of top stiff soil, ρ_{stiff}	2000 kg/m^3
Mass density of bottom soft soil, ρ_{soft}	1815 kg/m^3
Poisson's ratio, ν	0.499
Rate of shear strength increase, μ	0.1
Reference shear strain rate, $\dot{\gamma}_{\mathrm{ref}}$	0.024 s^{-1}
Soil sensitivity, S_t	2.0
Ratio of fully remoulded to initial shear strength, δ_{rem}	0.5
Accumulated absolute plastic shear strain for 95% reduction in strength due to remoulding, ξ_{95}	12

A typical value of 0.1 was assumed for μ, which is in a suggested range of 0.05-0.2 (Dayal and Allen, 1975; Graham et al., 1983; Biscontin and Pestana, 2001).

The reference shear strain rate $\dot{\gamma}_{ref}$ was taken as 0.024 s^{-1} same as the value suggested by Raie and Tassoulas (2009) in their conducted numerical study. The maximum shear strain rate $\dot{\gamma}_{max}$ was calculated incrementally as follows:

$$\dot{\gamma}_{max} = \frac{(\Delta\varepsilon_1 - \Delta\varepsilon_3)}{\Delta t} \tag{5-2}$$

where $\Delta\varepsilon_1$ and $\Delta\varepsilon_3$ are the cumulative major and minor principal strains over the time increment, Δt.

A typical value of 12 was taken for ξ_{95}, falling in the range of 10-25 recommended by Randolph (2004) (i.e. 1000 to 2500% cumulative plastic shear strain for a rapidly softening soil to a gradually one respectively). A value of 0.5 was adopted for the parameter δ_{rem} as the inverse of the soil sensitivity.

5.2.3. Mesh sensitivity analysis

A mesh sensitivity study was conducted to find the optimum mesh size satisfying both accuracy and computational effort. The analysis carried out with three different mesh densities, i.e., fine, medium and coarse. The element size was set uniformly with a minimum size in the hot spot areas going under large deformations and enlarging towards the maximum size in the areas with less importance. The minimum and maximum edge length of the elements were set to 0.25 m and 1.0 m for fine mesh, 0.5 m and 1.0 m for medium mesh, and uniformly 1.0 m for coarse mesh, respectively. In the performed mesh sensitivity analysis, the geometry of the model and the soil properties was selected based on Figure 5-2 and the Table 5-1 without implementing the effects of strain rate and strain softening in the soil model. The results of keel reaction forces and the subgouge soil deformation obtained from the mesh sensitivity analysis were plotted in Figure 5-3. Also,

Table 5-2 reports the elements size, number of elements and the corresponding analysis time for three case studies through mesh sensitivity study.

Table 5-2: Mesh sensitivity analysis for free-field ice gouge simulations

Case Study	Min. Element Size (m)	Max. Element Size (m)	Number of Eulerian Elements	Run Time on 76 CPUs
Coarse	1.0	1.0	71,250	0 hrs. 48 min.
Medium	0.5	1.0	292,600	3 hrs. 10 min.
Fine	0.25	1.0	1,083,760	17 hrs. 14 min.

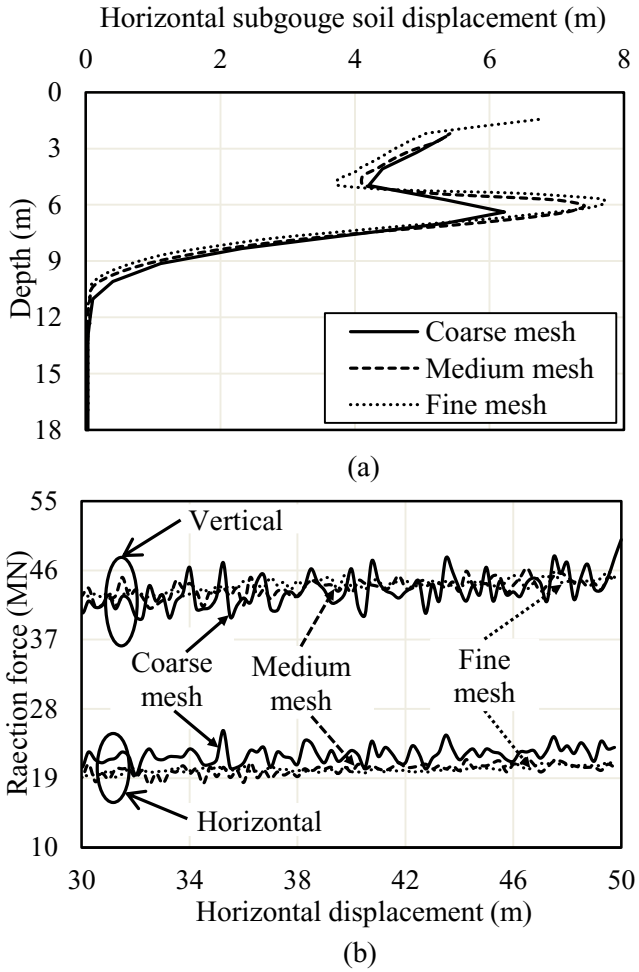

Figure 5-3: The results of mesh sensitivity analysis

The results showed that the subgouge deformation is underestimated using coarse mesh specially for soil particles located in bottom soft layer comparing the results of the other two mesh sizes (see Figure 5-3 (a)). As shown in Figure 5-3 (b), the coarse mesh overestimated the results of the horizontal reaction force and provided a noisy response for the vertical reaction force. A similar response was achieved for reaction forces using both medium and fine meshes. A good agreement was observed between the results of subgouge soil deformation and the keel reaction forces for two cases of medium and fine meshes, confirming the sufficiency of the medium case. However, to capture the soil layers interaction with a high accuracy, a fine mesh was considered for the conducted parametric study.

5.3. Parametric study

A comprehensive parametric study was conducted comprising 24 case studies (CS-1 to CS-24) to investigate the influence of the key parameters of the free-field ice gouging model including ice keel features, gouging configuration, soil strength characteristics and thicknesses of the layered soil strata. Table 5-3 summarizes the key parameters used in the proposed case studies.

Table 5-3: Parametric study layout

	Ice			Soil	
	Attack angle (°)	Gouge depth (m)	Keel width (m)	Soil layer thicknesses (m/m)	Soil strength conditions
CS-1	27	0.5	12	3/15	Stiff/Soft
CS-2	27	1.5	12	3/15	Stiff/Soft
CS-3	27	2.2	12	3/15	Stiff/Soft
CS-4	27	3.5	12	3/15	Stiff/Soft
CS-5	27	5	12	3/15	Stiff/Soft
CS-6	15	2.2	12	3/15	Stiff/Soft
CS-7	27	2.2	12	3/15	Stiff/Soft
CS-8	45	2.2	12	3/15	Stiff/Soft
CS-9	27	2.2	5	3/15	Stiff/Soft
CS-10	27	2.2	12	3/15	Stiff/Soft
CS-11	27	2.2	20	3/15	Stiff/Soft
CS-12	27	0.5	12	1/17	Stiff/Soft
CS-13	27	1.5	12	1/17	Stiff/Soft
CS-14	27	2.2	12	1/17	Stiff/Soft
CS-15	27	3.5	12	1/17	Stiff/Soft
CS-16	27	5	12	1/17	Stiff/Soft
CS-17	27	2.2	12	3/15	Uniform soft
CS-18	27	2.2	12	3/15	Uniform stiff
CS-19	27	5	12	3/15	$s_{ui\ \mathrm{Stiff}}$, doubled
CS-20	27	5	12	3/15	$s_{ui\ \mathrm{Stiff}}$, halved
CS-21	27	5	12	3/15	$s_{ui\ \mathrm{Soft}}$, doubled
CS-22	27	5	12	3/15	$s_{ui\ \mathrm{Soft}}$, halved
CS-23	27	3.5	12	3/15	Uniform soft
CS-24	27	3.5	12	3/15	Uniform stiff

The undrained shear strength profile of the layered seabed for the case studies, CS-1 to CS-11, was adopted by proposing a linear curve fit to some of the geotechnical site investigation data reported by Miller and Bruggers (1980). These tests have been conducted

on soil samples collected from the boreholes drilled in Alaskan Beaufort Sea and the profile was simplified to facilitate interpreting the analysis results (see Figure 5-4).

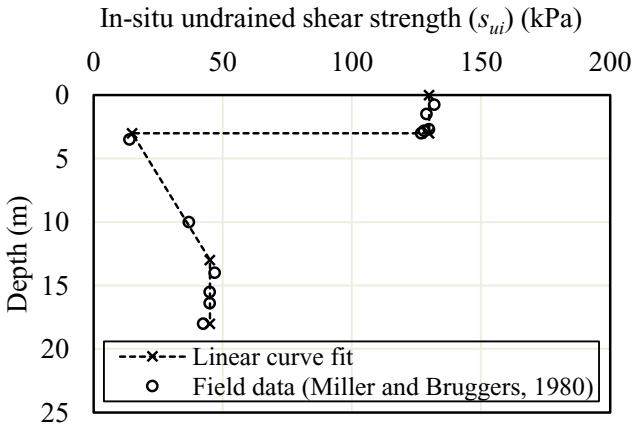

Figure 5-4**:** Undrained shear strength (s_{ui}) profile of the layered soil

In section 5.3.1 and section 5.3.2, the results obtained from the parametric study were discussed in details.

5.3.1. Effect of ice keel features and gouging configuration

The effects of different ice attack angle, ice width, and gouge depth on the performance of ice gouging in layered stiff over soft clay were investigated through CS-1 to CS-11. The horizontal and vertical keel reaction forces (RF1 and RF3) and the corresponding resultant subgouge soil deformations (combined horizontal and vertical deformations) are plotted in Figure 5-5.

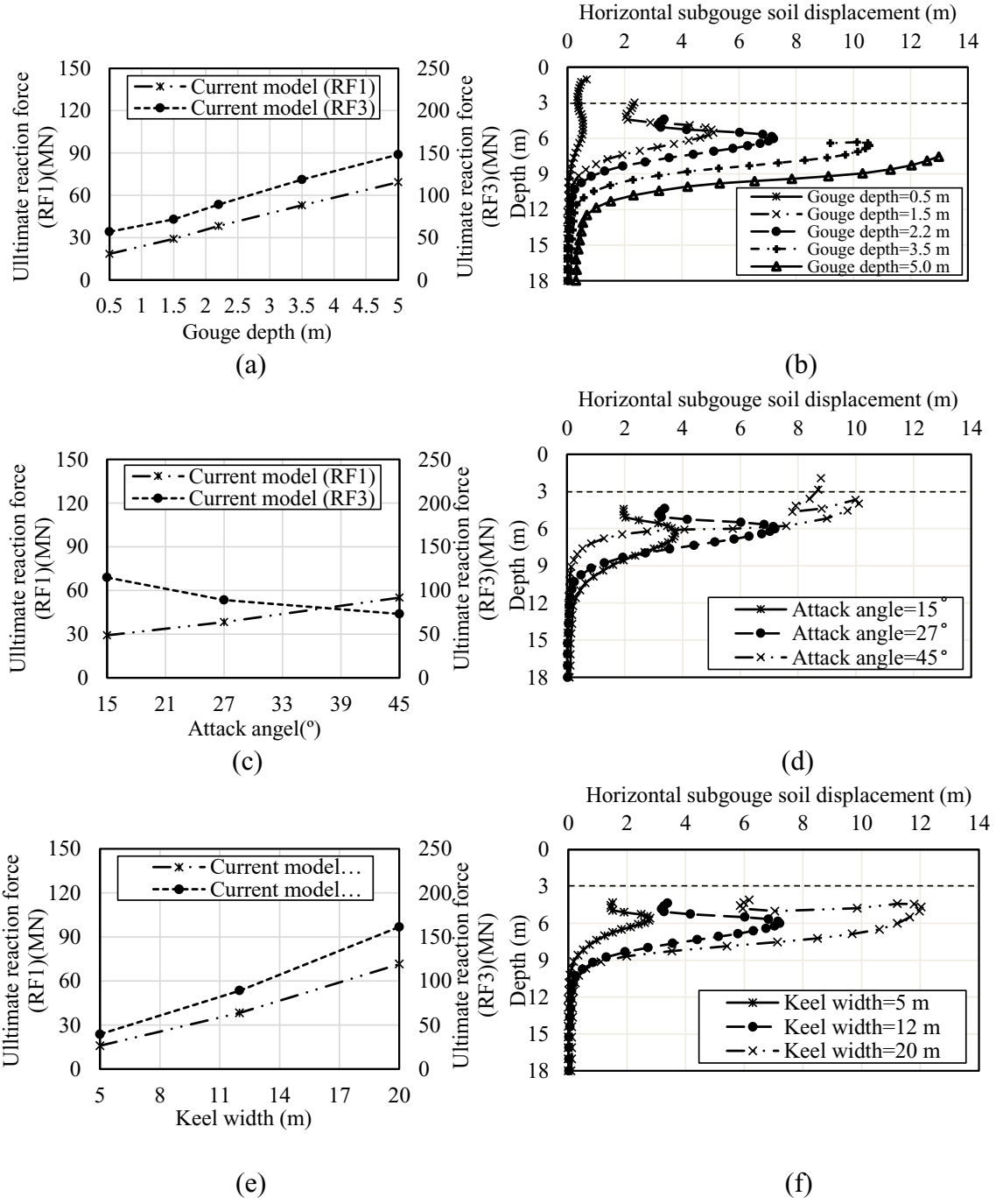

Figure 5-5**:** The effect of different attack angles, keel widths, and gouge depths on reaction forces and subgouge soil deformations (CS-1 to CS-11)

As shown in Figure 5-5 (a) and Figure 5-5 (e), the average reaction forces of the ice keel in the steady state gouging condition are increased with increasing the gouge depth and the keel width. This is similar to regular ice gouging analysis results in a uniform soil, where both of the reaction forces are usually increased with enlarging the contact area between the ice keel and the seabed (e.g., Eltaher, 2014; Pike and Kenny, 2016; and Hashemi and Shiri, 2022b). As seen in Figure 5-5 (c), by increasing the attack angle, the generated horizontal reaction force tends to increase and the vertical reaction force is decreased. This trend is in a similar fashion with uniform soil as well, where the compressive contact pressure in front of the ice keel tends to be a basal shearing zone, as the attack angle is increased. The same mechanism reduces the vertical contact between the ice keel and the seabed soil and results in reducing the vertical reaction force for sharper attack angles.

The results presented in Figure 5-5 (b), Figure 5-5 (d) and Figure 5-5 (f) show a very interesting and significantly important trend in subgouge soil deformation in layered stiff over soft clay. It was observed that the presence of stiff layer on top could cause large soil deformations much deeper in the soft layer. The peak point of these deformations are deeper than deformations expected in uniform soft and uniform stiff clay, which, in turn, shows the interactive nature of the layered seabed response to ice gouging. The generated wavy deformation has a peak value (heave) carried by soil particles located in bottom soft clay with a little distance from the interface. The peak value is intensified by increasing the gouge depth (e.g., from 0.5 m to 2.2 m), where the ice keel is displacing a larger volume of stiff clay. In addition, the subgouge soil deformation profile includes a nadir that is located in the stiff layer right in the proximity of the layer interface. The nadir is gradually faded by increasing the gouge depth stiff soil (e.g., from 3.5 m to 5 m). The intensity and

the peak value of the wavy subgouge soil deformation along with the reaction forces are increased by increasing the attack angle and the keel width (see Figure 5-5 (d), Figure 5-5 (e) and Figure 5-5 (f)).

In order to better understand the observed wavy soil deformation profile, the progressive plastic shear strains along with the side berms and frontal mounds resultant from ice gouging process with different gouge depth were produced and presented in Figure 5-6.

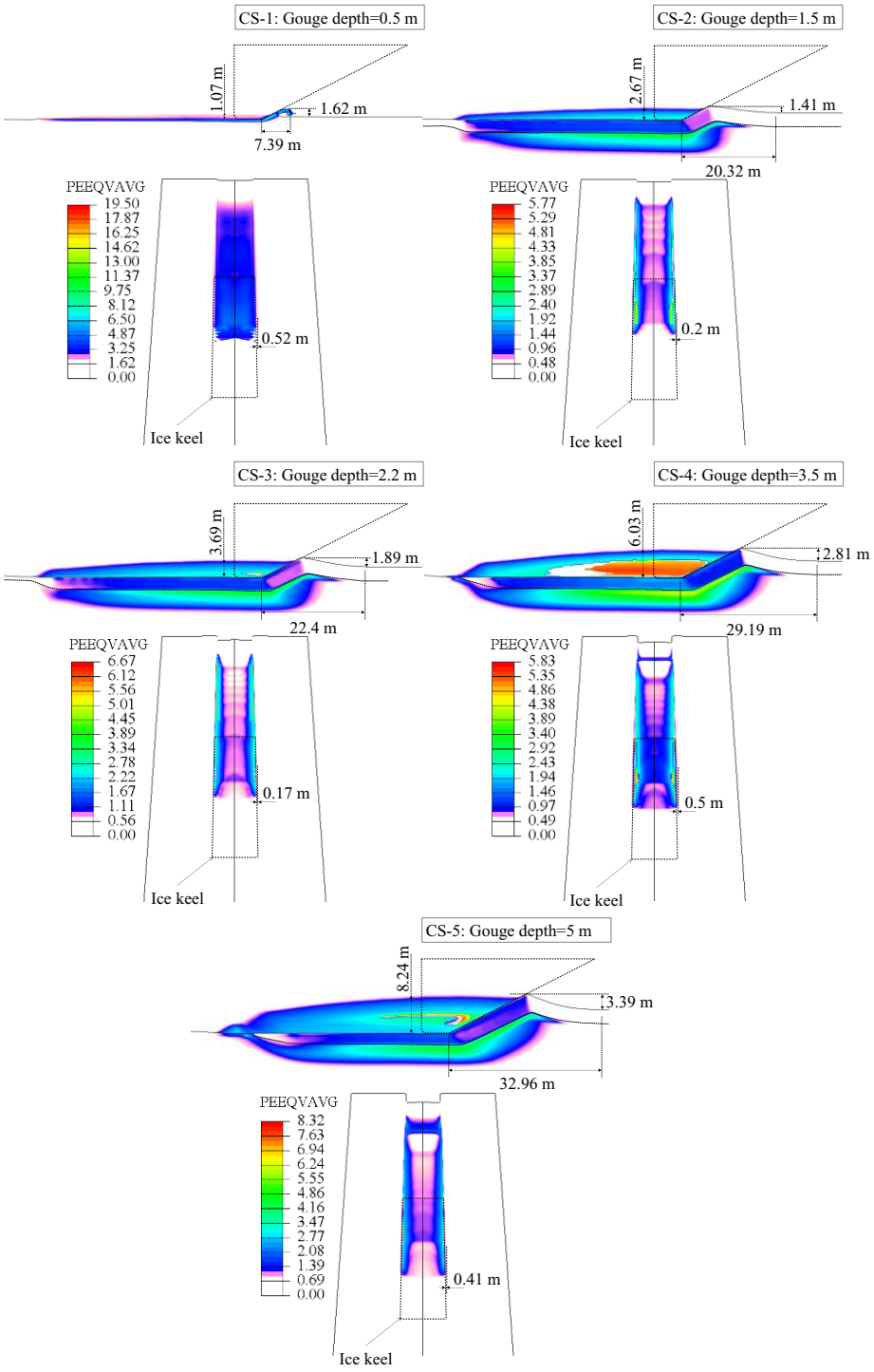

Figure 5-6**:** The effect of gouging with different depths on progressive plastic shear strain and quality of soil formation

Figure 5-6 shows that during the gouging process the stiff layer is interactively sandwiched in between the ice keel and the soft layer, transferring a large amount of plastic strain to the underlying soft layer. This intern results the soil particles in the soft layer to displace in a direction parallel to the attack angle. In addition, a failure curve in the soft layer is formed that crosses the interface of layers almost perpendicular to it (Figure 5-6, CS-2). The failure curve causes large soil deformation in the soft layer. As the gouge depth approaches the layer interface, this effect become tenser resulting in larger forward-upward deformations in the soft layer. By further deepening the gouge depth, the local effect of the stiff layer is faded, the wavy soil deformation is disappeared, and the subgouge soil deformation profile recovers its regular shape again but with deformation magnitudes larger than the uniform soft clay (Figure 5-6, CS-5). Also, the soil failure curve in the soft layer crosses the interface layer with a more inclined angle that is the reason behind fading of the front peak point in wavy subgouge soil deformation. Figure 5-7 shows the wavy displacement of tracing particle located in the soil body for CS-3 and CS-5 (Gouge depth of 2.2m and 5 m), where the compressed stiff layer in between the ice keel and the soft layer forces the soil particles in the soft layer and ahead of ice tip, to displace forward-upward parallel to the attack angle. As ice is passing over the soil particles, the particles are pushed downward.

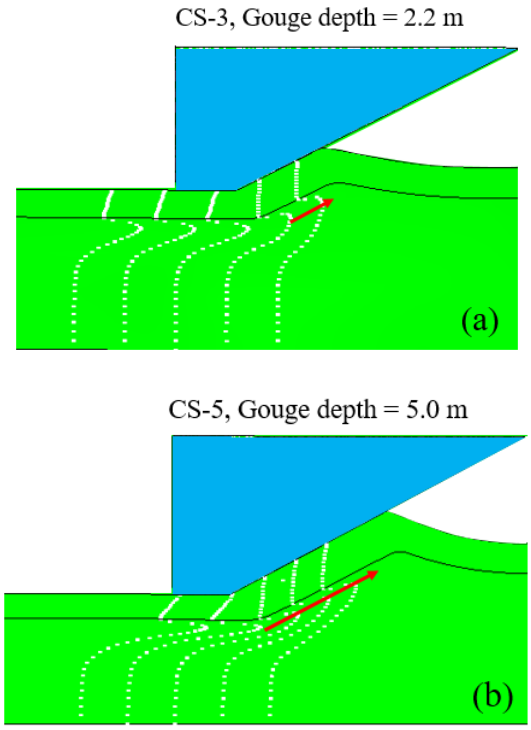

Figure 5-7: Tracing particle displacements showing the wavy subgouge soil deformation in stiff over soft layered seabed

Figure 5-6 shows that the size of the produced frontal mound and side berms are increased with increasing the gouge depth (from 0.5 m to 5 m), which is in agreement with all earlier studies.

The soil in the side berms undergoes high levels of plastic shear strain as well. The interactive mechanism shown in Figure 5-7 is significantly important and has not been captured before in the literature. These kinds of soft soil large displacement underlying stiff clay has been reported in studies investigating the lateral deformation of the retaining walls supporting vertically loaded stiff over soft clays, where the deep parts of the wall facing the soft soil undergoes larger deformations (e.g., Finno and Bryson, 2002). These results shown in Figure 5-6 and Figure 5-7 suggest that from practical standpoint,

simplifying stiff over soft clay as a uniform layer can be significantly misleading, hiding the large deformations in the soft layer and the large displacements trajectories of the buried pipe as well. Therefore, proper modeling of the layered still over soft clay is suggested to be conducted in practice.

5.3.2. Effect of layered soil strata

To further investigate the effect of having a layered stiff over soft clay seabed on the reaction forces and subgouge soil deformation, three different seabed configurations were studied and compared, including uniform soft seabed (CS-17 & CS-23), uniform stiff seabed (CS-18 & CS-24), and layered stiff over soft clay (CS-3 & CS-4). The undrained shear strength profiles of the uniform soft and uniform stiff seabed were extracted from the profile of layered seabed earlier shown in Figure 5-4 and presented in Figure 5-8

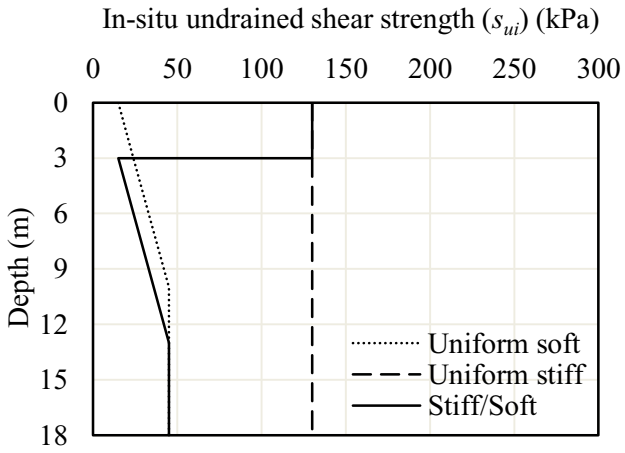

Figure 5-8**:** In situ undrained shear strength (s_{ui}) profile

The analyses were conducted with two different gouge depths, one inside the stiff layer (2.2 m) and another inside the soft layer (3.5 m). Figure 5-9 shows the comparison of the reaction forces and subgouge soil deformations for these three different seabed strata.

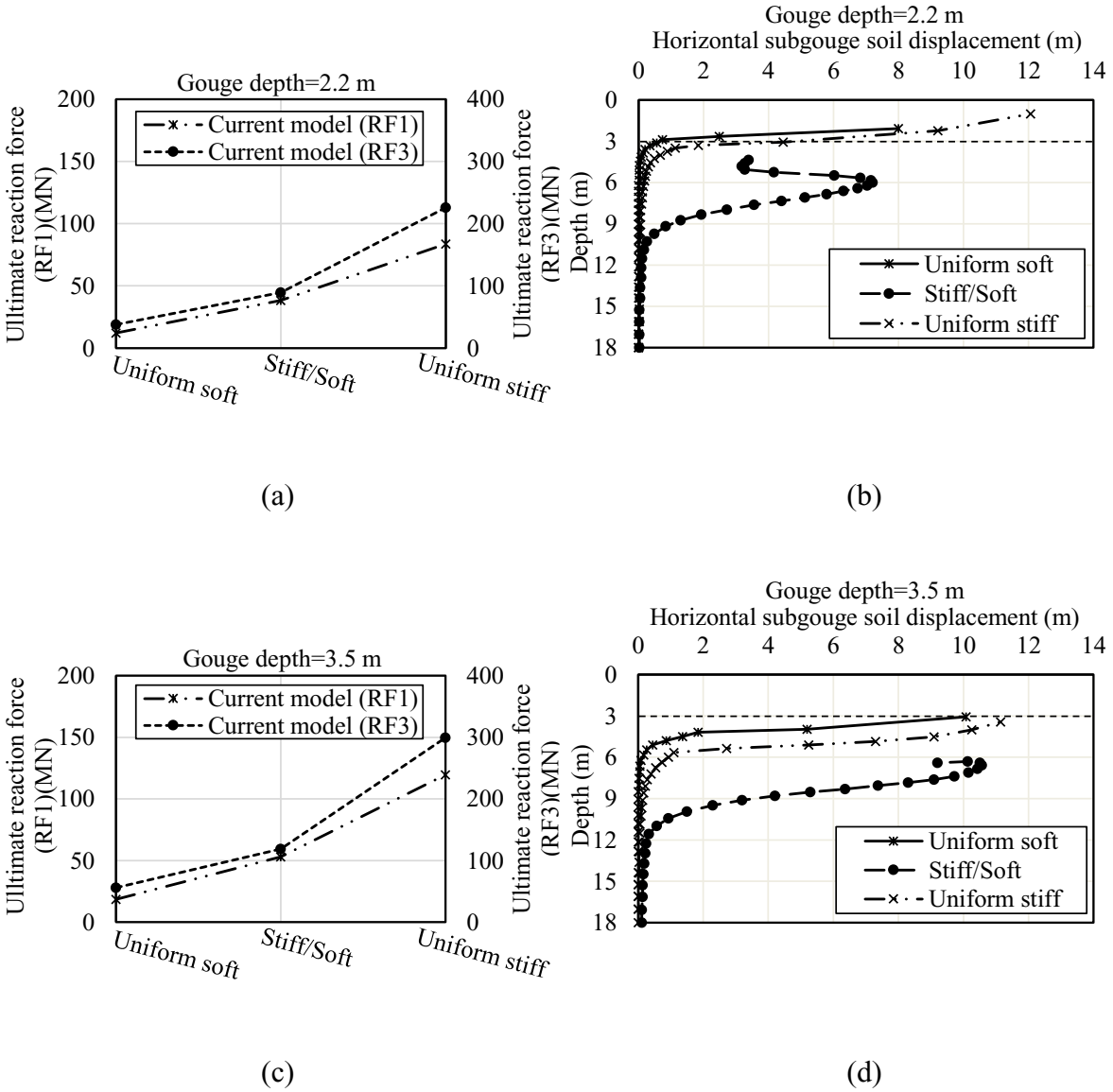

Figure 5-9**:** The effect of gouging in different layered soil strata on reaction forces and subgouge soil deformation

Figure 5-9 (a) and (c) shows that regardless of the gouge depth, ice gouging in uniform stiff soil generate larger reaction forces on the ice keel. The reaction forces obtained in stiff over soft layer is more than the uniform soft clay. The subgouge soil deformations presented in Figure 5-9 (b) and (d) show an interesting trend that is in perfect agreement

with the observations made in previous section. The subgouge soil deformation in uniform stiff clay is larger and deeper compared with the uniform soft clay for both gouge depths. The peak value of the wavy subgouge soil deformation in layered stiff over soft seabed is less than both uniform stiff and uniform soft seabed. The peak value is increased and approached to the corresponding magnitudes in uniform soil as the gouge depth is increased. However, the elevation of the peak value of subgouge deformation in layered stiff over soft clay is much lower than the uniform soils. From practical standpoint, these results suggests that considering the wavy profile of deformations in layered stiff over soft clay, the pipeline may not be buried two deep under the ice keel tip. Usually it is believed that a deeper trench is a safer one, although not the cheapest. However, these results question such a hypothesis. The results presented in this section show that deep burial of pipeline in a layered stiff over soft seabed may cause locating the pipe in the peak deformation point of the wavy profile and worsen the scenario. Therefore, care should be taken in determining the best burial depth in layered stiff over soft seabed.

The progressive plastic shear strains along with the side and front soil heaves were obtained and compared for different seabed configurations to look at the problem from a different angle. These results are presented in Figure 5-10.

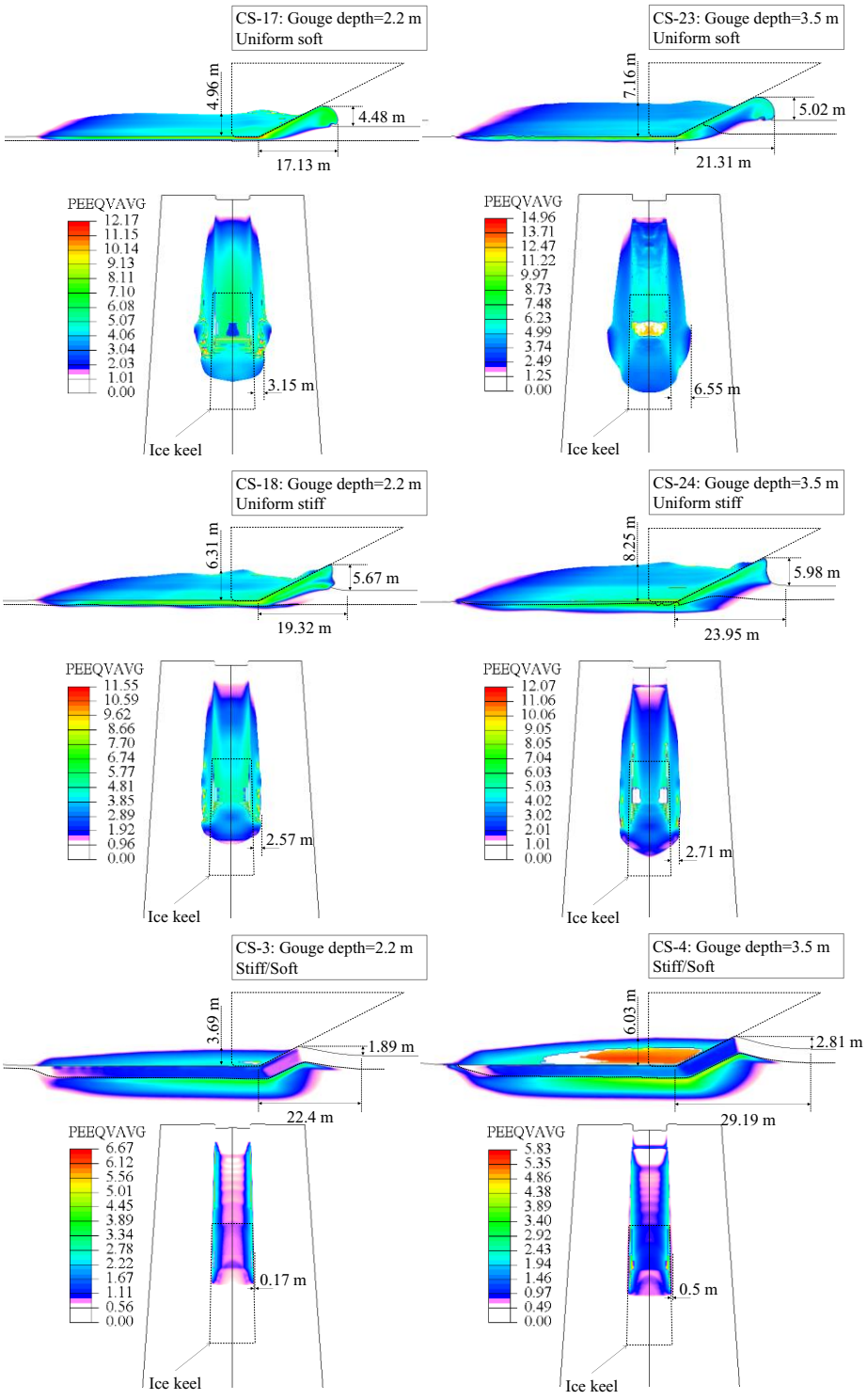

6.

Figure 5-10: The effect of gouging in different layered soil strata on progressive plastic shear strain and quality of soil formation

Figure 5-10 interestingly shows that the side soil berms and frontal mounds are significantly smaller in layered stiff over soft seabed (CS-3 and CS-4). Despite the uniform soft and stiff seabed, where large formations of side berms and frontal mounds are observed (CS-17, 18, 23, and 24), the interactive mechanism in between the seabed layers does not allow the same to happen in layered stiff over soft seabed. The overall shape of the side soil berms and frontal mounds are also different, forming a circular curve in uniform soft clay (CS-17 & CS-23), a steep and almost right angle slope in uniform stiff clay (CS-18 & CS-24), and a straight inclined line in layered stiff over soft seabed (CS-3 & CS-4). In uniform seabed (CS-17, 18, 23, and 24), the maximum plastic shear strain is localized in the contact areas near the keel chest and keel base. The maximum shear strain in layered seabed was observed in the contact area between the ice keel and side berms as well as the narrow area around the interface of two soil layers in bottom soft soil (CS-3 & CS-4).

5.3.3. Effect of different soil layer thicknesses

In order to further investigate the observations made in earlier sections the effect of different layer thicknesses were examined with three different gouge depths. The conducted cases studies include two configurations of 1 m stiff clay over 17 m soft clay, and 3 m stiff clay over 15 m soft clay, with gouge depths of 0.5 m, 2.2 m, and 3.5 m (CS-12, CS-14 and CS-15). Figure 5-11 shows the results of reaction forces and subgouge soil deformation obtained from these case studies.

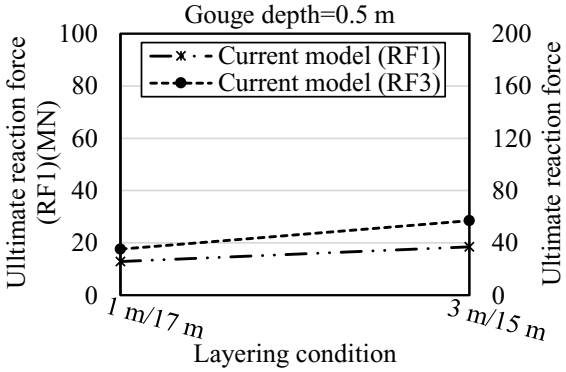
Gouge depth=0.5 m
Current model (RF1)
Current model (RF3)
Ulltimate reaction force (RF1)(MN)
Ultimate reaction force (RF3)(MN)
100
80
60
40
20
0
200
160
120
80
40
0
1 m/17 m
3 m/15 m
Layering condition

(a)

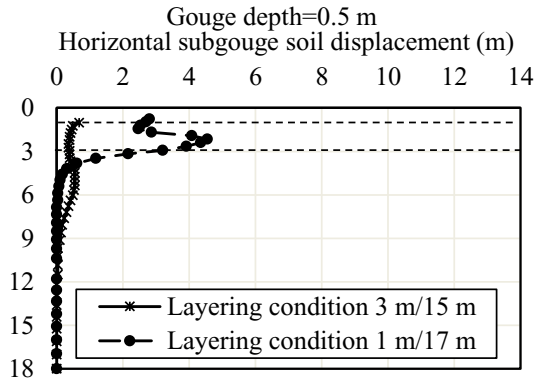
Gouge depth=0.5 m
Horizontal subgouge soil displacement (m)
0 2 4 6 8 10 12 14
Depth (m)
0 3 6 9 12 15 18
Layering condition 3 m/15 m
Layering condition 1 m/17 m

(b)

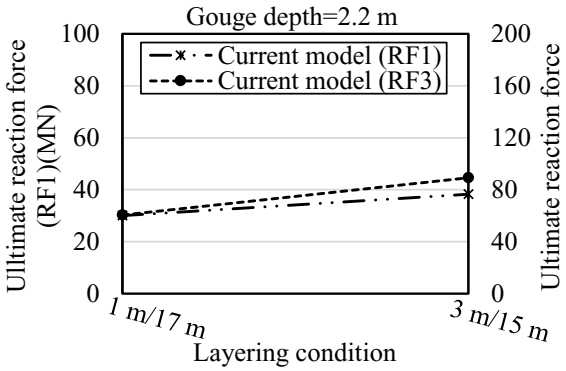
Gouge depth=2.2 m
Current model (RF1)
Current model (RF3)
Ulltimate reaction force (RF1)(MN)
Ultimate reaction force (RF3)(MN)
100
80
60
40
20
0
200
160
120
80
40
0
1 m/17 m
3 m/15 m
Layering condition

(c)

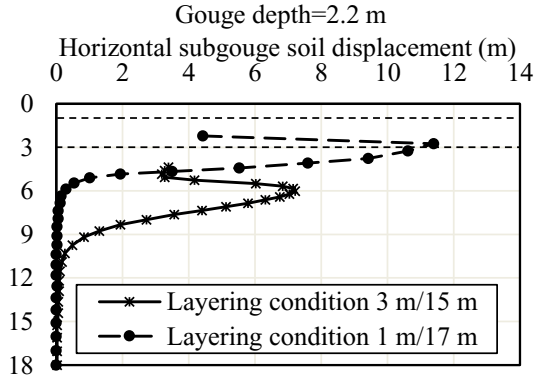
Gouge depth=2.2 m
Horizontal subgouge soil displacement (m)
0 2 4 6 8 10 12 14
Depth (m)
0 3 6 9 12 15 18
Layering condition 3 m/15 m
Layering condition 1 m/17 m

(d)

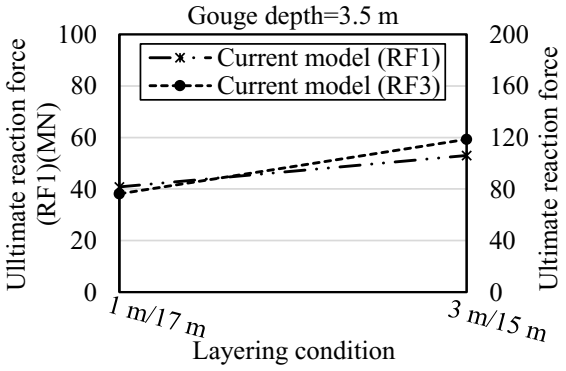
Gouge depth=3.5 m
Current model (RF1)
Current model (RF3)
Ulltimate reaction force (RF1)(MN)
Ultimate reaction force (RF3)(MN)
100
80
60
40
20
0
200
160
120
80
40
0
1 m/17 m
3 m/15 m
Layering condition

(e)

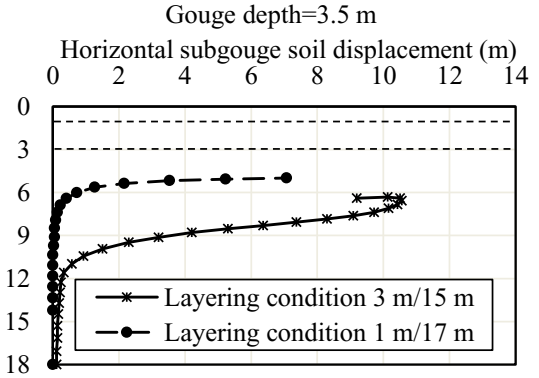
Gouge depth=3.5 m
Horizontal subgouge soil displacement (m)
0 2 4 6 8 10 12 14
Depth (m)
0 3 6 9 12 15 18
Layering condition 3 m/15 m
Layering condition 1 m/17 m

(f)

Figure 5-11: The effect of gouging in soils with different layered thicknesses on reaction forces and subgouge soil deformation

Figure 5-11 (b) shows that the less the distance between ice base and soft layer surface is (0.5 m compared with 2.5 m in distance), the more the magnitude of wave peak (heave) of subgouge soil deformation is. Figure 5-11 (d) and (f) confirms that when the ice base is located in the soft soil, in case of the same thickness of stiff layer (1 m), for the less amount of soft soil in front (1.2 m thickness compared with 2.5 m thickness), a larger magnitude of maximum subgouge soil deformation is obtained with a wavy deformation profile. In addition, the larger thickness of the stiff layer on top (3 m compared with 1 m) results in a larger vertical downward displacement of the soft soil particles (see Figure 5-11 (f)). The keel reaction forces are increased for a larger volume of stiff soil gouged by the ice (see Figure 5-11 (a), (c) and (e)).

To further investigate the failure mechanisms involved in these analyses, the progressive equivalent plastic shear strains along with the side berms and frontal mound formation were extracted and compared in Figure 5-12.

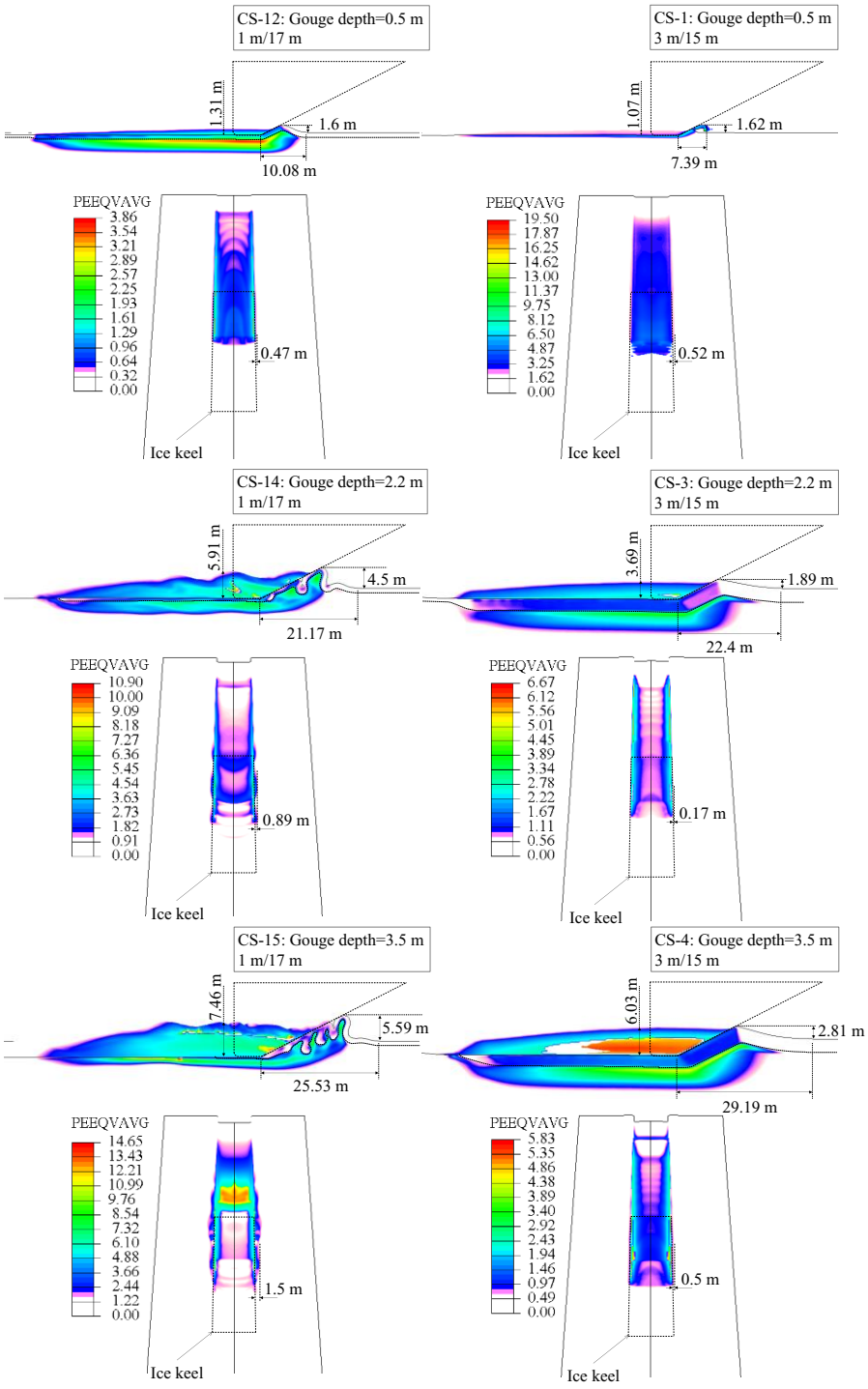

Figure 5-12: The effect of gouging in soils with different layered thicknesses on progressive plastic shear strain and quality of soil formation

The results shown in Figure 5-12 are quite interesting, particularly the case studies CS-14 and CS-15. The study showed that when the toping stiff layer is thin compared with the lower soft layer, and the gouge depth is well deeper than the stiff soil layer, the layered soil in front of the ice keel is wrinkled, the deeper the gough depth, the more wrinkles in the layered soil. This failure mechanism is totally different from the case studies with gouge depths located inside the thick stiff layer or slightly deeper than that (CS-3 and CS-4). In addition, wrinkled soil failure resulted in a larger side berm and frontal mound. The wrinkled soil failure happens when the stiff soil layer is thin and is not strong enough to transfer the stress to the soft layer. The wrinkled failure of stiff layer is followed by the wrinkled deformation in underlying soft layer as well. This wrinkled soil failure mechanism unlocks the reason behind the significant difference in subgouge soil deformations of case scenarios CS14 and CS-3 in Figure 5-11. From practical standpoint, these results can be very important, indicating that the ratio of layers thickness along with the gouge depth may change the soil failure mechanism and result in large soil deformations underneath and in front of the ice keel that may significantly affect the displacement and integrity of buried pipeline. These results emphasize on the importance of accurate modeling of ice gouging in layered stiff over soft clay with keeping an eye on the soil failure mechanism.

5.3.4. Effect of layers' strength ratio

The effect of different strength ratios between two layers of stiff and soft soils on the seabed response to ice gouging was investigated through case studies, CS-19 to CS-22 with a gouge depth of 5 m. For these case studies, the intercept values of undrained shear strength

for two layers were considered to be doubled and halved compared to the base case CS-5. Figure 5-13 and Table 5-4 shows the undrained shear strength profiles of these case studies.

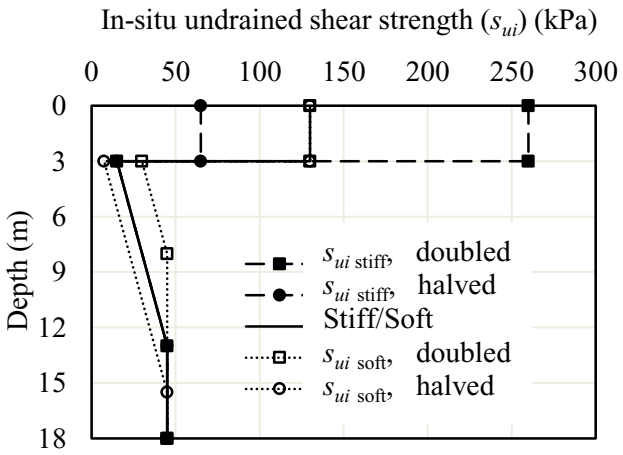

Figure 5-13: In situ undrained shear strength (s_{ui}) profile (CS-19 to CS-22)

Table 5-4: The intercept undrained shear strength magnitude of the soil layers

s_{ui} stiff / s_{ui} soft / 45 kPa		Case studies				
		CS-5	CS-19	CS-20	CS-21	CS-22
		Base	s_{ui} stiff, doubled	s_{ui} stiff, halved	s_{ui} soft, doubled	s_{ui} soft, halved
Intercept undrained shear strength magnitude (kPa)	Stiff	130	260	65	130	130
	Soft	15	15	15	30	7.5

The results of keel reaction forces and subgouge soil deformation for the defined case studies are presented in Figure 5-14.

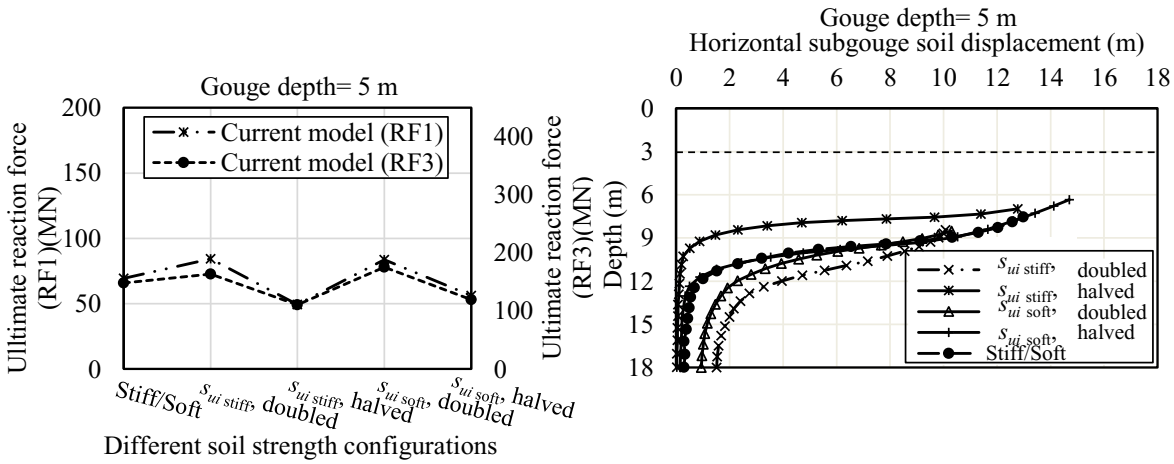

(a) (b)

Figure 5-14: The effect of different soil undrained shear strength profiles on reaction forces and subgouge soil deformations (CS-5 & CS-19 to CS-22)

Figure 5-14 (a) shows that higher value of reaction forces were obtained by increasing the strength of the stiff or soft layer (doubling). In a same fashion, lower magnitude of reaction forces were predicted by decreasing the strength of soft or stiff soil (halving).

Figure 5-14 (b) shows that by increasing the strength of stiff soil (CS-19), the soft soil particles in the bottom undergo more downward displacement compared with the base case of stiff over soft soil (CS-5). A reverse trend was observed, when the strength of stiff layer is decreased (CS-20). Also, by increasing the strength of stiff layer (CS-19), the maximum subgouge soil deformation is decreased compared to the based case scenario (CS-5).

By increasing the strength of both soil layer (CS-19 & CS-21), a large tendency were observed for soft soil particles located deeper to further move forward. The maximum subgouge deformation was obtained in the case, CS-22, where the strength of soft soil was decreased. The subgouge deformation curve for this case was quite similar to the base case (CS-5).

The corresponding progressive equivalent plastic shear strains along with the side berms and frontal mound formation are shown in Figure 5-15.

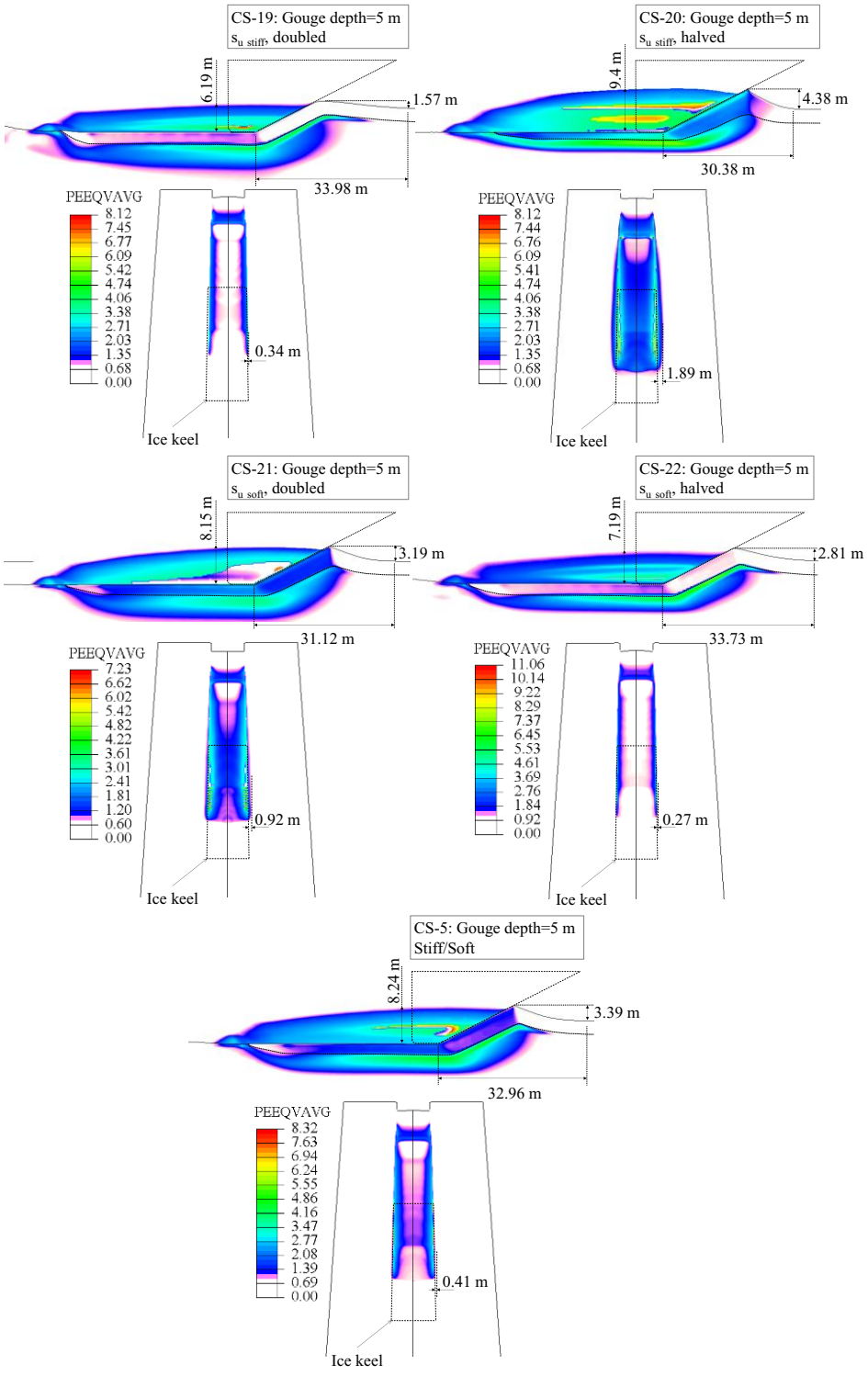

Figure 5-15: The effect of soil with different strength ratios on the progressive plastic shear strain and the quality of soil formation

Comparing with the base case results (CS-5), Figure 5-15 shows that by increasing the strength of toping stiff soil (CS-19) or by decreasing the strength of underlying soft soil (CS-22), the maximum shear strain are developed at soft soil around the interface of two soil layers. The magnitude of maximum shear strain is higher when the strength of soft soil is decreased (CS-22) compared to the other case (CS-19). In these two cases, the strength difference between two layers are at the highest level and the stiff layer in front of ice experiences the minimum plastic shear strain. From practical perspective, the results presented in Figure 5-15 shows that the strength ratio between the stiff and soft layer may have significant impact on increasing or decreasing of the subgouge soil deformations and the reaction forces in layered seabed. Therefore, care shall be taken in accurate modeling of layered stiff over soft clay seabed for ice gouging analysis. Simplifying the seabed as a uniform domian may cause significant uncertainity in the obtained results.

5.4. Conclusions

In this paper, ice gouging performance in layered stiff over soft clay was investigated by 3D large deformation finite element (LDFE) analysis using CEL approach. A modified Tresca soil model was coded as a user-defined subroutine (VUSDFLD) and incorporated into the ABAQUS/Explicit to capture the strain rate and strain softening effects. A comprehensive parametric study was conducted to explore the effects of ice keel and layered soil characteristics on the seabed response to the ice gouging in layered stiff over soft seabed. The following key observations were made:

- Replacing a layered stiff over soft clay seabed with a uniform seabed for ice gouging analysis can be a gross simplification. The study showed that the

interaction between the stiff and soft layers might result in a wavy shape subgouge soil deformation with a peak deformation much deeper than the uniform soil. The wavy shape subgouge deformation profile included a peak and a nadir point. The nadir point is located in the proximity of the interface between the soil layers and the peak point is located deep through the soft soil. As the ice keel moves forward, the stiff layer is inclined parallel to the attack angle and pushes the soft soil particles ahead of the keel forward-upward parallel to the attack angle. I was observed that as the ice keel pass over the soil particles, the uplifted soft soil is push downward again resulting in a maximum subgouge soil deformation which is not located right in the proximity of the soil layers interface. The study showed that as the gouge depth becomes deeper the wavy subgouge deformation profile is faded and the profile become similar to a deepened uniform soil. Also, it was observed the side berms and frontal soil mounds formed during the ice gouging process are much smaller in the layered stiff over soft soil compared with uniform soil. The wavy subgouge soil deformation can have a significant role in determining the best burial depth for protection of subsea pipelines against the iceberg attack in practice.

- The study showed that the soil failure mechanism in front of the ice keel could be significantly affected by the layered stiff over soft clay, resulting in subgouge deformations much larger than the uniform seabed. A wrinkled soil failure mechanism was observed when the stiff layer was thin and the gouge depth was well below the interface of the stiff and soft layers. The changing of the soil failure mechanism with the thickness of the layers emphasize on the interactive nature of

layered seabed response to the ice gouging and the importance of accurate modeling of the layers in practice.

- Different strength ratio in between the stiff and soft layers was found to have a remarkable effect on the subgouge soil deformation and the reaction forces. As the stiff layer becomes stiffer and the soft layer become softer, the subgouge soil deformation and ice keel reaction forces are decreased. Also, by increasing the strength of stiff soil, the soft soil particles on the bottom undergo more downward relocation and vice versa.

Overall, the revealed several important observations from ice gouging analysis in layered stiff over soft clay, all of which can have a significant effect in practical pipeline engineering design against the iceberg attack. Recommendations were made for practical applications based on the observations. It is recommended for the future to conduct experimental studies in layered stiff over soft seabed to further understand the interactive response of layered seabed to the ice gouging and its practical implications.

5.5. Acknowledgments

The authors gratefully acknowledge the financial support of this research by Wood PLC via establishing the Wood Group Chair in Arctic and harsh environment engineering at Memorial University, the NL Tourism, Culture, Industry and Innovation (TCII) via CRD collaborative funding program, the Natural Sciences and Engineering Research Council of Canada (NSERC) via CRD funding program, the Memorial University of Newfoundland through the school of graduate studies (SGS) baseline fund.

References

Alba, J. L. , 2015. Ice Scour and Gouging Effects With Respect to Pipeline and Wellhead Placement and Design, Bureau of Safety and Environmental Enforcement (BSEE), Wood Group Kenny, Report No. 100100.01.PL.REP.004, Houston, TX.

Allersma, H.G.B., and Schoonbeek, I.S.S., 2005. Centrifuge modelling of scouring ice keels in clay. Int. Conference on Offshore and Polar Engineering, ISOPE2005, Seoul, June 19-24, paper 2005-JSC-427, pp.404-409

Babaei, M. H., & Sudom, D., 2014. Ice-seabed gouging database: review and analysis of available numerical models. In *OTC Arctic Technology Conference*. Offshore Technology Conference.

Banneyake, R., Hossain, M. K., Eltaher, A., Nguyen, T., Jukes, P., 2011. Ice-soil pipeline interactions using coupled eulerian-lagrangian (CEL) ice gouge simulations extracts from ice pipe JIP. Paper presented at the OTC Arctic Technology Conference.

Biscontin, G., Pestana, J.M., 2001. Influence of peripheral velocity on vane shear strength of an artificial clay. Geotech. Test.J. 24(4), 423–429.

C-CORE, 1995e. Pressure Ridge Ice Scour Experiment, PRISE: Phase 3-Centrifuge Modelling of Ice Keel Scour: Draft Final Report. April 1995. Publication 95-C12, 52p.

C-CORE, 2008. Design Options for Offshore Pipelines in the US Beaufort and Chukchi Seas. April 2008. Report R-07-078-519.

Dayal, U., Allen, J. H., 1975. The effect of penetration rate on the strength of remolded clay and sand samples. Can. Geotech. J., 12(3),336–348.

DeGroot, D. J., DeJong, J. T., Yafrate, N. J., Landon, M. M., Sheahan, T. C., 2007. Application of recent developments in terrestrial soft sediment characterization methods to offshore environments. Proc., Offshore Technology Conf., Houston, OTC 18737.

DeJong, J., DeGroot, D., Yafrate, N., 2012. Evaluation of undrained shear strength using full-flow penetrometers. J. Geotech. Geoenviron. Eng.138(6),765–767.

Einav, I., Randolph, M. F., 2005. Combining Upper Bound and Strain Path Methods for Evaluating Penetration Resistance. International Journal for Numerical Methods in Engineering, Vol. 63, No. 14, pp. 1991-2016.

Eltaher, A., 2014. Gaps in Knowledge and Analysis Technology of Ice Gouge Pipeline Interaction. Proceedings of the Arctic Technology Conference, February 10 - 12, 2014, 10p.

Finno, R. J., Bryson, L. S., 2002. Response of Building Adjacent to Stiff Excavation Support System in Soft Clay. Journal of Performance of Constructed Facilities, Vol. 16, Issue 1, February 2002, https://doi.org/10.1061/(ASCE)0887-3828(2002)16:1(10).

Graham, J., Crooks, J. H. A., Bell, A. L., 1983. Time effects on the stress-strain behaviour of natural soft clays. Geotechnique, 33(3), 327–340.

Hashemi, S., Shiri, H. and Dong, X., 2022a. The influence of layered soil on ice-seabed interaction: Soft over stiff clay, Applied Ocean Research, Volume 120, March 2022, 103033, ISSN 0141-1187, https://doi.org/10.1016/j.apor.2021.103033

Hashemi, S., and Shiri, H., 2022b. Numerical Modeling of Ice–Seabed Interaction in Clay by Incorporation of the Strain Rate and Strain-Softening Effects. ASME. J. Offshore Mech. Arct. Eng. August 2022; 144(4): 042101. https://doi.org/10.1115/1.4053871

Hossain, MS, Randolph, MF, 2009. Effect of Strain Rate and Strain Softening on the Penetration Resistance of Spudcan Foundations on Clay. International Journal of Geomechanics, Vol 9, No 3, pp 122-132.

Konuk, IS., Gracie, R., 2004. A 3-dimensional Eulerian FE model for ice scour. IPC04-0075, pp.1911-1918.

Lach, P.R., 1996. Centrifuge modelling of large soil deformation due to ice scour, Ph.D., Memorial University of Newfoundland (Canada).

Lele, S., Hamilton, J., Panico, M., Arslan, H., Minnaar, K., 2011. 3D continuum simulations to determine pipeline strain demand due to ice-gouge hazards. Arctic Technology Conference, ATC.

Lunne, T., Andersen, K. H., 2007. Soft clay shear strength parameters for deepwater geotechnical design. Proc., 6th Int. Offshore Site Investigation and Geotechnics Conf.: Confronting New Challenges and Sharing Knowledge, Vol. 1, Society for Underwater Technology, London, 151–176.

Nobahar, A., Kenny, S., Phillips, R., 2007b. Buried pipelines subject to subgouge deformations. International Journal of Geomechanics, vol. 7, no. 3, pp. 206-216.

Peek, R., Nobahar, A., 2012. Ice gouging over a buried pipeline: Superposition error of simple beam-and-spring models. International Journal of Geomechanics, vol. 12, no. 4, pp. 508-516.

Pike, K., Kenny, S., 2016. Offshore pipelines and ice gouge geohazards: Comparative performance assessment of decoupled structural and coupled continuum models. Canadian Geotechnical Journal, 53(11), 1866-1881.

Phillips, R., Barrett, J., 2012. PIRAM: Pipeline Response to Ice Gouging. Proceedings of the Arctic Technology Conference, December 3 - 5, 2012, 6p.

Raie, M., Tassoulas, J., 2009. Installation of torpedo anchors: numerical modeling. J. Geotech. Geoenviron. Eng. 135 (12), 1805–1813.

Randolph, M. F., 2004. Characterization of soft sediments for offshore applications. Keynote Lecture, Proc., 2nd Int. Conf. on Site Characterization, Porto, Portugal, Vol. 1, Millpress Science Publishers, Rotterdam, 209–231.

Miller, D. L. and Bruggers, D. E., 1980. Soil and Permafrost Conditions in the Alaskan Beaufort Sea, Offshore Technology Conference OTC 3887.

Winters, W. J. and Lee, H. J. (1984). Geotechnical properties of samples from borings obtained in the Chukchi Sea, Alaska. USGS Report 85-23.

Woodworth-Lynas, C., Nixon, D., Phillips, R., Palmer, A., 1996. Subgouge Deformations and the Security of Arctic Marine Pipelines. Proc. 28th OTC, Vol. 4, Paper No. 8222, pp. 657–664.

Chapter 6

The Response of Layered Seabed to Ice Gouging: Sand over Clay

Seyedhossein Hashemi, as the main author, is credited for the methodology, modeling, data curation, visualization, investigation, validation and writing-original draft. Hodjat Shiri is credited for conceptualization, supervision, writing-review and editing and funding acquisition

This chapter is submitted as a journal manuscript to Ocean Engineering.

Abstract

Traveling icebergs may threat the structural integrity of the offshore pipelines in any territories that they can reach. Arctic offshore pipeline are usually buried for physical protection against ice gouging. The safe and cost-effective burial depth of these pipelines needs to be determined by accurate assessment of the subgouge soil deformation and the ice keel-seabed contact forces. Layered seabed soil strata that are found in many geographical locations adds to the complexity of assessing the ice keel-seabed interaction process. The currently used design codes have been developed for uniform soil strata that, in turn, may affect the accuracy and cost-effectiveness of the design. In this study, the significance of layered sand over clay seabed in the ice gouging process was investigated by performing large deformation finite element (LDFE) analysis using Coupled Eulerian-Lagrangian (CEL) approach. A comprehensive parametric study was conducted to assess the influence of ice gouging characteristics and soil properties on the subgouge soil deformation, developed plastic shear strains and the resultant ice keel reaction forces. The study showed that the seabed response to ice gouging is significantly dependent on the soil strata, where the layers interaction effects can alter the usual response expected from a uniform seabed. Practical suggestions were made for enhancing the pipeline design in layered sand over clay seabed soils.

Keywords: Ice gouging, Subgouge soil deformation, Layered seabed, Numerical simulation, Strain rate and strain-softening effects

6.1. Introduction

Floating icebergs or ice ridges during their long trip from Arctic oceans reach the shallow waters and start scouring the sea bottom by the ice keel tip. This is called “ice gouging”, an Arctic seabed geohazard that may jeopardize the structural integrity of subsea pipelines. Pipelines are buried below the deepest potential gouge depth for physical protection. However, due to the shear strength of the soil, the subgouge soil displacement may significantly extended deep through the soil. Determining the optimum burial depth for protection against iceberg attack is a challenging design aspect of Arctic offshore pipelines. The pipe response to ice gouging is currently determined by a decoupled approach in engineering practice. For this purpose, first, a free-field (with no pipeline) ice gouging analysis is conducted using continuum large deformation finite element analysis (LDFE). Then the obtained subgouge soil deformations are transferred to the end of a set of springs connected to a simple beam-spring model to capture the pipeline structural response (Woodworth-Lynas et al., 1996; Phillips and Barrett, 2012). Although the accuracy of this approach suffer from the superposition of idealization and directional load decoupling as two sources of errors (Konuk and Gracie, 2004; Nobahar et al., 2007b; Lele et al., 2011; Peek and Nobahar, 2012; Phillips and Barrett, 2012; Eltaher, 2014; Pike and Kenny, 2016), but this is still cost-effective solution that compromise some level of accuracy and is followed by the pipeline industry.

The accurate simulation of free-field ice gouging can have a significant impact on the ultimate results in the decoupled method. In free-field ice gouging analysis, the seabed stratum is usually simplified by uniform soil. This can be a gross simplification in the areas

with complex layered seabed strata. Modeling the ice gouging in layered sand over clay seabed has not been explored in the literature while such a non-uniform soil strata have been broadly observed in offshore Arctic areas with lots of gouging signatures (e.g., Chukchi Sea (Winters and Lee, 1984; C-CORE, 2008); Alaskan Beaufort Shelf (C-CORE, 2008); Russian Sakhalin Island (C-CORE, 1995e), etc.) (see Figure 6-1).

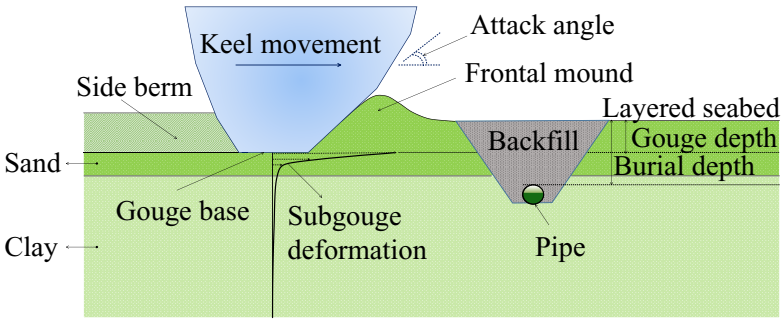

Figure 6-1: Schematic view of ice gouging process in sand over clay layered seabed

The significance and the need for investigation of the impact of layered seabed soil on ice gouging process has been highlighted and identified as a knowledge gap in the literature (e.g., NRC-PERD, 2014; BSEE-WGK, 2015; Winters and Lee, 1984; Babaei and Sudom, 2014; Alba, 2015). The geomechanical properties of the soil layers, soil strata configuration, and the ice features can significantly affect the ice-seabed interaction mechanisms and consequently the resultant subgouge soil deformation and ice keel reaction forces (Hashemi and Shiri, 2022a).

In the current study, the response of layered sand over clay seabed to ice gouging was investigated by performing large deformation finite element analysis (LDFE) using Coupled Eulerian-Lagrangian (CEL) algorithm in ABAQUS/Explicit. The CEL analysis allows the Eulerian domain (i.e., soil) to flow through the fixed Eulerian meshes without

any concern about the mesh over-distortion, while the Eulerian (soil) and Lagrangian (ice) domains interact with each other with no instability issues.

The sand layer on top was modeled using a built-in conventional Mohr Coulomb model from ABAQUS soil models' library. Using the formulation proposed by Einav and Randolph (2005), the underlying clay layer was modeled by coding a modified Tresca model as a user-defined subroutine (VUSDFLD) to incorporate the strain rate dependency and the strain softening effects on the undrained shear strength of the soil subjected to large plastic shear strains. The cohesive soil in ice gouging analysis is usually modeled as an elastic perfectly plastic material which is a fast and simple approach (e.g., Pike and Kenny, 2016). However, increasing the shear strain rate leads to increase in undrained shear strength when subjected to large shear strains, and gradual loss of shear strength caused by strain softening in clay (e.g., Biscontin and Pestana, 2001; DeGroot et al., 2007; Lunne and Andersen, 2007; Hossain and Randolph, 2009; DeJong et al., 2012). The strain rate dependency and strain softening in clay could affect the failure mechanisms, the mobilized soil resistance and the resultant subgouge soil deformation in ice gouging analysis.

A comprehensive parametric study was conducted to examine the effects of key parameters on the ice gouging, including ice features (i.e., keel width, gouge depth, and attack angle) and layered soil characteristics (soil layer thicknesses, layering configurations and soil strength characteristics). The resultant subgouge soil deformations, keel reaction forces, and the progressive plastic strains (PEVAVG as maximum principal plastic strain) distribution were investigated. The study revealed an interactive response between the soil layers that can completely distort the ultimate result if it is simplified by uniform soil strata.

The developed model can be used in current engineering practice as a simple but robust approach to assess the response of layered sand over clay seabed to ice gouging.

6.2. Numerical model

6.2.1. CEL model configuration

The model configuration was adopted from a published experimental ice gouging study in a sand over clay layered soil (i.e., Test #8 of the Pressure Ridge Ice Scour Experiments (PRISE) JIP, conducted by C-CORE (1995e)) to facilitate verifications and comparisons. To mitigate the computational efforts, a symmetric half-space model with overall dimensions of the Eulerian domain as 120 × 20 × 25 m (length, width, depth, respectively) was developed. The ice keel was discretized as a Lagrangian mesh and the soil layers as largely deformable material occupied the fixed Eulerian meshes. The Eulerian domain was modelled by using the 8-node linear Eulerian brick elements with reduced integration and hourglass control (EC3D8R). A constant element size was considered for the area of high strain, around the gouging zone, enlarging towards the areas with lower degree of attention. The element size was set to gradually increase to its maximum value in the vertical upward and downward directions. The ice keel was modelled as a rigid body and discretised by 8-node linear brick elements with reduced integration and hourglass control (C3D8R) with a base length of 8 m, a width of 7.5 m, and an attack angle of 15°. To initialize the analysis, the ice keel was initially pre-indented into the seabed at a depth of 1.58 m (Drive1 of PRISE 08) (see Figure 6-2).

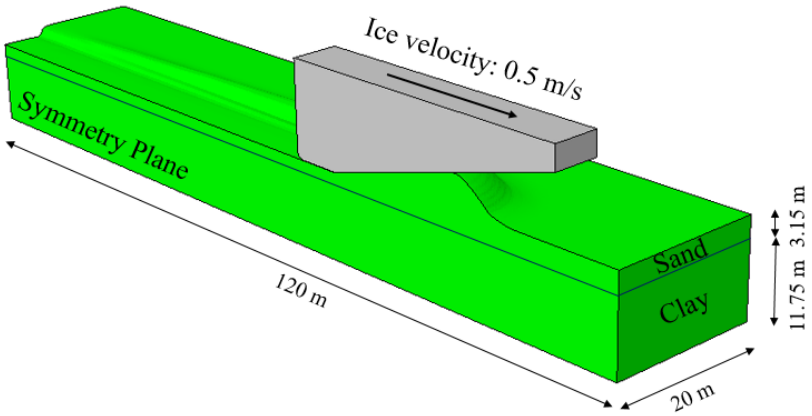

Figure 6-2: FEA model configuration

An extra void domain of 10 m high was created on top of the seabed to accommodate the soil frontal mound and side berm formations during the gouging process. Assigning the soil material to two reference parts, representing top sand and bottom clay layers (3.15 m sand overlaying an 11.75 m clay in the base analysis) was done by using the software volume fraction tools. Velocity boundary conditions were applied to constrain the soil movement in normal direction of each vertical faces and bottom of the Eulerian domain, and also to ensure that the soil as an Eulerian material will not be able to flow beyond the domain. The horizontal movement of the ice keel was modelled by applying a velocity boundary condition to the reference point located in the centre of mass of the ice keel. Two analysis steps were defined including an initial geostatic step to generate the in situ stress, followed by a dynamic Explicit step lasting 160 seconds to horizontally displace the ice keel at a constant velocity of 0.5 m/s.

A general "hard" contact algorithm offered by ABAQUS/Explicit was selected for interaction between the ice keel and the seabed soil. Following the isotropic coulomb friction model for tangential behaviour, friction coefficients (μ) of 1 and 0.3 were set for

the contact surfaces in ice keel-sand and ice keel-clay interaction, respectively. Also a maximum shear stress limit of 0.5 s_{ui} was defined for ice keel-clay contact, where s_{ui} was the value of measured in situ undrained shear strength in gouge depth (Pike and Kenny, 2016). The soil layers were defined as a single continuum domain with varying geomechanical properties through the layers.

6.2.2. Constitutive soil model

Soil properties were adopted from the centrifuge test No. 8 of PRISE JIP (sand over clay layer, C-CORE, 1995e). The sand layer on top was modeled by a conventional Mohr Coulomb model built-in in ABAQUS, using a set of parameters reported by C-CORE (1995e). The friction and dilation angles were set to 36.5 and zero degrees, respectively. A negligible value of 1.2 kPa was considered for the soil cohesion. The mass density, elastic modulus and poison's ratio were assumed to be 1500 kg/m^3, 36.5 MPa and 0.3, respectively.

The gouging velocity was sufficiently high to ensure the undrained condition for the clay layer. The undrained conditions was satisfied by taking the value of Poisson's ratio equal to 0.499 that was high enough to minimize the volumetric strains without any concerns about numerical instability. The clay layer was modelled as an elastic-perfectly plastic material obeying Tresca criterion. The icebergs are usually separated from the glaciers in the Arctic areas in the warm seasons, travel far away, and arrive in the subsea pipelines in the areas with seawater and seabed soil temperature above the zero. Therefore, the friction and dilation angles were set to zero in clay. The in situ undrained shear strength (s_{ui}) was linearly varying from 12 kPa at the interface to an ultimate value of 42 kPa (k=3 kPa/m)

through the soil depth. The Young's modulus was assumed as 500 s_{ui} and constant throughout the clay layer.

Using the equation proposed by Einav and Randolph (2005), the effect of strain rate dependency and strain softening were incorporated in constitutive soil model for clay by coding a user-defined subroutine VUSDFLD in ABAQUS. During the analysis, the user subroutine was being called by software to incrementally update the in situ undrained shear strength of the soil (s_{ui}) based on the incremental values of the current accumulated absolute plastic shear strain (ξ) and the average rate of maximum shear strain ($\dot{\gamma}_{max}$) in the previous time step:

$$s_u = \left[1 + \mu \times log\left(\frac{max\left(\left(|\dot{\gamma}_{max}|, \dot{\gamma}_{ref}\right)\right)}{\dot{\gamma}_{ref}}\right)\right] \times \left[\delta_{rem} + (1 - \delta_{rem})e^{-3\xi/\xi_{95}}\right]s_{ui} \quad (6\text{-}1)$$

In the first square bracket, the effect of strain rate and in the second one, the effect of strain softening on the in situ undrained shear strength is included. Both sections in the square brackets include two constants and one variable. The increase rate of the shear strength per log cycle (μ) and the reference shear strain rate ($\dot{\gamma}_{ref}$) are constant, while the maximum shear strain rate ($\dot{\gamma}_{max}$) is a variable. The ratio of fully remoulded to initial shear strength (or the inverse of the sensitivity) (δ_{rem}) and the value of accumulated absolute plastic shear strain resulting in 95% reduction in the remoulded shear strength (ξ_{95}) are constant while the incremental value of the current accumulated absolute plastic shear strain (ξ) is varying. The parameter s_{ui} is the undrained shear strength measured at the reference shear strain rate before making changes according to the effects.

The constant parameters for the clay soil model used in the benchmark analysis are shown in Table 6-1.

Table 6-1: Clay soil mechanical properties used in FE analysis

Parameter	Value
Mass density, ρ	1400 kg/m^3
Poisson's ratio, ν	0.499
Rate of shear strength increase, μ	0.1
Reference shear strain rate, $\dot{\gamma}_{ref}$	0.024 s^{-1}
Soil sensitivity, S_t	2.0
Ratio of fully remoulded to initial shear strength, δ_{rem}	0.5
Accumulated absolute plastic shear strain for 95% reduction in strength due to remoulding, ξ_{95}	12

As shown in Table 1, the value of μ, rate of shear strength increase, was taken as 0.1. A value in range of 0.05 to 0.2 was suggested for this parameter in the literature (Dayal and Allen, 1975; Graham et al., 1983; Biscontin and Pestana, 2001). The reference shear strain rate $\dot{\gamma}_{ref}$ was taken as 0.024 s^{-1} following the research work has been done by Raie and Tassoulas (2009) on numerical modelling of torpedo Anchors installation. The variable parameter $\dot{\gamma}_{max}$, maximum shear strain rate, was calculated incrementally using equation (6-2) during the analysis:

$$\dot{\gamma}_{max} = \frac{(\Delta\varepsilon_1 - \Delta\varepsilon_3)}{\Delta t} \tag{6-2}$$

where $\Delta\varepsilon_1$ and $\Delta\varepsilon_3$ are the cumulative major and minor principal strains over the time increment, Δt.

A typical value of 12 was selected for ξ_{95} in range of 10 to 25 suggested by Randolph (2004) for typical soft marine clays (for soil from rapidly softening soil to gradually softening). The δ_{rem} was taken as 0.5 as the inverse of the assumed soil sensitivity.

The ratio of the mobilized undrained shear strength to the in situ values (FV= s_u /s_{ui}) as a field variable is calculated incrementally for each individual Gaussian point of every soil element located in different depths. During this process, the FV in the current increment is calculated following the coded VUSDFLD subroutine based on the two variable parameters $\dot{\gamma}_{max}$ and ξ which were delivered by the solver and required for the formulation. Then the solver updates the value of the in situ undrained shear strength (s_{ui}) based the calculated FV in the current increment and start to solve the problem in the next increment using the updated undrained shear strength (s_u). Figure 6-3 shows the flowchart of the main solver calling the subroutine VUSDFLD.

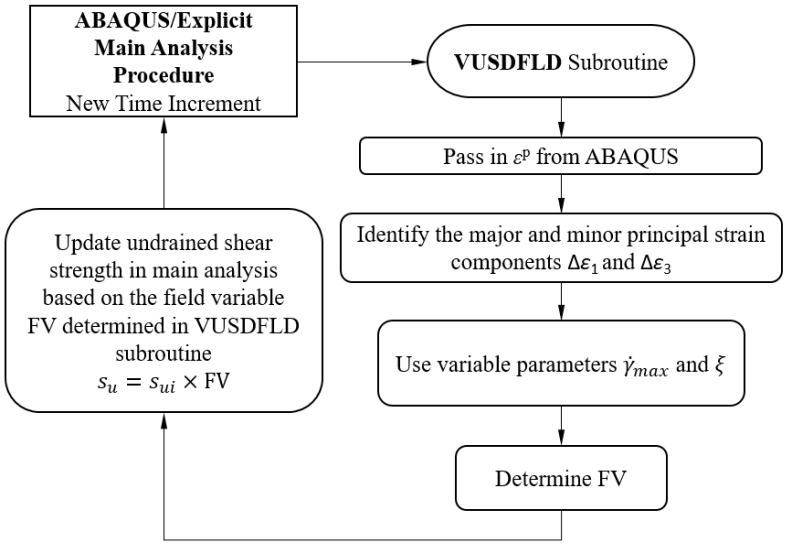

Figure 6-3: Flowchart declaring the interaction between the solver and the user subroutine, VUSDFLD

6.2.3. Mesh sensitivity analysis

Mesh sensitivity analysis was conducted to find the optimum mesh size in terms of accuracy and computational effort. Three different mesh sizes were investigated, including a fine mesh size of 0.25 m, a medium mesh size of 0.5 m, and a coarse mesh size of 1.0 m. The horizontal reaction forces and the ratio of vertical to horizontal reaction forces were obtained from the analyses using different mesh sizes and plotted in Figure 6-4.

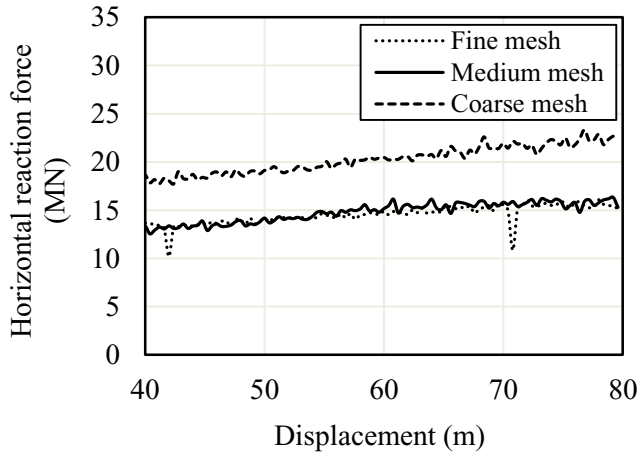

(a)

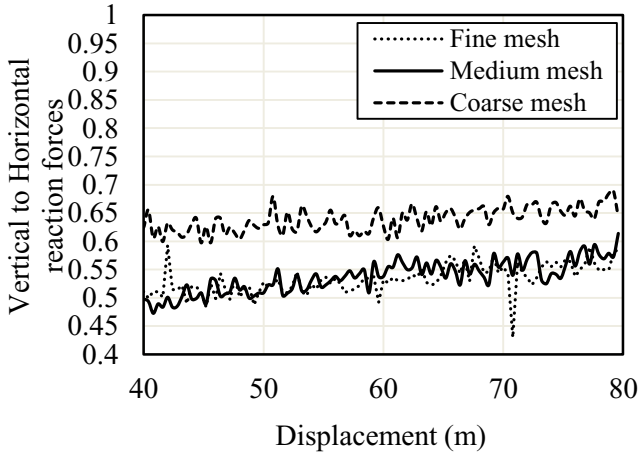

(b)

Figure 6-4: The results of mesh sensitivity analysis

The number of elements and the corresponding run time showing the computational efforts required for analysis are summarized in Table 6-2.

Table 6-2: Mesh convergence analysis for free-field ice gouge simulations

Case	Min. Element Size (m)	Max. Element Size (m)	Number of Eulerian Elements	Run Time on 76 CPUs
1	1.0	1.0	98,000	2 hrs. 10 min.
2	0.5	1.0	392,000	10 hrs. 6 min.
3	0.25	1.0	1,519,840	83 hrs. 55

As shown in Figure 6-4, a good match was observed between the responses obtained from the medium and fine mesh cases (Case 2 and 3), while the coarse mesh (Case 1) provided a slightly conservative predictions. A similar trend could be observed in Figure 6-4 (b) for the ratio of vertical to horizontal reaction forces of the ice keel. Comparing the results obtained in the Figure 6-4 (a) and (b) and the solution run time in Table 6-2, the medium mesh size (Case 2) was selected for the model verification analysis and the comprehensive parametric study to achieve an optimal balance between the computation efficiency and solution accuracy.

6.3. Model verification

The developed model was verified by making comparisons with the classical Mohr-Coulomb (MC) model predictions for the clay layer and the experimental study results (i.e., Test No. 8 of PRISE conducted by C-CORE (1995e)). During that specific test, ice attacked to a sand over clay layered soil strata (3.15 m sand overlaying an 11.75 m clay) with an attack angle of 15° in a gouge depth of 1.58 m. Figure 6-5 shows the comparison of the predicted and tested keel horizontal reaction force (a) and the ratio of the vertical to horizontal reaction forces (b).

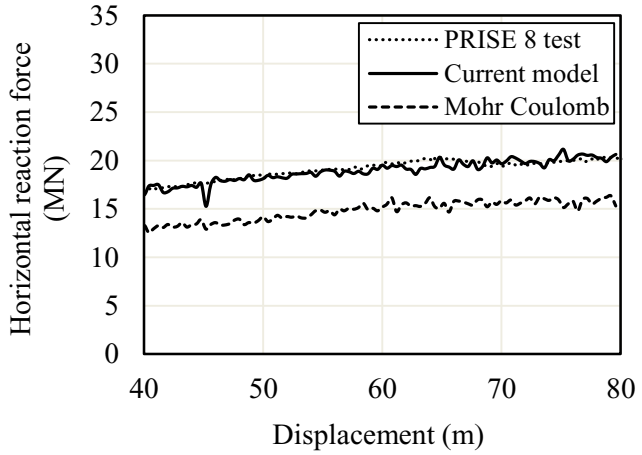

(a)

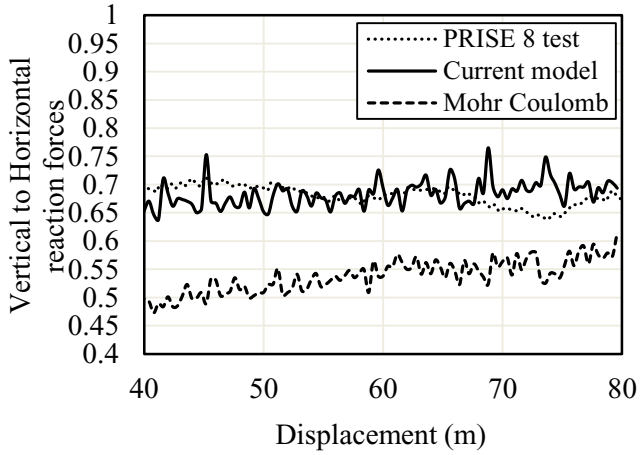

(b)

Figure 6-5: The Comparison of the tracked soil deformation

The obtained keel horizontal reaction force and the ratio of vertical to horizontal reaction forces match well with the experimental results (C-CORE, 1995e). The remarkable underestimation of the reaction forces by the classical MC model considered for the clay layer emphasized the significance and importance of incorporating the strain rate dependency and strain-softening effects into the modified Tresca model simulating the plastic behaviour of clay soil in the bottom. By accounting these effects in the modified Tresca model for the clay layer, the in situ undrained shear strength (s_{ui}) of the bottom clay

soil under shearing increased by a factor of 2.11 in the areas with high shear strain rate and resulted in a stiffer soil response compared with the classical MC model.

6.4. Parametric study

A comprehensive parametric study was performed including 26 different case scenarios (CS-1 to CS-26) as shown in Table 6-3. These case studies contributed to assessment of the influence of the key parameters of the free-field ice gouging model, including the geometry of the ice keel (attack angle and keel width), gouge depth of the ice keel, the thickness and configuration of the layered soil on the resultant reaction forces, subgouge soil deformation, and the side berms and frontal mound formations.

Table 6-3: Parametric study layout

	Ice			Soil	
	Attack angle (°)	Gouge depth (m)	Keel width (m)	Soil layer thicknesses (m/m)	Soil layering configurations
CS-1	27	0.5	12	3/15	Loose sand/Soft clay
CS-2	27	1.5	12	3/15	Loose sand/Soft clay
CS-3	27	2.2	12	3/15	Loose sand/Soft clay
CS-4	27	3.5	12	3/15	Loose sand/Soft clay
CS-5	27	5	12	3/15	Loose sand/Soft clay
CS-6	15	2.2	12	3/15	Loose sand/Soft clay
CS-7	27	2.2	12	3/15	Loose sand/Soft clay
CS-8	45	2.2	12	3/15	Loose sand/Soft clay
CS-9	27	2.2	5	3/15	Loose sand/Soft clay
CS-10	27	2.2	12	3/15	Loose sand/Soft clay
CS-11	27	2.2	20	3/15	Loose sand/Soft clay
CS-12	27	0.5	12	1/17	Loose sand/Soft clay
CS-13	27	2.2	12	1/17	Loose sand/Soft clay
CS-14	27	3.5	12	1/17	Loose sand/Soft clay
CS-15	27	2.2	12	3/15	Loose sand/Soft clay
CS-16	27	2.2	12	3/15	Loose sand/Stiff clay
CS-17	27	3.5	12	3/15	Loose sand/Soft clay
CS-18	27	3.5	12	3/15	Loose sand/Stiff clay
CS-19	27	2.2	12	3/15	Very loose sand/Soft clay
CS-20	27	2.2	12	3/15	Very loose sand/Stiff clay
CS-21	27	3.5	12	3/15	Very loose sand/Soft clay
CS-22	27	3.5	12	3/15	Very loose sand/Stiff clay
CS-23	27	2.2	12	3/15	Dense sand/Soft clay
CS-24	27	2.2	12	3/15	Dense sand/Stiff clay
CS-25	27	3.5	12	3/15	Dense sand/Soft clay
CS-26	27	3.5	12	3/15	Dense sand/Stiff clay

The undrained shear strength profile of the bottom soft clay soil layer in the parametric study was adopted to vary linearly from 15 kPa at the interface to 60 kPa at the deepest

point (k=3 kPa/m) while a uniform strength profile, 130 kPa constant through depth, was considered for bottom stiff clay soil (see Figure 6-6).

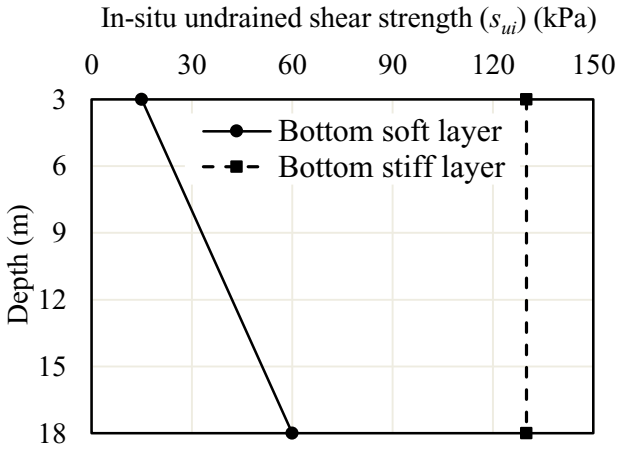

Figure 6-6: Undrained shear strength (s_{ui}) profile of the clay soil layer

In section 6.4.1 and section 6.4.2, the results obtained on the effects of ice keel features and layered soil configurations are presented.

6.4.1. Effect of ice keel features and gouging configuration

The case studies CS-1 to CS-11 were conducted to investigate the effect of gouge depth, ice keel attack angle and ice keel width on the resultant reaction forces and subgouge soil deformations. As shown earlier in Table 6-3, a gouge depth of 2.2 was considered for the case studies investigating the effect of attack angle and keel width.. Figure 6-7 shows the results of ice keel horizontal and vertical reaction forces (RF1 and RF3) and subgouge soil deformation obtained from these case studies.

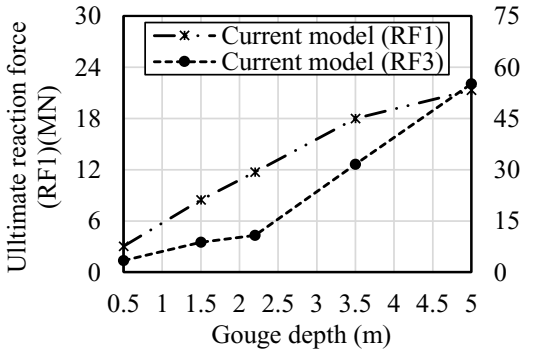
Ulltimate reaction force (RF1)(MN)
Current model (RF1)
Current model (RF3)
Gouge depth (m)

(a)

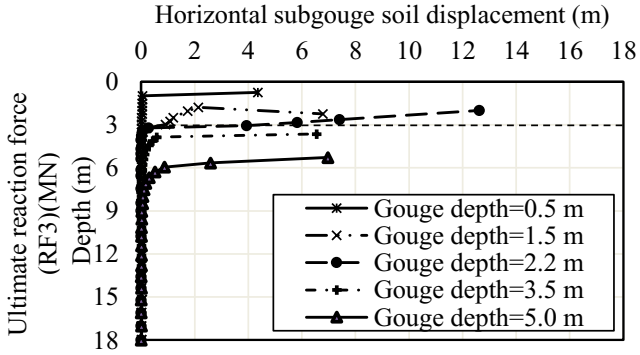
Horizontal subgouge soil displacement (m)
Ultimate reaction force (RF3)(MN)
Depth (m)
Gouge depth=0.5 m
Gouge depth=1.5 m
Gouge depth=2.2 m
Gouge depth=3.5 m
Gouge depth=5.0 m

(b)

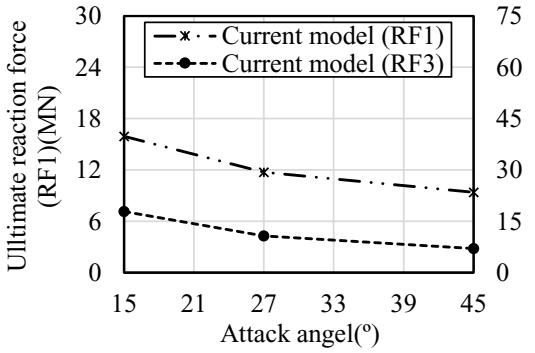
Ulltimate reaction force (RF1)(MN)
Current model (RF1)
Current model (RF3)
Attack angel(°)

(c)

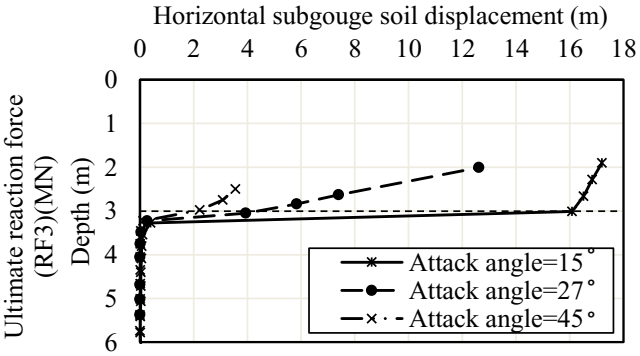
Horizontal subgouge soil displacement (m)
Ultimate reaction force (RF3)(MN)
Depth (m)
Attack angle=15°
Attack angle=27°
Attack angle=45°

(d)

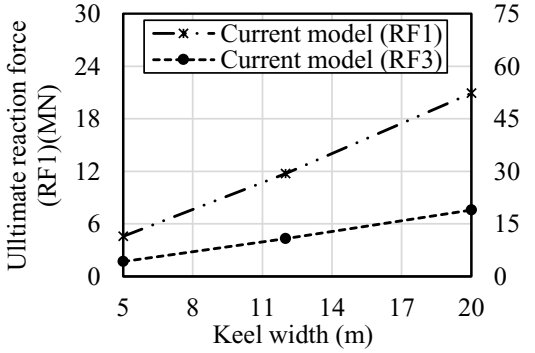
Ulltimate reaction force (RF1)(MN)
Current model (RF1)
Current model (RF3)
Keel width (m)

(e)

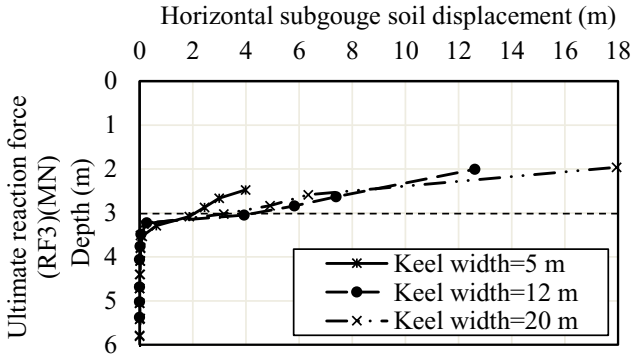
Horizontal subgouge soil displacement (m)
Ultimate reaction force (RF3)(MN)
Depth (m)
Keel width=5 m
Keel width=12 m
Keel width=20 m

(f)

Figure 6-7: The effect of different attack angles, keel widths, and gouge depths on reaction forces and subgouge soil deformations (CS-1 to CS-11)

As shown in Figure 6-7 (a) both the horizontal and vertical reaction forces of the ice keel in the steady state were increased by increasing the gouge depth. A sharp basal shear zone was observed under the ice keel tip located in the loose sand, where the subgouge soil deformation was not transferred from loose sand to the soft clay layer (see Figure 6-7 (b)). As the gouge becomes deeper, the subgouge soil deformation profile recovers its usual shape in soft clay, and the displacements are further extended to the deeper areas.

The larger keel attack angle resulted in smaller subgouge soil deformation (see Figure 6-7 (d)) and smaller reaction forces (see Figure 6-7 (c)). Also, the larger keel width produced larger subgouge soil deformation (see Figure 6-7 (f)) and larger reaction forces (see Figure 6-7 (e)) which is in agreement with earlier studies.

To visualize the soil failure mechanisms, Figure 6-8 illustrates the influence of gouging with different depths on the resultant progressive plastic strain (PEVAVG as maximum principal plastic strain) and the formation of side berms and frontal mound.

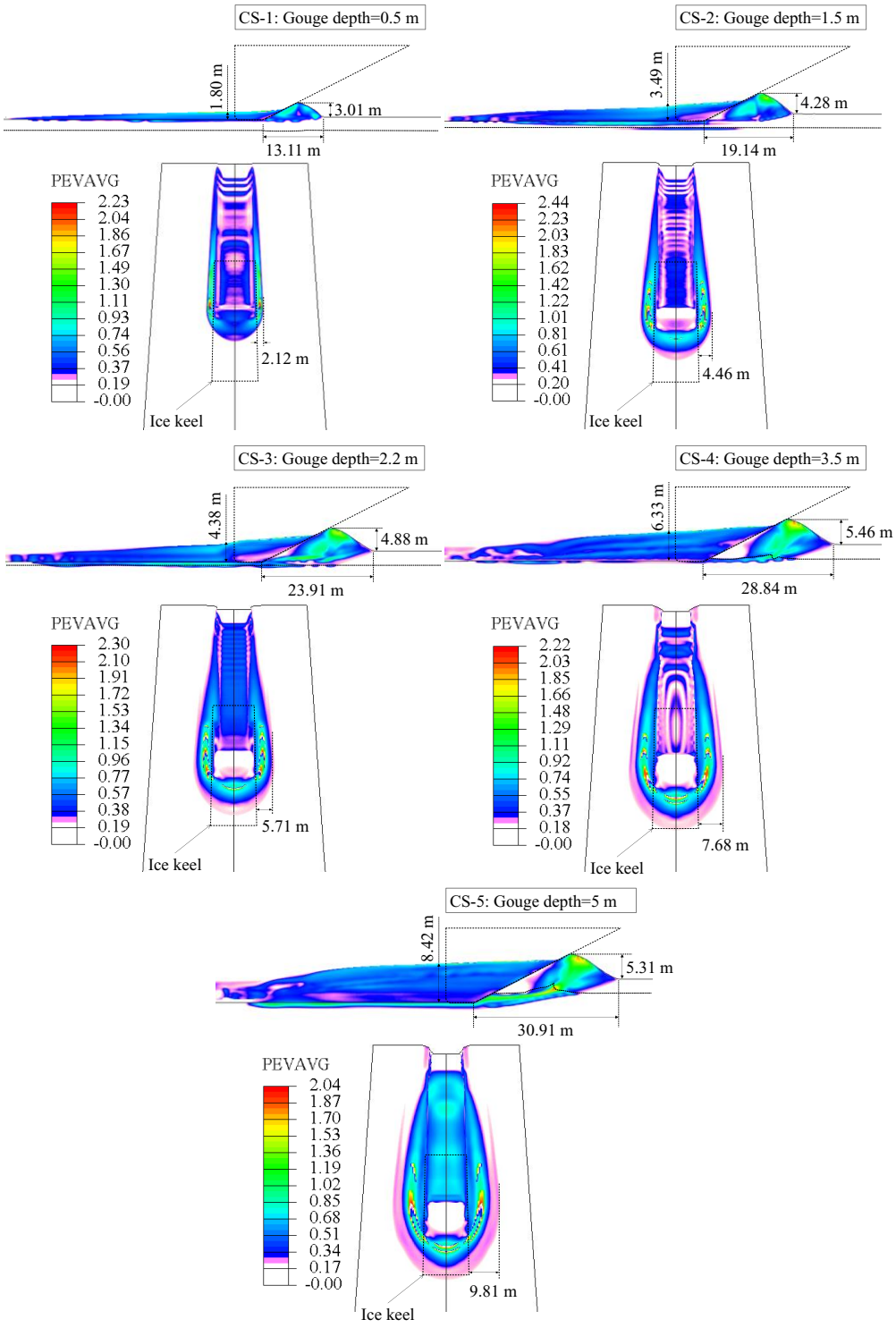

Figure 6-8: The effect of gouging with different depths on progressive plastic strain and quality of soil formation

Figure 6-8 shows that by increasing the gouge depth, the size of frontal mound and side berms are increased. The maximum plastic strain (PEVAVG as maximum principal plastic strain) was found generally localizing on top of the frontal mound, which is further developed through the bottom soft clay as the gouge depth is increased and the ice tip reaches the soft clay (CS-4 & CS-5). Development of dead sand wedges with zero plastic strain was observed right underneath the keel base and the contact area between the ice chest and the top sand layer. A wrinkling mechanism was also observed in the interface of the sand and clay layers that becomes tenser with increasing the gouge depth.

6.4.2. Effect of different layer strengths

Three different strengths for sand, including very loose, loose and dense sand, and two different strengths for clay, including soft and stiff clay were investigated. Three different sets of friction and dilation angles were adopted for very loose, loose and dense sands, i.e., (20°, 0°), (32°, 0°) and (38°, 8°) respectively. The undrained shear strength profiles of soft and stiff clays followed the distribution presented at Figure 6-6. The key outputs were compared for ice gouging with two different gouge depths 2.2 m and 3.5 m with the ice tip located in top sand and the bottom clay, respectively.

Figure 6-9 compares the reaction forces and subgouge soil displacements obtained from these analyses for the case scenarios of very loose sand over soft clay (VLS/SoC), loose sand over soft clay (LS/SoC) and dense sand over soft clay (DS/SoC).

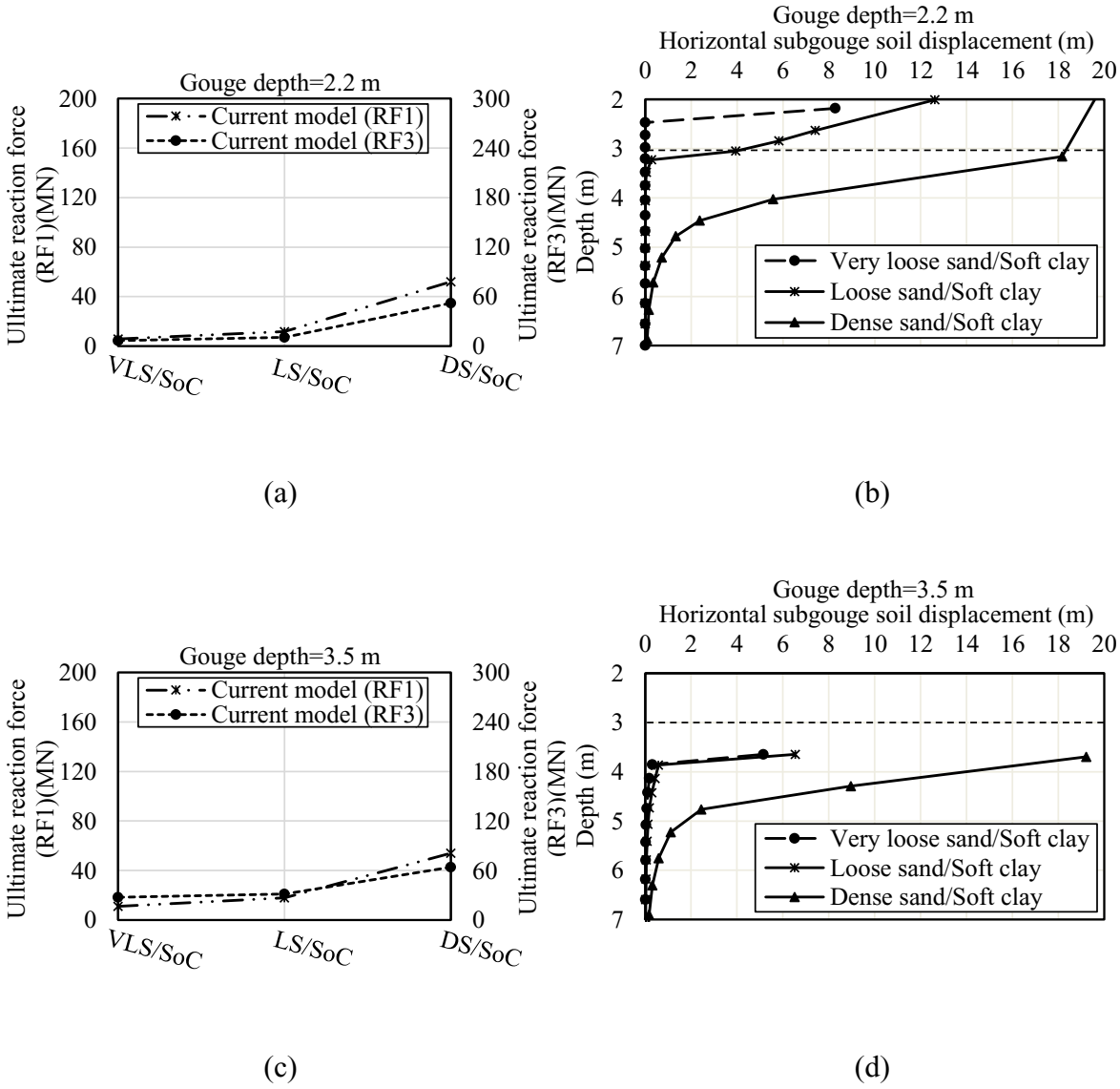

Figure 6-9: The effect of gouging in sand over soft layered seabed on reaction forces and subgouge soil deformation

Figure 6-9 (a) and (c) show that the reaction forces are higher for gouging in dense sand over soft clay. Figure 6-9 (c) shows that the reaction forces are higher for deeper gouges in very loose and loose sand over soft clay. For deeper gouge, the reaction forces in dense sand over soft clay (CS-25) are almost identical comparing with shallower gouge depth

(CS-23). Figure 6-9 (b) and (d) show that the subgouge soil displacement in dense sand over soft clay is further extended through the soil depth and become larger compared with two other cases. As can be seen in Figure 6-9 (b) and (d), the basal shear mechanism in sand is faded as the relative strength of the sand layer is increased. Also, as the top sand layer becomes denser, the soil particles tend to have more vertical downward displacement.

Figure 6-10 compares the progressive plastic strains (PEVAVG as maximum principal plastic strain) along with frontal mound, side berm formation, and the layers interaction in sand over soft clay seabed with different seabed strengths.

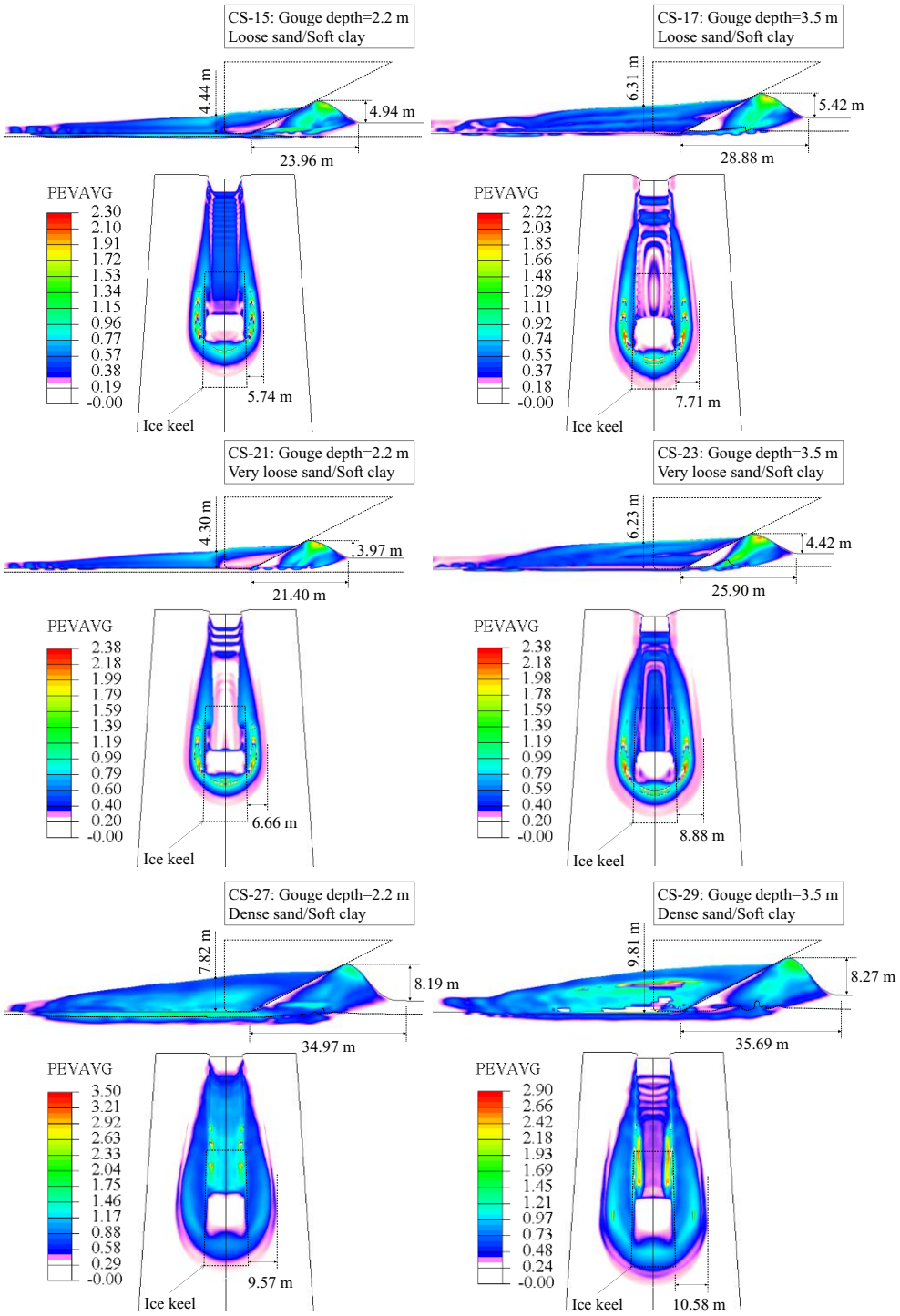

Figure 6-10: The effect of gouging in sand over soft clay layered seabed on progressive plastic strain and quality of soil formation

Figure 6-10 shows that by increasing the relative density of the top sand layer (very loose, loose and dense), the size of frontal mound and side berms are increased. For the cases with very loose sand on top layer, the maximum plastic strain was locally developed on top of the frontal mound and extended in a narrow zone towards the bottom soil. The maximum plastic strain is more extended in a wider area for loose sand and is minimized on top of frontal mound for dense sand. In addition, the maximum plastic strain was extended from frontal mound to the side berms when the top layer is very loose or loose sand. For the case with dense sand, the maximum plastic strain was developed through the contact area between the keel base and the bottom soil, and the keel wall and the side berms. From a practical standpoint, it will be important to know that presence of a dense layer of sand on top can results in further extension of the subgouge soil deformations through the underlying soft layer of clay.

A similar set of studies were conducted replacing the bottom soft layer of clay with stiff clay.

Figure 6-11 compares the reaction forces and subgouge soil displacements resulted for three different seabed configurations, very loose sand over stiff clay (VLS/StC), loose sand over stiff clay (LS/StC) and dense sand over stiff clay (DS/StC).

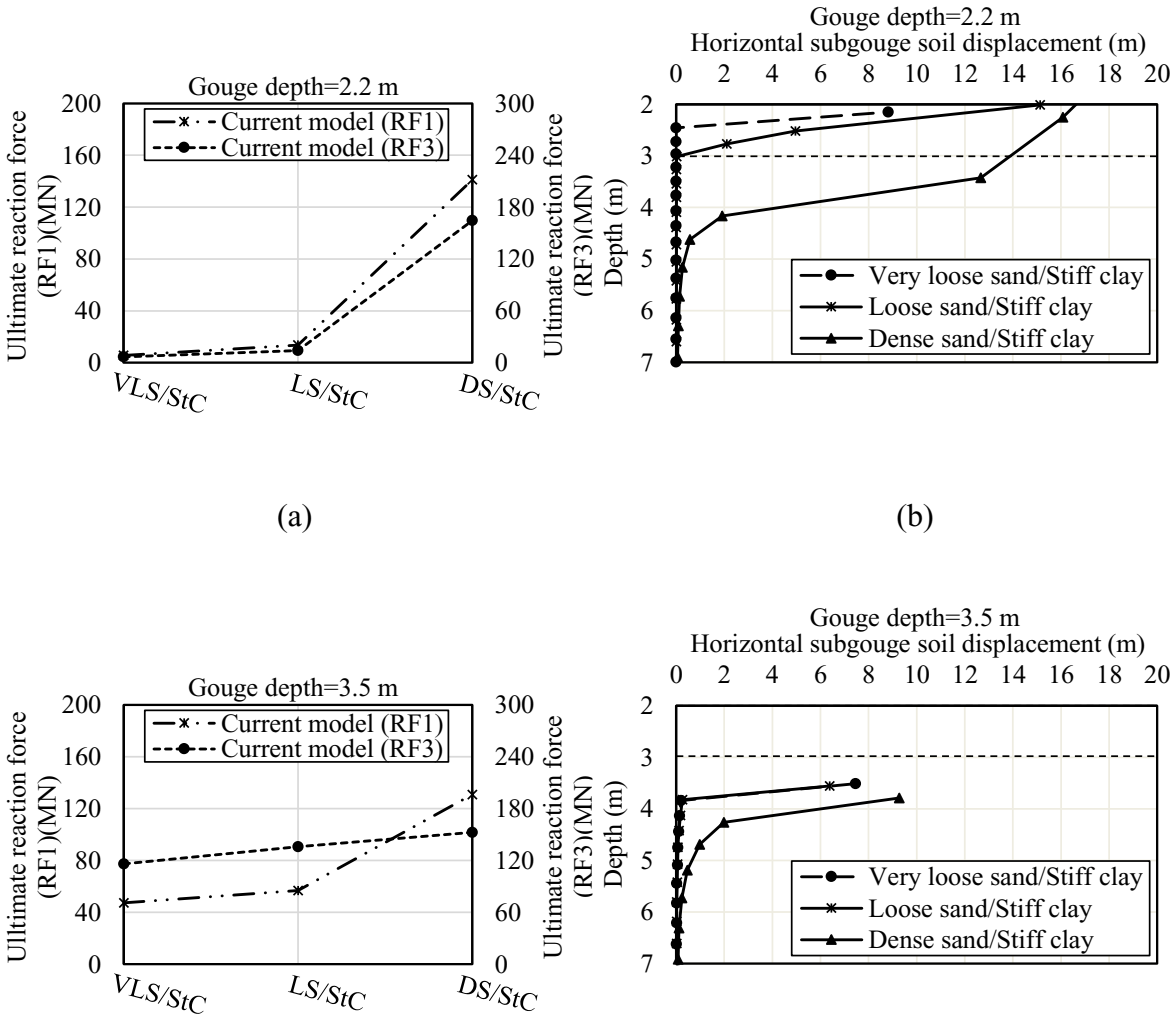

Figure 6-11: The effect of gouging in sand over stiff clay layered seabed on reaction forces and subgouge soil deformation

Almost similar trends with the previous study were observed but with a less extension of the subgouge soil deformation through the depth of stiff clay.

Figure 6-12 compares the progressive plastic strains (PEVAVG as maximum principal plastic strain) along with frontal mound, side berm formation, and the layers interaction in sand over stiff clay seabed with different seabed configurations.

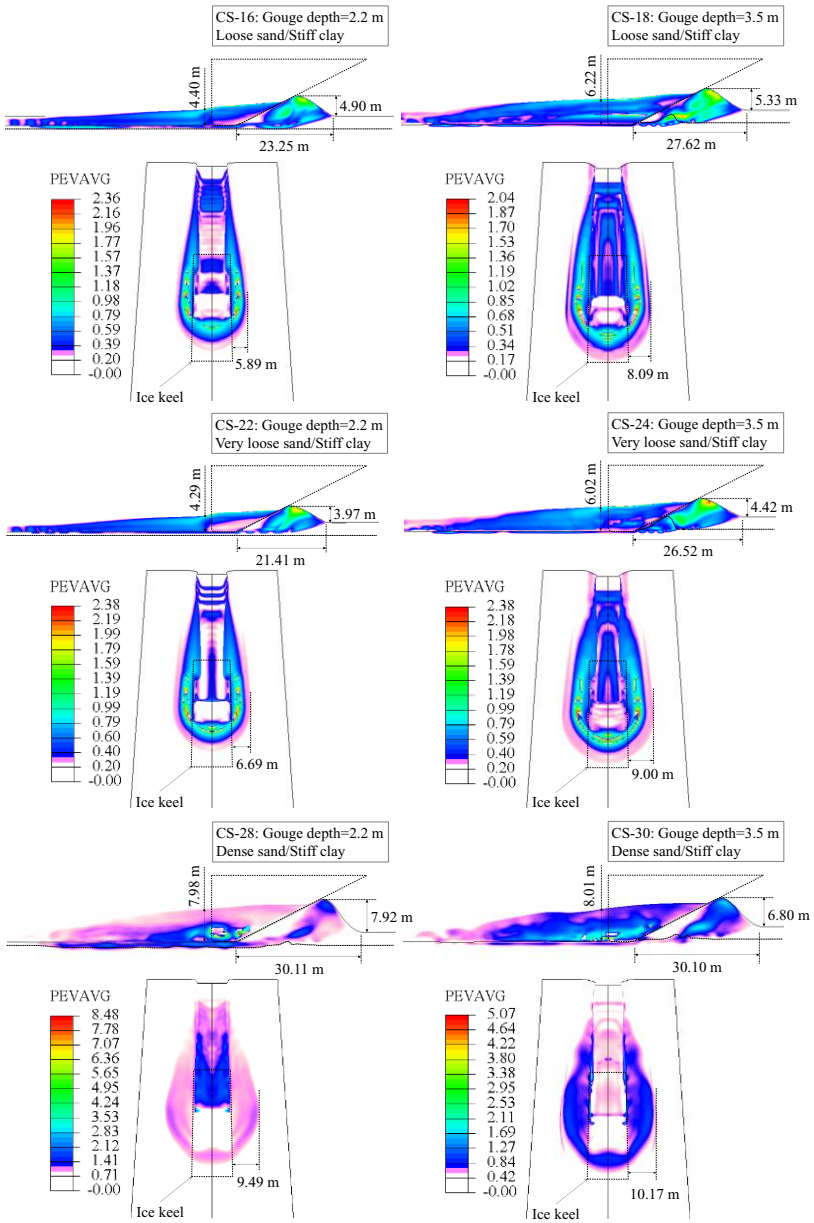

Figure 6-12: The effect of gouging in sand over stiff seabed on progressive plastic strain and quality of soil formation

Overall, these results show that the relative strength in between the top sand layer and bottom clay layer has a significant impact on both the reaction forces and subgouge soil deformations. As the strength difference between the top sand layer and the bottom clay layer is increased, the soil failure mechanism tends to be basal shear with less extension of displacements through the depth. Inversely, as the strength of the layers become less different, the subgouge soil deformation is deeper extended through the bottom soil more like a uniform soil stratum. These finding are important from practical point of view, showing that spectial attention is required when a combination of cohesionless and cohesive layers are encountered with large difference in strength classifications.

6.4.3. Effect of different soil layer thicknesses

The effect of soil layers with different thicknesses on ice gouging was studied through three case studies, i.e., CS-12 to CS-14. Considering a loose sand over soft clay as the base case scenario, ice gouging was conducted in two layered soil strata, including 1 m loose sand over 17 m soft clay, and 3 m loose sand over 15 m soft clay. Figure 6-13 shows the comparison the results of reaction forces and subgouge soil deformation obtained from theses case studies.

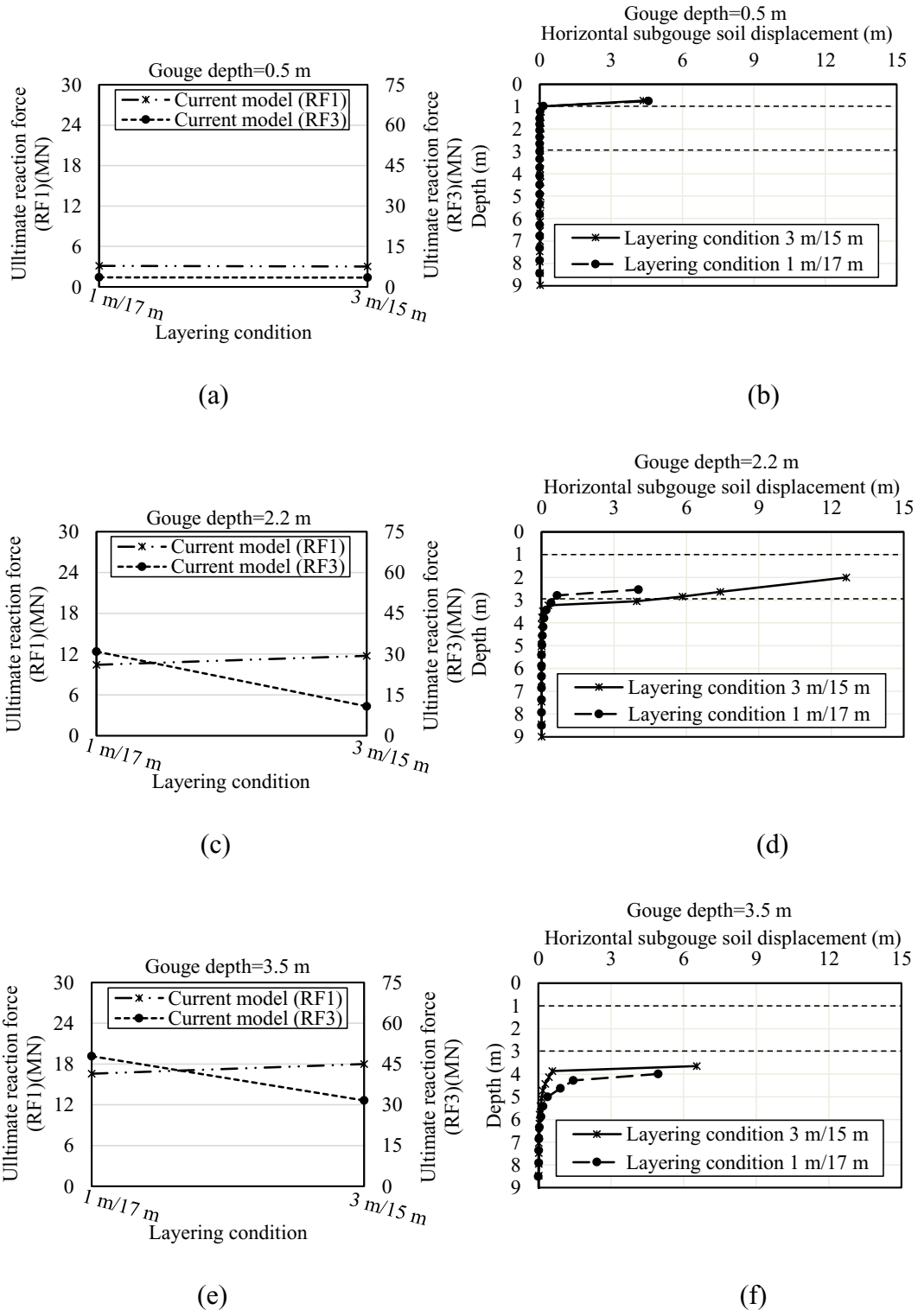

Figure 6-13: The effect of gouging in loose sand over soft clay seabed with different layered thicknesses on reaction forces and subgouge soil deformation

The results was almost identical for two cases with gouge depth equal to 0.5 m, CS-12 & CS-1, in which the ice keel bottom were located initially in top sand layer and didn't touched the bottom soft clay (see Figure 6-13 (a) and (b)). Figure 6-13 (c) and (d) Compare the results of two cases, CS-13 with two types of soils located in front of keel, and the case, CS-3, with the keel bottom still located in the top layer and CS-3 as well. The results show higher vertical reaction forces and lower horizontal reaction forces for the case CS-13 compared with CS-3. The magnitude of maximum subgouge soil deformation was smaller for the case, CS-13, compared with the case, CS-3 (Figure 6-13 (d)). Figure 6-13(e) and (f) compares the results of CS-14 and CS-4, where the bottom soil was touched by the keel base, the larger the volume of the bottom soft clay carried by the keel front (CS-14); the higher the vertical reaction force, and the less the resulted value of subgouge soil deformation.

Figure 6-14 compares the progressive plastic strains (PEVAVG as maximum principal plastic strain) along with frontal mound, side berm formation, and the layers interaction in loose sand over soft clay seabed with different layer thicknesses.

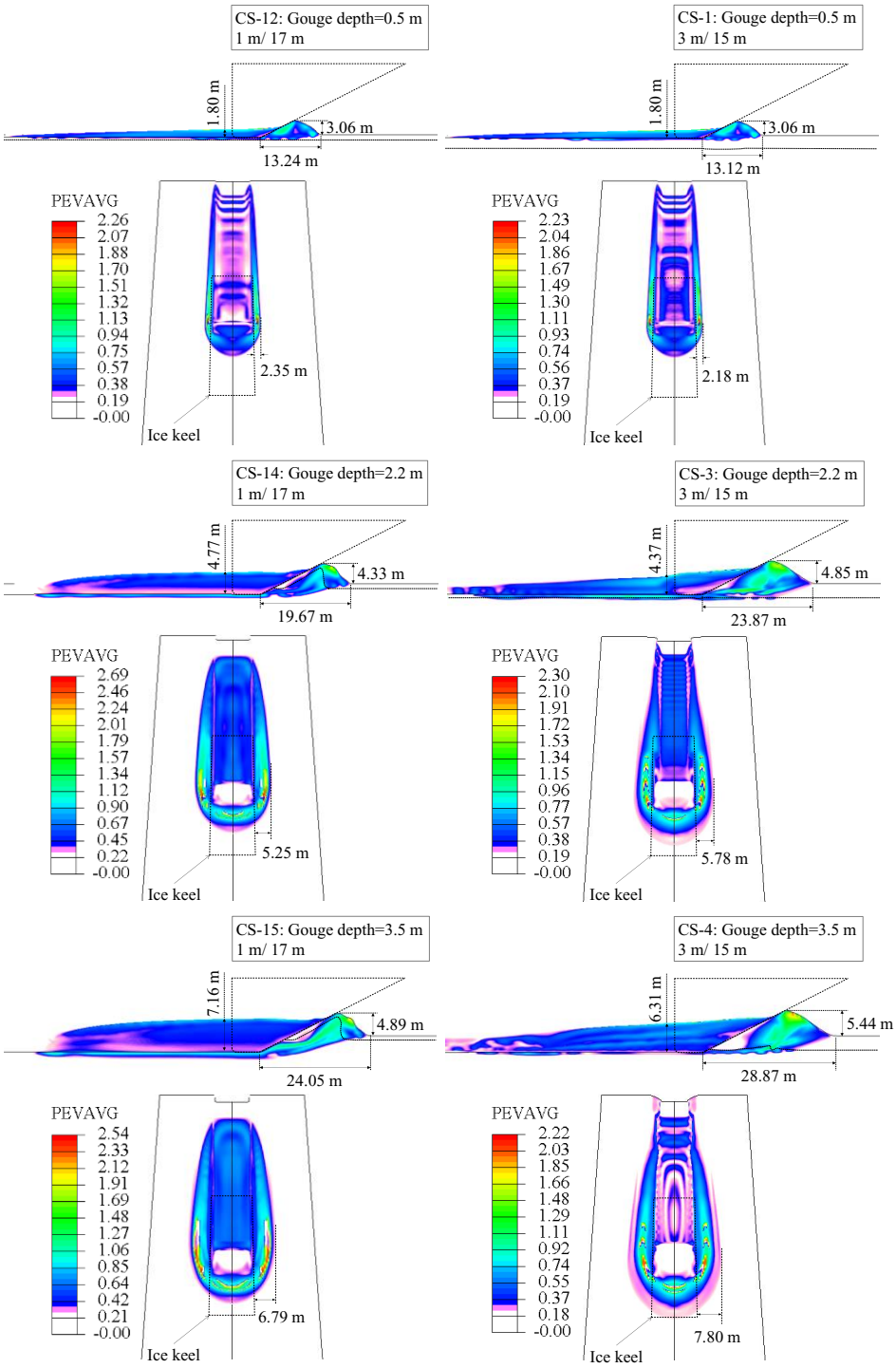

Figure 6-14: The effect of gouging in loose sand over soft clay seabed with different layered thicknesses on progressive plastic strain and quality of soil formation

Figure 6-14 shows the same trend in distribution of progressive plastic strain (PEVAVG as maximum principal plastic strain) for two cases with gouge depth less than 1 m (CS-12 and CS-1). Compared with the cases of the keel tip located in loose sand (CS-3), a less volume of soil was mobilized in front of keel, when the keel bottom was in contact with the bottom soft clay (CS-14). Also, the more the keel base initially penetrates in to the clay soil (CS-15), the less volume of soil is mobilized in front of the keel and a smaller dead wedge is developed in the keel chest and base.

6.5. Conclusions

The response of layered sand over clay seabed to the ice gouging was investigated. Using the CEL algorithm offered by ABAQUS/Explicit, large deformation finite element analysis of ice gouging was conducted. A built-in conventional Mohr Coulomb model was used for sand and a modified Tresca soil model was coded to a user-defined subroutine to account for the effects of strain rate dependency and strain softening on the mobilized undrained shear strength of the clay layer. The developed numerical model was verified against published experimental studies. A comprehensive parametric study was conducted to investigate the effects of ice keel features and layered sand over clay characteristics on the resultant ice keel reaction forces and the subgouge soil deformations. The key findings of the study can be summarized as follows::

- The study further revealed the significance of accurate modeling of the layered sand over clay seabed and noted that replacing the layered seabed with a uniform soil stratum may result in significant distortion of the ultimate results.

- The significance of accounting for the strain rate dependency and the strain softening in clay layer was observed, even if the gouge depth does not reach the underlying clay layer.
- It was observed that as the relative difference between the strength classification of the toping sand layer and the bottom clay layer is increased, the basal shear failure mechanism dominances and the subgouge soil deformations are less extended deeper in the underlying clay layer. Accordingly, the reaction forces are also decreased. From practical standpoint, the results suggest that special care shall be taken on the assessment of the reaction forces and subgouge soil deformations, when the strength classification of the layers is converging.
- The study showed that by increasing the relative density of the top sand layer (very loose, loose and dense), the size of frontal mound and side berms were increased. The reaction forces are higher for the gouge results in dense sand over soft clay, compared with two other cases.
- The subgouge soil deformation was found to be larger in shallow gouge depths. The subgouge soil displacement was observed to be larger in dense sand over stiff clay, compared with very loose and loose sands. Also, the soil particles observed to have more tendency for vertical downward displacement in cases with dense sand.

Overall, the study revealed the significance of considering layered sand over clay through continuum finite element analysis. The developed model can be used as a simple but robust tool for daily engineering practice. Further developments are suggested to incorporate the

pre-peak strain hardening and the post-peak strain softening of the dense sand in the simulations for refined results.

6.6. Acknowledgments

The authors gratefully acknowledge the financial support of this research by Wood PLC via establishing the Wood Group Chair in Arctic and harsh environment engineering at Memorial University, the NL Tourism, Culture, Industry and Innovation (TCII) via CRD collaborative funding program, the Natural Sciences and Engineering Research Council of Canada (NSERC) via CRD funding program, the Memorial University of Newfoundland through the school of graduate studies (SGS) baseline fund.

References

Alba, J. L., 2015. Ice Scour and Gouging Effects With Respect to Pipeline and Wellhead Placement and Design, Bureau of Safety and Environmental Enforcement (BSEE), Wood Group Kenny, Report No. 100100.01.PL.REP.004, Houston, TX.

Babaei, M. H., & Sudom, D., 2014. Ice-seabed gouging database: review and analysis of available numerical models. In *OTC Arctic Technology Conference*. Offshore Technology Conference.

Biscontin, G., Pestana, J.M., 2001. Influence of peripheral velocity on vane shear strength of an artificial clay. Geotech. Test.J. 24(4), 423–429.

BSEE-WGK, 2015. Ice Scour and Gouging Effects with Respect to Pipeline and Wellhead, Final Report, 100100.01.PL.REP.004, Rev0.

C-CORE, 1995e. Pressure Ridge Ice Scour Experiment, PRISE: Phase 3-Centrifuge Modelling of Ice Keel Scour: Draft Final Report. April 1995. Publication 95-C12, 52p.

C-CORE, 2008. Design Options for Offshore Pipelines in the US Beaufort and Chukchi Seas. April 2008. Report R-07-078-519.

Dayal, U., Allen, J. H., 1975. The effect of penetration rate on the strength of remolded clay and sand samples. Can. Geotech. J., 12(3),336–348.

DeGroot, D. J., DeJong, J. T., Yafrate, N. J., Landon, M. M., Sheahan, T. C., 2007. Application of recent developments in terrestrial soft sediment characterization methods to offshore environments. Proc., Offshore Technology Conf., Houston, OTC 18737.

DeJong, J., DeGroot, D., Yafrate, N., 2012. Evaluation of undrained shear strength using full-flow penetrometers. J. Geotech. Geoenviron. Eng.138(6),765–767.

Einav, I., Randolph, M. F., 2005. Combining Upper Bound and Strain Path Methods for Evaluating Penetration Resistance. International Journal for Numerical Methods in Engineering, Vol. 63, No. 14, pp. 1991-2016.

Eltaher, A., 2014. Gaps in Knowledge and Analysis Technology of Ice Gouge Pipeline Interaction. Proceedings of the Arctic Technology Conference, February 10 - 12, 2014, 10p.

Graham, J., Crooks, J. H. A., Bell, A. L., 1983. Time effects on the stress-strain behaviour of natural soft clays. Geotechnique, 33(3), 327–340.

Hashemi, S., Shiri, H. and Dong, X., 2022a. The influence of layered soil on ice-seabed interaction: Soft over stiff clay, Applied Ocean Research, Volume 120, March 2022, 103033, ISSN 0141-1187, https://doi.org/10.1016/j.apor.2021.103033

Hossain, MS, Randolph, MF, 2009. Effect of Strain Rate and Strain Softening on the Penetration Resistance of Spudcan Foundations on Clay. International Journal of Geomechanics, Vol 9, No 3, pp 122-132.

Konuk, IS., Gracie, R., 2004. A 3-dimensional Eulerian FE model for ice scour. IPC04-0075, pp.1911-1918.

Lele, S., Hamilton, J., Panico, M., Arslan, H., Minnaar, K., 2011. 3D continuum simulations to determine pipeline strain demand due to ice-gouge hazards. Arctic Technology Conference, ATC.

Lunne, T., Andersen, K. H., 2007. Soft clay shear strength parameters for deepwater geotechnical design. Proc., 6th Int. Offshore Site Investigation and Geotechnics Conf.: Confronting New Challenges and Sharing Knowledge, Vol. 1, Society for Underwater Technology, London, 151–176.

Nobahar, A., Kenny, S., Phillips, R., 2007b. Buried pipelines subject to subgouge deformations. International Journal of Geomechanics, vol. 7, no. 3, pp. 206-216.

NRC-PERD, 2014. Ice-Seabed Gouging Database: Review & Analysis of Available Numerical Models (Babae, M.H. and Sudom, D. (2014)); Physical Simulations of Seabed Scouring by Ice: Review and Database (Barrette, P. and Sudom, D. (2014)).

Peek, R., Nobahar, A., 2012. Ice gouging over a buried pipeline: Superposition error of simple beam-and-spring models. International Journal of Geomechanics, vol. 12, no. 4, pp. 508-516.

Pike, K., Kenny, S., 2016. Offshore pipelines and ice gouge geohazards: Comparative performance assessment of decoupled structural and coupled continuum models. Canadian Geotechnical Journal, 53(11), 1866-1881.

Phillips, R., Barrett, J., 2012. PIRAM: Pipeline Response to Ice Gouging. Proceedings of the Arctic Technology Conference, December 3 - 5, 2012, 6p.

Raie, M., Tassoulas, J., 2009. Installation of torpedo anchors: numerical modeling. J. Geotech. Geoenviron. Eng. 135 (12), 1805–1813.

Randolph, M. F., 2004. Characterization of soft sediments for offshore applications. Keynote Lecture, Proc., 2nd Int. Conf. on Site Characterization, Porto, Portugal, Vol. 1, Millpress Science Publishers, Rotterdam, 209–231.

Winters, W. J. and Lee, H. J.,1984. Geotechnical properties of samples from borings obtained in the Chukchi Sea, Alaska. USGS Report 85-23.

Woodworth-Lynas, C., Nixon, D., Phillips, R., Palmer, A., 1996. Subgouge Deformations and the Security of Arctic Marine Pipelines. Proc. 28th OTC, Vol. 4, Paper No. 8222, pp. 657–664.

Chapter 7

Conclusions and Recommendations

In this project, the response of different layered seabed comprising soft over stiff clay, stiff over soft clay, and the loose and dense sand over soft and stiff clay to the ice gouging were investigated by performing large deformation finite element (LDFE) analysis using a Coupled Eulerian Lagrangian (CEL) algorithm. The results were compared with uniform soil strata and published studies. The strain rate and strain softening effects of the cohesive soil was incorporated by coding a modified Mohr Coulomb soil model into a user-defined subroutine (VUSDFLD) and linked to the main solver in ABAQUS/Explicit. Inclusion of these effects improved the accuracy of simulating the ice gouging process in layered seabed as a high velocity geotechnical problem involving large deformations. During the analysis, the user subroutine is incrementally called by ABAQUS to update the undrained shear strength of the soil based on the incremental values of the currently accumulated absolute plastic shear strain and the calculated maximum shear strain rate with zero value adopted for friction and dilation angles. The performance of the modified soil model was verified through comparisons with published experimental studies and conventional soil models. Comprehensive parametric studies were conducted to examine the ice keel-seabed interaction in a range of layered seabed with different configurations. The effect of different input parameters including the ice keel geometry, gouge depth, seabed soil strength, and layering condition on the keel reaction forces, subgouge soil deformation, the side berm and frontal mound formations, and the progressive plastic shear strain distribution were examined through a large number of case scenarios.

A series of interesting observations were made showing that replacing a layered seabed with a uniform seabed for simplicity could significantly distort the subgouge soil deformation magnitudes and keel reaction forces. Based on the observations, technical advices were provided to improve the design practice. The summary of key findings and practical recommendations are as follows:

- **Key Conclusions and Technical Advice for Practice**

- The developed model with incorporation of the strain rate dependency and strain-softening effects was found to be a simple but robust tool for simulation of free-field ice gouging process in clay. Compared with earlier numerical and the MC model, the developed model achieved a significantly improved agreement with the published test results.
- The incorporation of strain rate and strain-softening effects in a uniform soil stratum resulted in reaction forces higher than MC model and subgouge soil deformation smaller than MC model. The strain rate and strain-softening produced higher values of undrained shear strength around the scour area and a stiffer seabed response with high localized plastic shear strain in the proximity of the ice keel. The study showed the dominance of the strain rate effects compared with strain-softening effects. The strain-softening contributed to a broader extend of plastic shear strain under and in the front of the ice keel. This, in turn, resulted in a larger frontal mound and also a smaller subgouge soil deformation. Eventually, the strain rate effects governed the ice keel-seabed interaction.

- The interactions between the soil layers in a soft over stiff clay seabed with different strengths could significantly override the usual seabed response to ice gouging in a uniform soil. In the soft over stiff clay, for the gouge depths less than the thickness of the soft layer, the subgouge soil deformation was truncated in the interface of the soil layers. This suggests that the trench depth can be safely limited to thickness of soft layer, and the pipeline buried in stiff layer with its crown touching the soft layer. This in turn would need new trenching technics to excavate an opening in the trench bed to locate the pipe.
- The effects of strain rate dependency and strain softening were found to be significant in the loading area with high developed plastic shear strain. These areas include the interface of soft and stiff soil layers, and the proximity of ice keel soil contact zone. It was observed that the conventional soil models might overestimate the subgouge soil deformation and reaction forces.
- The seabed reaction forces in layered soft over stiff clay are in between the ones from uniform layers, i.e., lower than uniform stiff clay and higher than uniform soft clay. The magnitude of difference depends on the thickness and shear strength of each layer, and also the gouge depth. This shows the significance of modeling layers seabed soil strata where applicable.
- Same as the uniform soil, the intensity of the ice gouging in layered seabed could be influenced by the geometry of the ice keel. In both horizontal and vertical direction, the reaction force of the ice keel decreased with increasing the attack angle, and increased with increasing the keel width.

- Replacing a layered stiff over soft clay seabed with a uniform seabed for ice gouging analysis can be a gross simplification. The study showed that the interaction between the stiff layer on top and the soft layer in the bottom might result in a wavy shape subgouge soil deformation profile with a peak deformation much deeper than the uniform soil. The wavy shape subgouge deformation profile included a peak and a nadir point. The nadir point is located in the proximity of the interface between the soil layers and the peak point is located deep through the soft soil.
- It was observed in stiff over soft clay that as the ice keel moves forward, the stiff layer is inclined parallel to the attack angle and pushes the soft soil particles ahead of the keel forward-upward parallel to the attack angle. As the ice keel passes over the soil particles, the uplifted soft soil is push downward again resulting in a maximum subgouge soil deformation, which is not located right in the proximity of the soil layers interface.
- In stiff over soft seabed, as the gouge depth becomes deeper the wavy subgouge deformation profile is faded and the profile become similar to a deepened uniform soil. Also, it was observed the side berms and frontal soil mounds formed during the ice gouging process are much smaller in the layered stiff over soft soil compared with uniform soil. The wavy subgouge soil deformation can have a significant role in determining the best burial depth for protection of subsea pipelines against the iceberg attack in practice.
- The study showed that the soil failure mechanism in front of the ice keel could be significantly affected by the layered stiff over soft clay, resulting in subgouge

deformations much larger than the uniform seabed. A wrinkled soil failure mechanism was observed when the stiff layer was thin and the gouge depth was well below the interface of the stiff and soft layers. The changing of the soil failure mechanism with the thickness of the layers emphasize on the interactive nature of layered seabed response to the ice gouging and the importance of accurate modeling of the layers in practice.

- Different strength ratio in between the stiff and soft layers was found to have a remarkable effect on the subgouge soil deformation and the reaction forces. As the stiff layer becomes stiffer and the soft layer become softer, the subgouge soil deformation and ice keel reaction forces are decreased. Also, by increasing the strength of stiff soil, the soft soil particles on the bottom undergo more downward relocation and vice versa.
- When a stiff layer is located on top of a soft clay seabed, further deepening of the trench will not only improve the safety of the pipeline, but also endanger it by increasing the probability of locating the pipe in the peak point of the wavy subgouge soil deformation.
- In sand over clay seabed, as the relative difference between the strength classification of the toping sand layer and the bottom clay layer is increased, the basal shear failure mechanism dominances and the subgouge soil deformations become less extended deeper in the underlying clay layer. Accordingly, the reaction forces are also decreased. From practical standpoint, the results suggest that special care shall be taken on the assessment of the reaction forces and subgouge soil deformations, when the strength classification of the layers is converging.

- By increasing the relative density of the top sand layer (very loose, loose and dense), the size of frontal mound and side berms were increased. The reaction forces are higher for the gouge results in dense sand over soft clay, compared with two other cases.
- The subgouge soil deformation in sand over clay seabed was found to be larger in shallow gouge depths. The subgouge soil displacement was observed to be larger in dense sand over stiff clay, compared with very loose and loose sands. In addition, the soil particles observed to have more tendency for vertical downward displacement in cases with dense sand.

- **Recommendation for future studies**

- The current study is limited to numerical simulations using CEL algorithm. To further investigate the observed failure mechanisms in the layered seabed, and to propose analytical solutions, performing experimental studies are recommended.
- In this study, it was assumed that the ice gouging velocity is high enough to consider undrained conditions for cohesive soil. Ice gouging with low velocity has been observed in the field. Therefore, it is required to model the partial drained and drained condition and investigate the rate effects. The observed trends and failure mechanisms may not be valid for partial drained and fully drained conditions. It is recommended to incorporate the consolidation and rate effects in the constitutive soil models and verify it against the experimental studies.

- In this study, the classical Mohr Coulomb model was used for modeling the sand layer. It is recommended to incorporate the pre-peak strain hardening and post-peak strain softening effects into the dense sand layer for improved analysis. It is also recommended to include the effect of sand particles crushing in contact with the ice keel.
- The conducted studies are recommended to be extended by inclusion of trench and pipeline for a coupled analysis of the pipeline response to ice gouging in layered seabed.

Further investigations are recommended to propose analytical solution for the layered seabed and improve the existing beam-spring models in the decoupled approach for ice gouging analysis.